GENETIC ANALYSIS OF ADIPOSE LINEAGE AND

DEVELOPMENT

APPROVED BY SUPERVISORY COMMITTEE

Jonathan M. Graff, MD., Ph.D.

Michelle Tallquist, Ph.D.

David Mangelsdorf, Ph.D.

Robert Hammer, Ph.D.

To My Mom and Dad,

Runtian Tan and Xihai Tang

To My Husband,

Tao Wang

ACKNOWLEDGEMENTS

I am extremely grateful to my mentor, Dr. Jon Graff, who provides me the precious opportunity to be trained under his guidance in his laboratory. During the past few years, Jon has guided me through all the ups and downs of my career, trained me to be an independent researcher, and taught me everything I know about science. Jon sets a good model for me as a successful scientist who always strives for excellence in science. His passion and love for science and his work ethic have great influence on my scientific career.

I would like to express my deep appreciation to my thesis committee members, Drs. Michelle Tallquist, David Mangelsdorf, Rober Hammer, for whom I have great respect as excellent scientists and great teachers. Their continuous support, encouragement and supervision have guided me through my graduate school years.

I am very grateful to the past and present members in the Graff lab — Ed Fortuno III, Angela Cade, Xiaohuan Gao, Yuan Xu, Kellee Gilmour, Ying Dong, Jim McKay, Renee McKay, Jaemyoung Suh, Jin Seo, Daniel Zeve, Drew Stenesten and Zack Salo. I am fortunate enough to work with such a wonderful group of people, who have helped me in every aspect of my life and career. I will always remember the days I spent with them.

I would like to thank Ms. Shawna Kennedy for her excellent technical support for the FACS work, and to Dr. Mitsu Osawa for his generous help on my research.

I would like to thank all my friends, who make my graduate school years enjoyable and full of happy memories.

My deep gratitude goes to my parents, whose value of education impacts my whole life.

Their love and belief in me have sustained me through times of difficulties.

Most importantly, I would like to thank my husband, Tao Wang, for his unfailing love and patience for me.   He is always there for me whenever I need help, encouragement or comfort. I deeply appreciate all the sacrifice he has made and all the love and joy he has brought to my life.

GENETIC ANALYSIS OF ADIPOSE LINEAGE AND DEVELOPMENT

by

WEI TANG

DISSERTATION

Presented to the Faculty of the Graduate School of Biomedical Sciences

The University of Texas Southwestern Medical Center at Dallas

In Partial Fulfillment of the Requirements

For the Degree of

DOCTOR OF PHILOSOPHY

The University of Texas Southwestern Medical Center at Dallas

Dallas, Texas

June, 2008

GENETIC ANALYSIS OF ADIPOSE LINEAGE AND DEVELOPMENT

Wei Tang, Ph.D.

The University of Texas Southwestern Medical Center at Dallas, 2008

Supervising Professor: **Jonathan M. Graff, M.D., Ph.D.**

Adipose tissues protect against traumatic and thermal insults, and regulate lifespan, reproduction and metabolism. The importance of forming the appropriate number of adipocytes is highlighted by the significant metabolic disturbances that accompany too few (lipodystrophy) or too many (obesity) adipocytes. Most of our current understanding about adipocyte formation comes from *in vitro* culture studies. Little is known about adipose development *in vivo* because of the lack of genetic tools. To this end, I generated a few knock-in mice that offer both spatial and temporal controls to manipulate gene expression in adipose tissues. Here I demonstrate the application of one of the tools, PPARγ-tTA, in exploring some important aspects of

adipose development, such as the adipose depot specification, the identity of adipocyte progenitor cells and their anatomical niche.

Adipose tissues form throughout the body in various places in a stereotypical pattern, with each adipose depot displaying distinctive properties. As the first step to understand depot specificity, I used the PPARγ-tTA mice for lineage tracing on adipose tissues, and found that each adipose depot is specified at very distinctive developmental stages, suggesting that different adipose depots are derived from distinct origins.

With new genetic tools, I also marked and isolated adipogenic progenitors. I found that the majority of adipocytes descend from a pool of PPARγ-expressing proliferating progenitors already committed early in post-natal life, prior to the development of most adipocytes. These progenitors are morphologically and molecularly distinct from adipocytes, have high potential to undergo adipogenesis both *in vitro* and *in vivo* after transplantation. Interestingly, some progenitors reside in the mural cell compartment of blood vessels that supply adipose depots and not in vessels of other tissues. The identification of the adipocyte progenitor and localization to the blood vessel wall indicate the presence of a vascular niche in adipose development and provide a basis to examine the interplay between adipogenesis and angiogenesis that could be exploited as a new avenue for obesity and diabetes therapies.

TABLE OF CONTENTS

Chapter I

**Generation and Characterization of Genetic Tools
for Adipose Lineage Studies**   1

Chapter II

Lineage Tracing on Adipose Tissues Using the PPARγ-tTA Tool   34

Chapter III

Chapter IV

VITAE

LIST OF PUBLICATIONS

1. Tang W., Sun X., Fang J.S., Zhang M. and Sucher N.J. (2004) Flavonoids from Radix Scutellariae as potential stroke therapeutic agents by targeting the second postsynaptic density 95 (PSD-95)/disc large/zonula occludens-1 (PDZ) domain of PSD-95. Phytomedicine. 11(4):277-84.

2. Tang W., Zeve D., Suh J.M., Bosnakovski D., Kyba M., Tallquist M. and Graff J.M. (2008) Adipogenic progenitors reside in the adipose vasculature. (Submitted)

LIST OF FIGURES

LIST OF TABLES

LIST OF ABBREVIATIONS

aP2   adipocyte P2

ACC1   acetyl-CoA carboxylase 1

ACSL1   acyl-CoA synthetase long-chain family member 1

APC   anti-allophycocyanin

ATGL   adipose triglyceride lipase

ATP   adenosine 5'-triphosphate

BAT   brown adipose tissue

BCA   bicinchoninic acid

bFGF   basic fibroblast growth factor

BMI   body-mass index

BrdU   5-bromo-2-deoxyuridine

CCLR   Cell Culture Lysis Reagent

cDNA   complementary DNA

C/EBP   CCAA/enhancer-binding protein

CKI   casein kinase I

CMV   Cytomegalovirus

DAPI   4',6-diamidino-2-phenylindole

DMEM   Dulbecco's Modified Eagle's Medium

DNase   Deoxyribonuclease

Dox   Doxycycline

ER	estrogen receptor
ES	embryonic stem
FACS	fluorescence-activated cell sorting
FAS	fatty acid synthase
FBS	fetal bovine serum
GATA	GATA-binding protein
GFP	green fluorescent protein
GSK	glycogen synthase kinase
GWAT	gonadal white adipose tissue
HEK	human embryonic kidney cell line
HSL	hormone-sensitive lipase
H&E	hematoxylin and eosin
ICC	Immunocytochemistry
IHC	Immunohistochemistry
IL-6	interleukin-6
ISWAT	interscapular white adipose tissue
IWAT	inguinal white adipose tissue
KI	knock-in
lacZ	β-D-galactosidase
LBD	ligand binding domain
LPL	lipoprotein lipase
MCP	macrophage capping protein
MMP	matrix metalloproteinase
MWAT	mesenteric white adipose tissue

MMLV	Moloney murine leukemia virus
NG2	chondroitin sulfate proteoglycan
NMR	nuclear magnetic resonance
PAI-1	plasminogen activator inhibitor-1
PBS	phosphate-buffered saline
PCR	polymerase chain reaction
PDGFRβ	platelet-derived growth factor receptor β
PE	Phycoerythrin
PECAM	platelet/endothelial cell adhesion molecule 1
PPARγ	peroxisome proliferators-activated receptor γ
PPARγ-GFP	PPARγ-tTA; tetO-Cre; R26R
PPARγ-R27R	PPARγ-tTA; tetO-H2B-GFP
Pref-1	preadipocyte factor-1
PWAT	perirenal white adipose tissue
qPCR	quantative polymerase chain reaction
R26R	ROSA26 reporter
RNA	ribonucleic acid
rtTA	reverse tetracycline-controlled transactivator
RWAT	retroperitoneal white adipose tissue
SEM	standard error of the mean
SMA	smooth muscle actin
Smo	Smoothened
SV	stromal-vascular

SVF	stromal-vascular fraction
SVP	stromal-vascular particulate
TNF-α	tumor necrosis factor-α
TRE	tet-response element
tTA	tetracycline-controlled transactivator
TZD	Thiazolidinedione
UCP-1	uncoupling protein-1
VEGF	vascular endothelial growth factor
WAT	white adipose tissue
WHR	waist-hip ratio
Wisp2	Wnt-1-inducible signaling parthway protein-2
WT	wild-type

Chapter I

Generation and Characterization of Genetic Tools

for Adipose Lineage Studies

Abstract

Adipose tissue protects against traumatic and thermal insults, and plays an important role in regulating metabolism, lifespan, and reproduction. Most of our current understanding about adipogenesis comes from *in vitro* culture studies. Surprisingly little is known about adipose development *in vivo* because of the lack of genetic tools. Here I report the generation of three strains of knock-in mice: PPARγ-tTA, PPARγ-rtTA and aP2-CreER^{T2}. One of the strains, PPARγ-tTA, displays high tTA activity specifically in adipose tissues, and this activity can be efficiently suppressed by doxycycline (Dox). These genetic tools offer both spatial and temporal controls to manipulate gene expression, which would expand the scope of our study to explore various aspects of fat biology, including development, function and pathology.

Introduction

Adipose Tissue and Metabolism

Adipose tissue is the connective tissue composed mainly of adipocytes. Adipose tissue stores excess energy in the form of fat, and thus helps organisms to survive during periods of feast and famine. Adipose tissue has long been considered a passive storage place for fat until the groundbreaking discovery of the first adipose-secreted factor, leptin, in 1994 (Zhang et al., 1994). Mice deficient in leptin displayed severe hyperphagia, obesity and diabetes. Leptin was shown to be secreted by adipose tissue and to regulate food intake and energy expenditure (Friedman and Halaas, 1998). With research on fat biology growing exponentially thereafter, adipose tissue is now recognized as an endocrine organ that actively regulates metabolism, energy homeostasis, reproduction and longevity (Bulcao et al., 2006). However, western diets and life style with excess food intake and limited energy expenditure challenge the ability of adipose tissue to maintain a balanced metabolism.

During the past decades, obesity, which is the excessive accumulation of fat to an extent that adversely affects health and longevity (Kopelman, 2000), has risen to be the second leading cause of death and diseases in the United States (Mokdad et al., 2004). A simple and frequently used index to assess body fat is body-mass index (BMI). Today, about 2 out of 3 American adults are overweight (BMI$\geq$25), and 1 out of 3 is obese (BMI$\geq$30) (Ogden et al., 2007). Obesity is not merely a cosmetic problem; more importantly, it is closely associated with a panel of metabolic syndromes, such as hyperlipidemia, hyperinsulinemia, type 2 diabetes mellitus, hypertension, and cardiovascular diseases (Kopelman, 2000). For example, a 15-lb increase in body weight will increase the risk of diabetes by 50%; conversely, losing 11-lb will reduce the

risk of diabetes by 50% (Daniels, 2006). In fact, the extent of individual level of obesity has been routinely used as an important predictor of decreased longevity (Kopelman, 2000).

To attempt to combat obesity, much research has been carried out to understand how adipose tissue works. When caloric intake exceeds energy expenditure, adipose tissues store the excess energy in the most efficient form—lipids. Dietary fat enters the bloodstream in the form of chylomicrons, and in response to elevated insulin, adipose tissue absorbs and stores the lipids in the form of triglycerides (Nelson and Cox, 2000). In times of restrictive caloric intake, adipose tissue releases free fatty acids into the circulation to provide lipid fuel to other parts of the body (Nelson and Cox, 2000). Besides its central role in lipid metabolism, adipose tissue also actively participates in glucose metabolism and is well recognized for its endocrine function (Avram et al., 2005). White adipose tissue (WAT) communicates extensively with the central nervous system and peripheral tissues by secreting a variety of factors, collectively called adipokines, into the humoral system. The wide spectrum of adipokines reflects the variety of activities that WAT regulates, such as immune response (e.g. MCP-1, TNF-α, IL-6), energy homeostasis (e.g. leptin), glucose and lipid metabolism (e.g. adiponectin, retinol binding protein) and vascular function (e.g. VEGF, PAI-1, angiotensinogen) (Trayhurn et al., 2006).

Obesity reflects the severe disturbance of metabolism and energy homeostasis. Excess or dysfunction of adipose tissue results in high level of lipids circulating in the bloodstream (hyperlipidemia), and inappropriate deposition of lipids in organs such as muscle and liver, which are important for glucose metabolism. The lipid toxicity then causes insulin resistance within muscle and liver, eventually resulting in diabetes. The excess lipids circulating in the bloodstream can also deposit on the blood vessel wall and form plaques, leading to atherosclerosis. Moreover, too much adipose tissue will release excess hormones and

proinflmmatory cytokines, many of which are known to directly induce insulin resistance in the whole organism and lead to diabetes (Daniels, 2006; MacDougald and Mandrup, 2002).

Adipose Development

Given the importance of adipose tissue in metabolism, surprisingly little is known about adipose development *in vivo*. During adipose development, adipose tissue enlarges by proliferation and accumulating more lipids in adipocytes. Then adipose tissue reaches a plateau where it can only expand by increasing in size (Bjorntorp, 1974). However, adipocytes cannot grow in size infinitely. As obesity progresses, growth in adipose tissues generally involves both growth in cell size (hypertrophy) and cell number (hyperplasia) (Hausman et al., 2001). So to know the source of proliferation and the mechanism underlying proliferation control will help us combat obesity. How do adipocytes form during adipose development? How is proliferation in adipose tissue regulated? What are the progenitors for adipocytes? What are the dynamics of progenitors and how are they regulated during development and obesity? What is the niche for progenitors? All of these questions fundamental to adipose development remain unanswered. Understanding the molecular mechanism of adipose development would open up possible avenues for battling obesity.

It has long been postulated that in adipose tissue, mesenchymal stem cells give rise to early progenitors called adipoblasts, which in turn give rise to committed preadipocytes that eventually differentiate into mature adipocytes under appropriate stimuli (Ailhaud et al., 1992; Gesta et al., 2007). However, no morphological characteristics or molecular markers were ever found to clearly identify any of these speculative populations. Therefore, the *in vivo* developmental steps prior to adipocyte formation remain a mystery.

The differentiation process from preadipocytes to mature adipocytes has been studied extensively using cell culture models, contributing to most of our current knowledge on adipogenesis. In 1970s, Green and colleagues established immortal preadipocyte cell lines (3T3-L1 and 3T3-F442A) from mouse embryonic fibroblasts (Green and Kehinde, 1975, 1976); these preadipocytes rapidly accumulate lipid and differentiate into adipocytes upon induction with insulin and glucocorticoids. The establishment of cell culture models greatly facilitates the study on adipogenesis. During *in vitro* adipogenesis, cells are grown to confluence and undergo growth arrest due to contact inhibition. Adipogenic inducers are then added, which in turn induce one or two rounds of cell division, known as "clonal expansion", before activation of the transcriptional program. The cells then go through early differentiation and then terminal differentiation, becoming lipid-laden adipocytes (Rangwala and Lazar, 2000). The *in vitro* cell culture models can recapitulate some of the characteristics of adipocyte differentiation *in vivo*. For example, 3T3-L1 cells, when injected into mice, differentiated and formed fat pad which was indistinguishable from normal adipose tissues (Green and Kehinde, 1979). Some of the *in vitro* findings have been successfully translated to the *in vivo* system, such as the central role of PPARγ in adipogenesis and the inhibitory effect of Wnt signaling on adipogenesis (Farmer, 2006; Ross et al., 2000; Lazar, 2005). However, the cell culture models are still considered oversimplified (MacDougald and Mandrup, 2002). For example, the inducers used in cell culture are at much higher concentration than the physiological condition. Some genes displayed differential effects *in vitro* and *in vivo* (Tanaka et al., 1997). The growth arrest due to contact inhibition and the subsequent clonal expansion might be specific for cell culture system and not occur *in vivo*. Moreover, the cell culture model cannot reflect the differential characteristics of various adipose depots, which has significant physiological relevance (see

Chapter II). Therefore, it is necessary to seek the answers to developmental questions *in vivo*, within the context of the whole organism during development.

Lineage Tracing in Adipose Tissue

One potential approach to identify adipocyte progenitor cells is to perform lineage tracing in adipose tissues. Lineage tracing specifically and irreversibly labels a population of cells expressing a marker for a certain lineage during development, and traces the fate of these labeled cells at a later stage. Two components are indispensable to lineage tracing: a spatially and temporally controlled gene manipulation system expressed under a lineage specific promoter, and an indelible marker.

However, the adaptation of this approach to adipose lineage is limited by the lack of genetic tools. In the field of fat biology, the only available tool is the aP2-Cre transgenic strain. aP2 is one of the terminal differentiation genes. Transgenic aP2-Cre has often been used as an adipose-specific deleter to study gene function specifically in adipose tissue, but in reality, aP2 has been reported to have a broader expression pattern, such as in macrophages (Makowski et al., 2001). So if gene functional studies rely solely on this tool, the resulting phenotypes could potentially be complicated by effects in other tissues. Also, there are some intrinsic problems associated with transgenic mice. For example, the expression pattern is affected by the fidelity of the promoter used; the positional effect of transgenic strains has to be vigorously tested. These problems associated with aP2-Cre trangenics are highlighted by the fact that two studies, using independently generated aP2-Cre transgenic mice to delete PPARγ in adipose tissues, produced surprisingly different results. When challenged with high-fat diet, the fat-specific PPARγ deficient mice from the Evans Lab showed severe insulin resistance while the mice from

the Magnuson Lab showed improved insulin sensitivity (Jones et al., 2005; He et al., 2003). The lack of temporal control of aP2-Cre was circumvented by the generation of an aP2-CreER[T2] transgenic strain (Imai et al., 2004). However, the problems associated with transgenic mice remain. Therefore, it is imperative to generate new complementary adipose-specific tools for developmental and functional analysis. By comparing and contrasting the phenotypes from using the existing aP2-Cre lines and the new tools, any adipose-specific effects could be easily dissected out. For these reasons, I decided to generate new genetic tools using gene targeting technology to facilitate my studies on adipose development.

In search for the appropriate driver for adipose-specific genetic tools, I examined the genes currently available. aP2, the commonly used adipose driver, is a terminal differentiation gene. Its expression does not peak until the adipocytes are mature (Jones, 2005). If aP2 is used as a driver, the phenotypes could be milder than expected due to its late expression. I therefore examined more upstream genes in the adipogenesis hierarchy. Pref-1 (preadipocyte factor1), a widely accepted marker for preadipocytes, has broad expression in a variety of embryonic tissues and adult organs (Villena et al., 2002), which excludes its usefulness as a lineage marker. PPARγ, with its high expression in adipose tissues and critical roles in adipose lineage determination, stood out as an attractive candidate.

PPARγ and Adipogenesis

In 1994, Spiegelman and colleagues discovered that peroxisome proliferators-activated receptor γ (PPARγ), a nuclear hormone receptor, can potently stimulate unspecific fibroblast cells into lipid-laden adipocytes (Tontonoz et al., 1994). Since then, PPARγ has been shown to be the master regulator of the adipogenic program. In cell culture, upon hormonal induction, the

transcription factors C/EBPβ and C/EBPδ are induced, and in turn activate PPARγ and

C/EBPα (Ntambi and Young-Cheul, 2000). In a positive feedback loop PPARγ and C/EBPα

promote the expression of each other to a level that induces downstream differentiation genes

(Ntambi and Young-Cheul, 2000), causing cells to differentiate and become lipid-laden

adipocytes. This transcriptional cascade is depicted in Figure 1.1. Although PPARγ and

C/EBPα are at the center of adipogenic program, PPARγ seems to be dominant (Gesta et al.,

2007). PPARγ is necessary and sufficient for *in vitro* adipogenesis and also plays an essential *in*

vivo role (Farmer, 2006; Lazar, 2005).
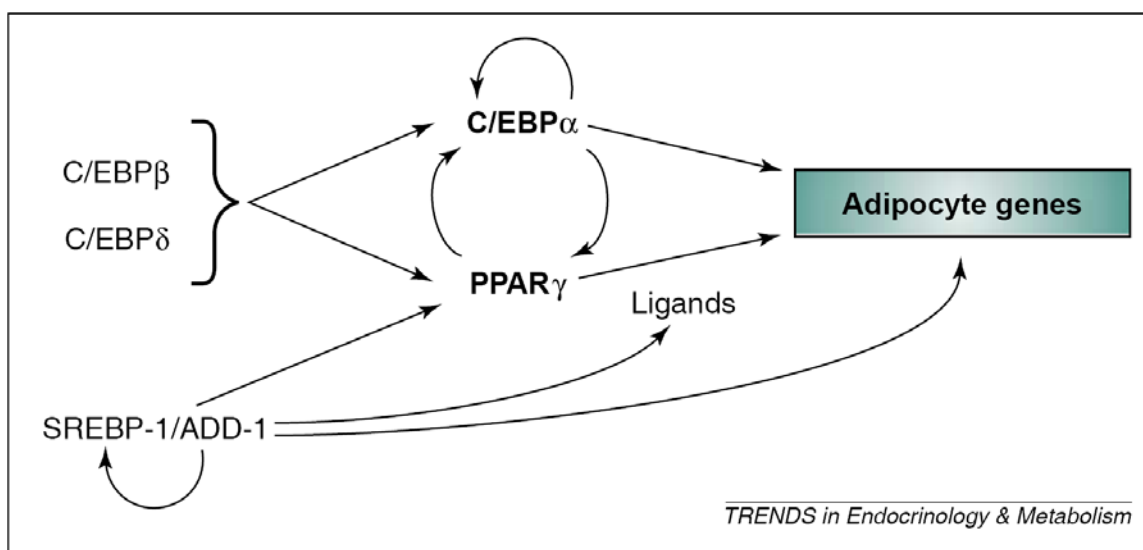
Figure 1.1. The transcriptional cascade in adipocyte differentiation. (Adapted from MacDougald and Mandrup, 2002) (See the text for detail.)

PPARγ has two isoforms, PPARγ1 and PPARγ2, which share the majority of the coding

sequence but have different amino termini due to alternative splicing (Tontonoz et al., 1994).

Each isoform has its individual promoter and 5'-untranslated region, and PPARγ2 has additional

30 amino acids at the amino terminus of the PPARγ1 ATG start codon (Tontonoz et al., 1994).

PPARγ was shown to express predominantly in adipose tissues, the expression of which is at least 20 times higher than in other tissues (Tontonoz et al., 1994). PPARγ-lacZ knock-in mice have been generated that disrupt both PPARγ1 and γ2 (Barak et al., 1999). Based on lacZ reporter expression, PPARγ displays an adipose-restricted expression, suggesting that this PPARγ knock-in strategy could be useful to drive expression specifically in adipose tissues. However, PPARγ knock-in mice seem to have some haploinsufficiency effects. PPARγ null mice have been shown to be embryonic lethal due to placental defects and an epiblast-specific deletion of PPARγ results in mice nearly devoid of any adipose tissue and with severe diabetes (WT, JMG, unpublished data). However, PPARγ heterozygous mice do not display any abnormality in either adipose tissue or metabolism under a standard diet, but are resistant to high-fat diet-induced obesity (Kubota et al., 1999). So PPARγ heterozygous mice should still be useful for studying adipose development and gene function. However, when metabolic phenotyping is involved, especially under high-fat diet conditions, PPARγ haploinsufficiency should be taken into consideration, and proper controls should be included to control for the potential haploinsufficiency effects produced by PPARγ heterozygosity.

Tet System and Inducible Cre System

The Tet and inducible Cre systems are the most widely used transcription control systems. In the Tet-off system, tTA (tetracycline-controlled transactivator) binds to the tetO promoter and activates downstream gene expression; the presence of doxycycline (Dox) prevents the binding of tTA to the tetO promoter and therefore abolishes the gene expression. The Tet-on system is complementary to the Tet-off system where rtTA (reverse tetracycline-controlled transactivator) requires Dox to bind to the tetO promoter and activate downstream gene expression. The Tet

systems offer some unprecedented advantages, making them a popular system to use. Tet systems provide low background, high activity, and high sensitivity to Dox (1-5ng/ml for tTA, 50-100ng/ml for rtTA) (Gossen and Bujard, 2002). Dox has been widely used in humans and animals for decades, and it has high tissue and cell penetration allowing the effective dosage to be easily reached. Also, it can be delivered to embryos through the placenta and to pups through milk (Gossen and Bujard, 2002). Therefore, it is particularly suitable for embryonic studies which are important for lineage tracing. For these reasons, I chose the Tet systems to generate the adipose-specific gene manipulation tools.

Inducible Cre is another widely used system. Cre recombinase is fused to the mutated ligand binding domain (LBD) of human estrogen receptor (ER), and sequestered to the cytoplasm (Imai et al., 2001). Upon binding of the appropriate ligand to the ER LBD, Cre is transported to the nucleus where it causes site-specific recombination between direct repeats of *loxP* sites. CreER^{T2} has been successfully applied to the analysis of adipose tissues with the aP2-CreER^{T2} transgenic mice (Imai et al., 2001). To circumvent the potential problems associated with transgenics, I decided to generate an aP2-CreER^{T2} knock-in strain. aP2 knock-out mice have been shown to be developmentally and metabolically normal (Hotamisligil et al., 1996), so haploinsufficiency should not affect aP2-CreER^{T2} knock-in heterozygous mice.

Here I report the generation of three strains of knock-in mice: PPARγ-tTA, PPARγ-rtTA and aP2-CreER^{T2}. One of the strains, PPARγ-tTA displays high tTA activity in an adipose-restricted manner, which can be efficiently suppressed by doxycycline. These genetic tools offer both spatial and temporal controls to manipulate gene expression, which will expand the scope of our study to explore various aspects of fat biology, including development, function and pathology.

Results

***In vitro* Testing of PPARγ-tTA/rtTA Fusion Activity**

The preexisting PPARγ-lacZ knock-in mice successfully disrupted the PPARγ allele while lacZ reproduced the expression pattern of endogenous PPARγ (Barak et al., 1999).   So I decided to adopt this strategy to generate the KI mice (Figure 1.2).
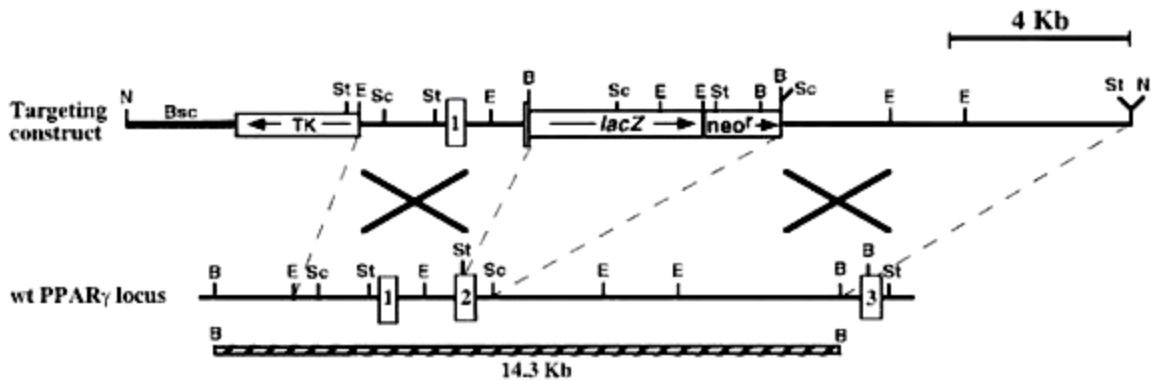
Figure 1.2.   PPARγ targeting strategy. (Adapted from Barak et al., 1999)
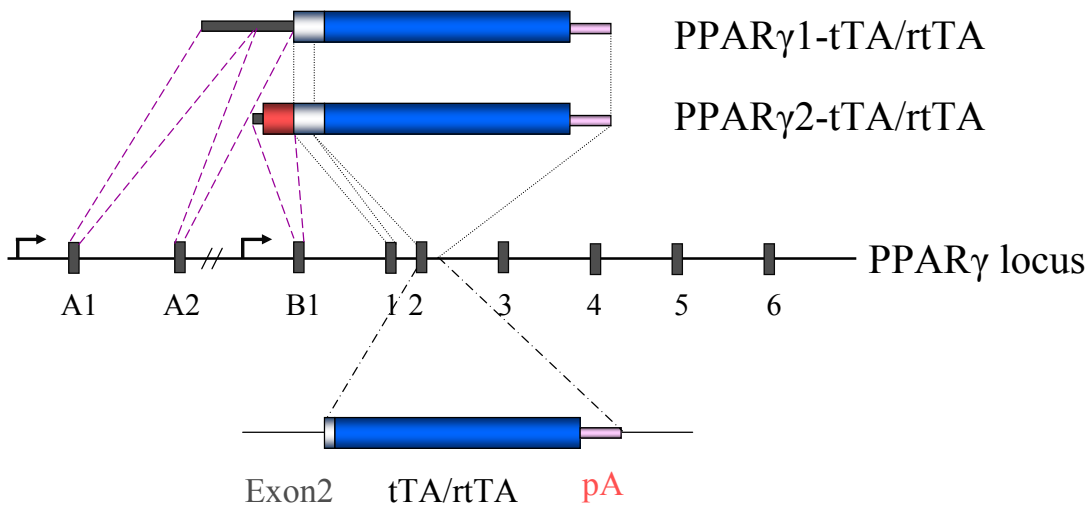
Figure 1.3.   Gene products from PPARγ-tTA/rtTA knock-in targeted allele. (See the text for detail)

Using this knock-in strategy, part of exon 2 was replaced with tTA or rtTA. The products expressed from PPARγ promoters will be a short fragment of PPARγ1 or PPARγ2 fused to tTA or rtTA (Figure 1.3). The fusion protein might not necessarily fold or function properly. Before making the KI mice it was imperative to test whether the fusion tTA and rtTA could still turn off or turn on gene expression in a Dox-dependent way.

To test the fusion proteins *in vitro*, I cloned the fusion fragments under a CMV promoter. Several nonsense mutations have to be introduced into tTA to facilitate making of the targeting construct, so I included the same mutations into the test constructs. I co-transfected these test constructs along with a TRE-luciferase (*firefly*) reporter into Hela cells. Then I treated the cells with Dox or without Dox and measured the luciferase activity. The transfection efficiency was controlled by a co-transfected *Renilla* luciferase construct. The *firefly* luciferase activity was normalized against *Renilla* luciferase.
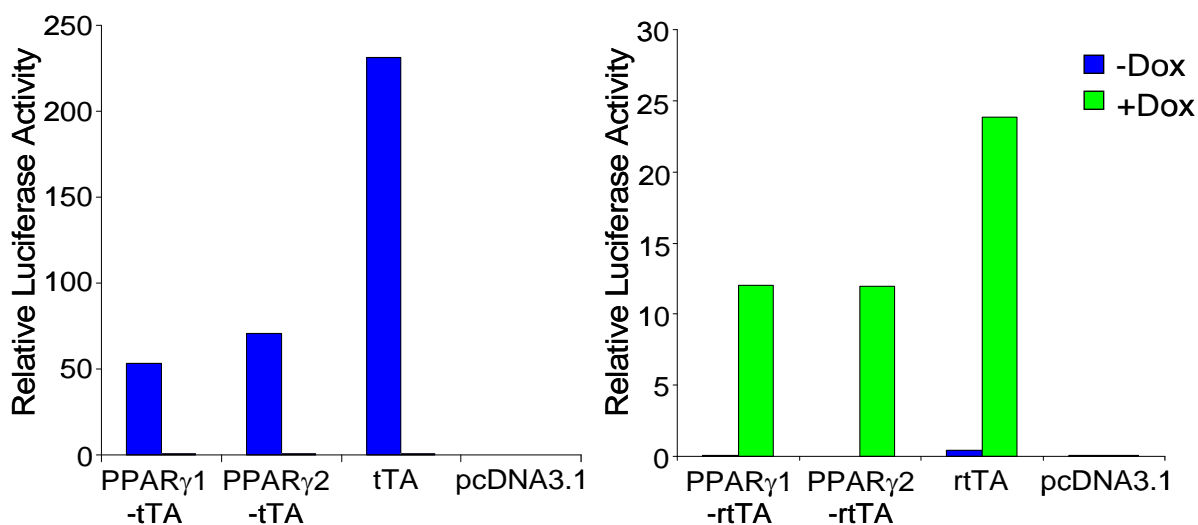
Figure 1.4. tTA and rtTA fusions have reduced activity. Original constructs (tTA and rtTA) and fusion constructs were co-transfected into NIH3T3 cells along with a TRE-luciferease reporter and *Renilla* luciferase plasmid, and the cells were cultured in the absence (blue bars) and presence (green bars) of doxycycline (Dox). pcDNA3.1(-) served as a negative control. Luciferase activity was measured and normalized against *Renilla* luciferase activity.

Consistent with the literature, tTA is active in the absence of Dox and suppressed by Dox, whereas rtTA is activated only in the presence of Dox (Gossen and Bujard, 2002). When activated, tTA is about 10 times more active than rtTA; at the same time tTA also displayed much lower background activity than rtTA (Figure 1.4).

The activity of fusion tTAs (PPARγ1-tTA and γ2-tTA) was reduced 70% compared to the intact tTA (Figure 1.4). Importantly, fusion tTAs were completely suppressed by Dox. Given the high activity of tTA (compared to rtTA), a 70% reduction could still be useful to drive target gene expression. Fusion rtTAs (PPARγ1-rtTA and γ2-rtTA), when induced by Dox, were reduced 40% compared to the intact rtTA (Figure 1.4). However, the background activity (in the absence of Dox) of fusion rtTAs was also much lower compared to the intact rtTA. Together, these results suggest that the fusion forms partially maintain activity and remain responsive to Dox. So I decided to make the targeting constructs.

Generation of PPARγ-tTA (rtTA) Knock-in Mice

I digested out the lacZ-Neo fragment from the original targeting constructs. Besides replacing the original lacZ with tTA or rtTA, I replaced the original PGKNeo cassette with another PGKNeo cassette flanked by FRT sites with the notion that I could easily remove the Neo cassette later on when necessary, which has been reported to affect neighboring gene expression in some cases (Pham et al., 1996). Removing the Neo cassette was later shown to be critical for the usefulness of the tools.

In screening for targeting events by Southern blot, I got 10 positive clones out of 600 clones. After confirming the recombination using both 5' and 3' arm (Figure 1.5), two clones were injected into blastocysts to generate chimeric mice. Germline transmission was confirmed

for both PPARγ-tTA and PPARγ-rtTA.
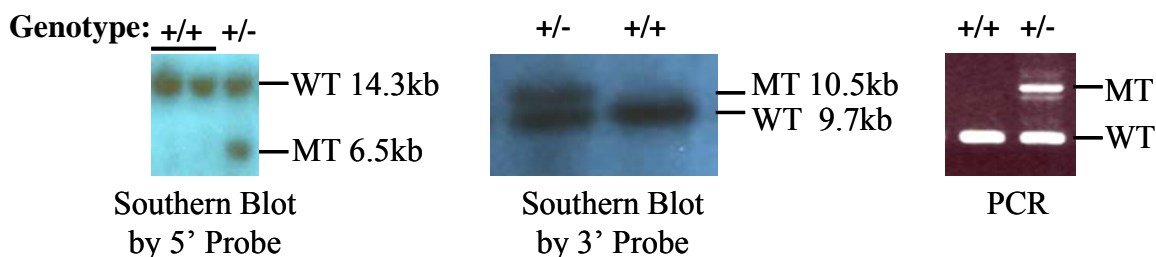
Figure 1.5.   Southern blots and PCR identified the PPARγ-tTA (rtTA) targeted allele. Southern blots were performed on ES cell clones after electroporation and selection. PCR genotyping was performed on tail biopsies to confirm germline transmission and identify progeny carrying the targeted allele.   The wild-type (WT) and mutant (MT) bands and the corresponding sizes are as indicated.   PPARγ-tTA and PPARγ-rtTA gave the same pattern, so only the PPARγ-tTA results are shown.

Characterization of PPARγ-tTA Knock-in Mice

Removal of Neo cassette improves the expression pattern

To test the usefulness of the system, I bred the PPARγ-tTA KI mice with reporter mice containing tetO-Cre; ROSA26-flox-stop-flox-LacZ (R26R for ROSA26 reporter) (Soriano, 1999; Yu et al., 2005). In the cells that express PPARγ, Cre expression is driven from tetO promoter, and the stop cassette upstream of β-galactosidase in ROSA26 locus, which is flanked by *loxP* sites, will be permanently deleted, and these cells will express β-galactosidase from ROSA26 locus, which expresses ubiquitously in almost every tissue (Soriano, 1999).   I examined the adult adipose tissues directly for β-galactosidase activity (Figure 1.6).   The adipose depots I examined were inguinal, interscapular, gonadal, mesenteric and retroperitoneal white adipose tissues.   These adipose depots are the white adipose tissues with well-defined shapes and locations in mice, as shown in Figure 2.1.   I found that every adipose depot was stained blue. However, the staining was not homogenous across the various depots.   For example, in gonadal

WAT, there was only some patchy staining.   This was unexpected because PPARγ-lacZ staining revealed a homogenous pattern (Barak et al., 1999).   To test whether the reporter tetO-Cre; R26R was responsible for this phenomenon, I bred the mice to another reporter, tetO-H2B-GFP (Tumbar et al., 2004).   Although it was more difficult to observe the patchy pattern, PPARγ-tTA; tetO-H2B-GFP also gave the similar depot-specific variation in GFP intensity (not shown).   So the defects I observed most likely resulted from PPARγ-tTA.

One way to possibly improve this PPARγ-tTA tool was to remove the Neo cassette in case it was affecting neighboring gene expression.   To determine if this was the case, I removed the Neo cassette by breeding the mice with Flipper (ROSA26-FLP) mice.   In these mice, the FLP recombinase (identified in flies) was knocked into the ROSA26 locus to achieve a ubiquitous expression of FLP (Farley et al., 2000), especially in germ cells.   Once the FRT flanked gene was bred together with ROSA26-FLP, recombination occurred between direct repeats of FRT sites so that the FRT flanked cassette was removed by FLP.   This deleted form was then passed onto the descendents through germ cells.   I removed the ROSA26-FLP allele from the progeny by selecting against this allele, and bred the desired mice to the reporters.   Adipose depots from these mice displayed homogeneous and strong X-gal staining without any patchy pattern (Figure 1.6), suggesting that the presence of PGKNeo did affect the neighboring tTA expression/activity by reducing or even blocking tTA expression or activity in some cells in adipose tissues.   Thus the removal of the PGKNeo cassette improved the PPARγ-tTA tool tremendously.   Therefore, I adopted the Neo-deleted version of PPARγ-tTA for my studies.
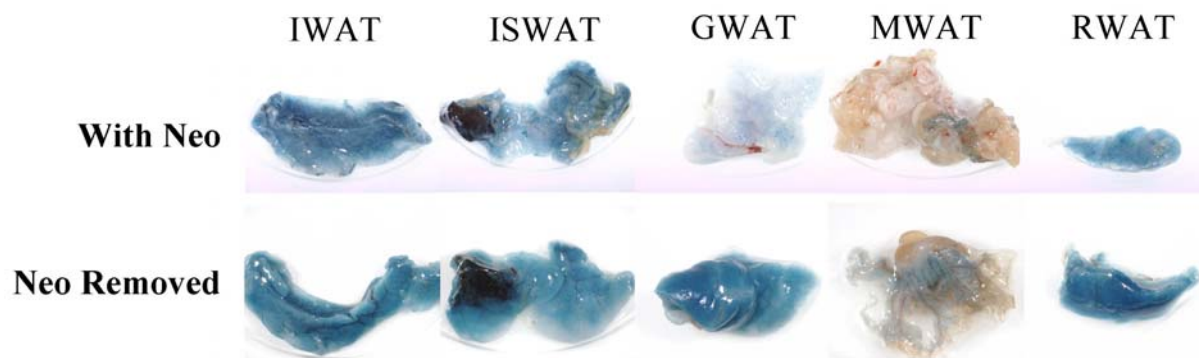
Figure 1.6.   Removal of the Neo cassette from the PPARγ-tTA knock-in allele improved the expression pattern of PPARγ-tTA.   Original PPARγ-tTA mice (with Neo) and PPARγ-tTA mice with Neo removed were bred to the tetO-Cre; R26R reporter, and adipose tissues harvested and stained for β-galactosidase activity (blue).   IWAT: inguinal white adipose tissue; ISWAT: interscapular white adipose tissue; GWAT: gonadal white adipose tissue; MWAT: mesenteric white adipose tissue; RWAT: retroperitoneal white adipose tissue.

Adipose-restricted expression

As described above, I used two sets of reporters to analyze PPARγ-tTA: tetO-Cre; R26R and tetO-H2B-GFP.   In Chapter III, I will describe in detail the properties and usage of each reporter.   Briefly, when tTA activates the tetO promoter, it drives the expression of Cre or H2B-GFP.   Cre will further delete the stop cassette upstream of lacZ in the ROSA26 locus, which drives ubiquitous expression in many tissues, and permanently turns on lacZ expression. I found that the tetO promoter used to drive Cre expression is somewhat leaky (Figure 1.7). Even in the absence of tTA, the combination of tetO-Cre and R26R resulted in some background blue staining in some adipose tissues, such as inguinal WAT.   This leakiness mostly occurred in a small subset of vasculature, but not so much in adipocytes *per se*.   The leakiness of tetO-Cre was particularly severe in subdermal WAT, in which the presence or absence of PPARγ-tTA didn't show any appreciable difference (not shown).   This defect of tetO-Cre reporter excluded the possibility of performing lineage tracing studies in subdermal WAT.   For this reason,

subdermal WAT will not be discussed in the rest of my studies.

To further characterize PPARγ-tTA, the tissue-specific expression pattern should be scrutinized.   So I examined various organs in the PPARγ-tTA; tetO-Cre; R26R mice for reporter expression (Figure 1.7).   Since tetO-Cre; R26R is an indelible marker, the staining pattern is a result of accumulated staining over time.   None of the other organs had a similar level of lacZ expression as adipose tissues (Figure 1.7), which is consistent with the adipose-specific role of PPARγ.   However, the organs examined did have some spotty staining, lung and pancreas being the strongest.   Due to the indelible aspect of the reporter, the staining pattern might not reflect the dynamics of PPARγ expression. So I used the complementary tetO-H2B-GFP reporter, although the intrinsic property of H2B-GFP also limits its ability to mirror PPARγ expression in a timely fashion (see Chapter III for details).   When other whole organs were examined, no obvious GFP was observed, however the adipose tissues were very bright (Figure 1.8), again confirming the predominant adipose-specific expression of PPARγ.   However, when the organs were sectioned and examined carefully for GFP+ signal, some punctate signals were observed (not shown), indicating that PPARγ-tTA does have some scattered expression outside of adipose tissue.   For lineage tracing studies, this non-specific expression might not affect the analysis since adipose lineage is my major focus.   However, we have to be extra careful in terms of interpreting results from functional studies, especially for metabolic phenotypes, because some metabolically active organs, such as muscle, liver and pancreas, do have some scattered expression of PPARγ, which could potentially contribute to the phenotypes observed.
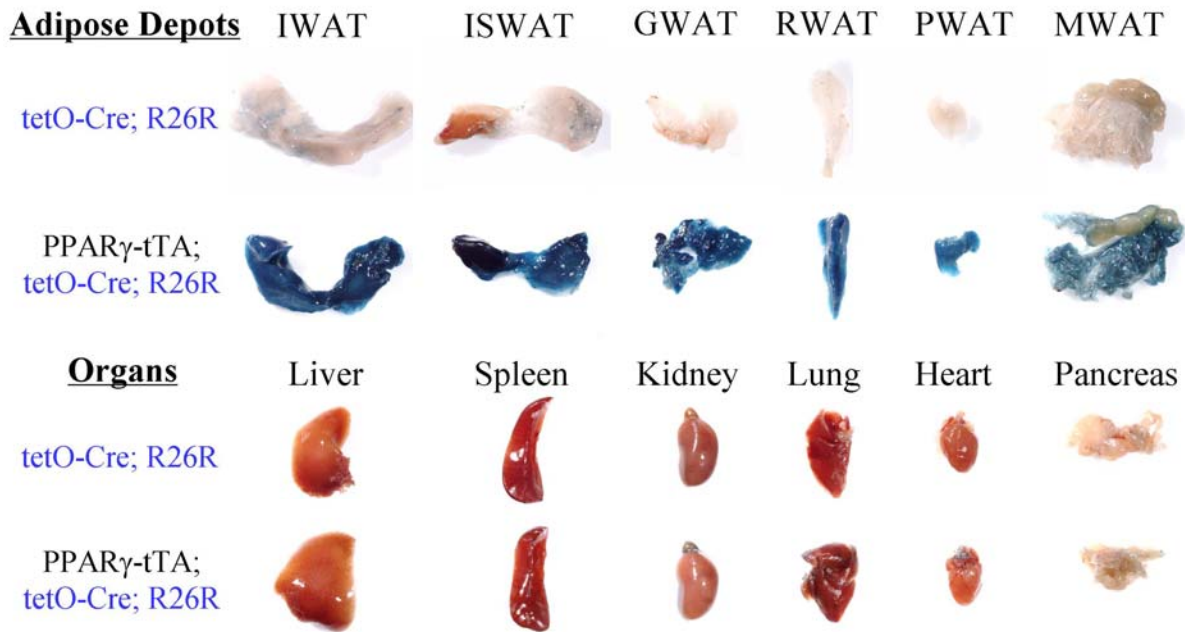
Figure 1.7. PPARγ-tTA displayed adipose-restricted expression (by tetO-Cre; R26R reporter).   Adipose tissues and organs as indicated were harvested from PPARγ-tTA; tetO-Cre; R26R mice and stained for β-galactosidase activity (blue).   PWAT: perirenal white adipose tissue.
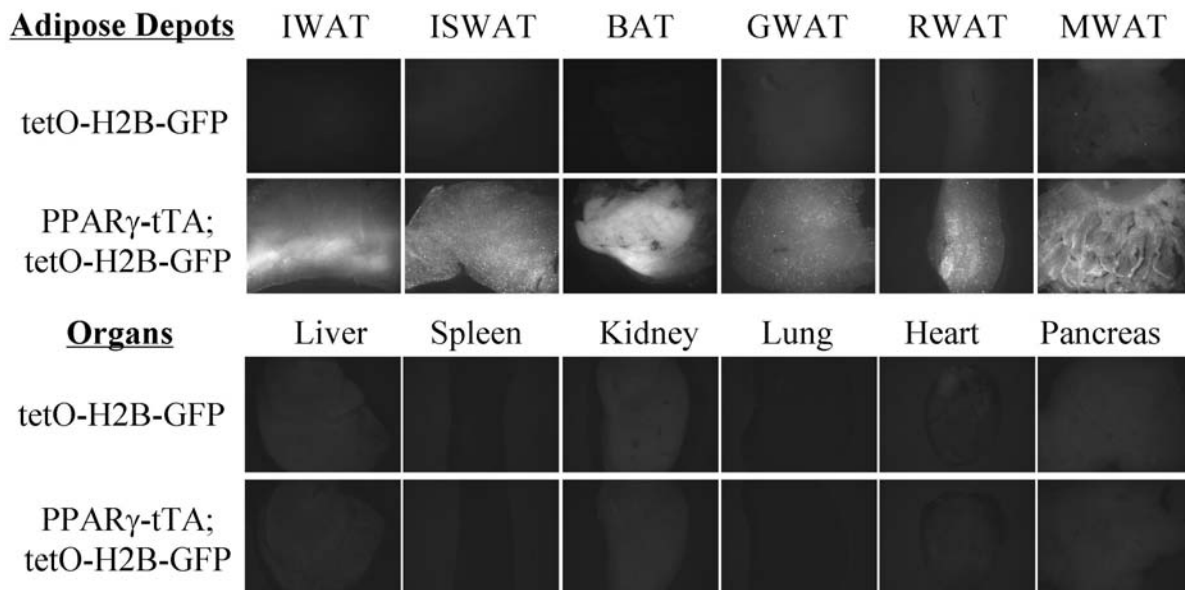
Figure 1.8. PPARγ-tTA displayed adipose-restricted expression (by tetO-H2B-GFP reporter).   Adipose tissues and organs as indicated were harvested from PPARγ-tTA; tetO-H2B-GFP mice and examined for GFP.

Doxycycline-dependent suppression

Next I wanted to examine the inducible aspect of PPARγ-tTA, that is to test how well Dox can suppress tTA activity.   The tetO-Cre; R26R reporter seemed to provide a more stringent test because any trace of activation in the history will be reflected or even amplified at the time of examination.   So I treated PPARγ-tTA; tetO-Cre; R26R with Dox from embryonic day 0 (E0) until postnatal day 30 (P30), and performed X-gal staining on adipose tissues.   When compared to tetO-Cre; R26R control, I did not find any noticeable difference in terms of staining pattern and intensity (Figure 1.9).   TetO-H2B-GFP reporter gave a similar result (Figure 1.9). This suggested that in PPARγ-tTA knock-in mice, tTA can be effectively suppressed by doxycycline, and tTA, when suppressed, does not have any detectable background activity.

In summary, the results suggested that PPARγ-tTA knock-in mice function as expected, displaying strong tTA activity in an adipose-restricted manner which can be effectively suppressed by Dox.   PPARγ-tTA knock-in mice are therefore a useful tool to study adipose lineage and function.

Unfortunately, when I did a similar set of experiments on the PPARγ-rtTA knock-in mice, I could not turn on rtTA activity, as shown by reporter expression, by administering Dox to the mice either by injection or through drinking water.
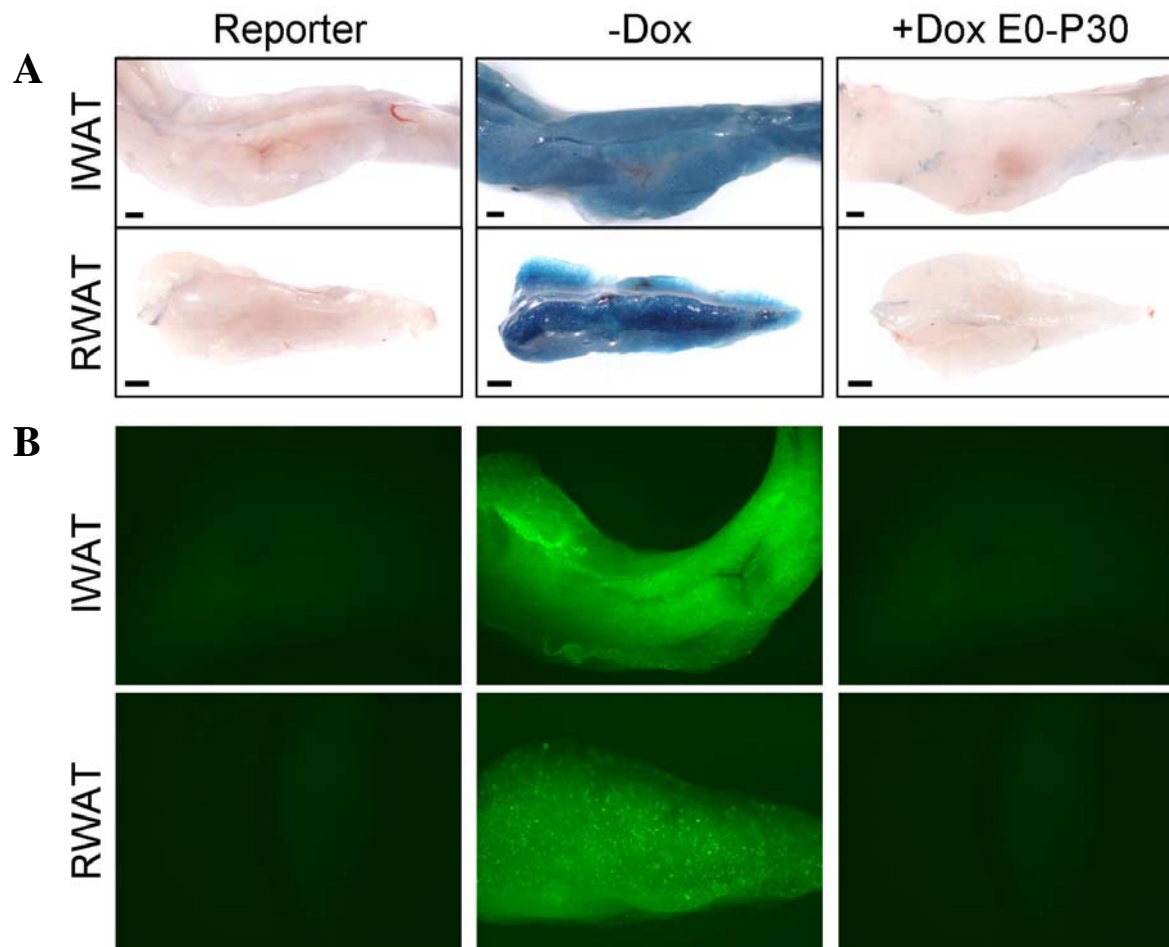
Figure 1.9.   Doxycycline can completely suppress tTA activity in PPARγ-tTA mice.
(A) PPARγ-tTA; tetO-Cre; R26R (PPARγ-R26R) or (B) PPARγ-tTA; tetO-H2B-GFP (PPARγ-GFP) mice were treated from embryonic day 0 (E0) until postnatal day 30 (P30) without or with Dox and then inguinal white adipose tissues (IWAT) and retroperitoneal white adipose tissues (RWAT) were stained for β-galactosidase expression (blue).   Left panels are depots of non-Dox treated mice containing reporter alone.

Generation and Characterization of aP2-CreER^T2 Knock-in Mice

To make the aP2-CreER^{T2} targeting construct, I designed the targeting strategy as shown in Figure 1.10.   I cloned CreER^{T2}-pA with PGK-Neo into the ATG of the aP2 open reading frame flanked by two arms, which were 2.2kb and 2.6kb, respectively.   I electroporated the targeting construct into ES cells and then screened ~1600 clones by Southern blotting using a 5'

external probe. I found 9 positive clones. These clones were further confirmed by Southern

blotting using a 3' probe (Figure 1.11). I picked two clones to generate chimeric mice, and

successful germline transmission was confirmed by PCR. Two independent lines were

generated, and these two lines behaved similarly.
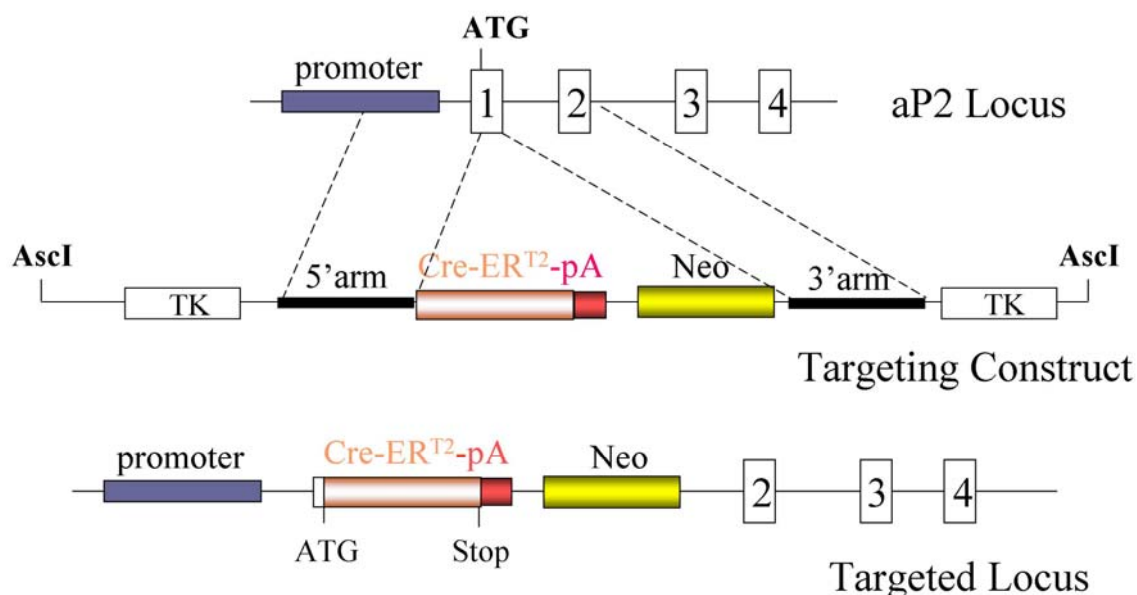
Figure 1.10. Knock-in strategy to generate aP2-CreER^{T2}. (See the text for details.)
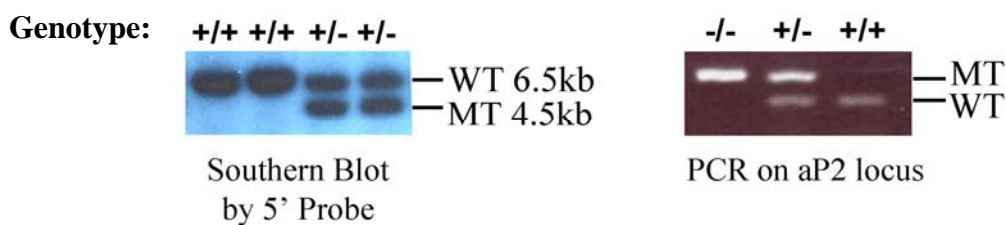
Figure 1.11. Southern blot and PCR identified the aP2-CreER^{T2} knock-in allele. The wild-type (WT) and mutant (MT) bands and the corresponding sizes are as indicated.

I tested the activity of aP2-CreER^{T2} by breeding the mice to the R26R reporter, induced

Cre activity at 1 month old by injecting the mice with tamoxifen for 5 consecutive days.

Adipose tissues were dissected and stained for β-galactosidase activity (Figure 1.12). I found

that at 1mg and 3mg dosage of tamoxifen, Cre activity was successfully induced. In some

depots, induction was dose-dependent while in some other depots, this relationship was less obvious (Figure 1.12).   It suggested that tamoxifen might penetrate differentially into various depots.   However, when the mice were injected with vehicle only, aP2-CreER^{T2}; R26R adipose tissues also displayed some weak background staining, suggesting that aP2-CreER^{T2} is leaky in adipose tissues, although the similar level of leakiness was not reported in other organs (Indra et al., 1999; Li et al., 2000).   This effect could be because aP2-CreER^{T2} is activated stochastically in some adipocytes.   Alternatively, the highly lipophilic feature of adipose tissue, which likely attracts estradiol homologues in the body more efficiently than other organs, might explain the particularly high background activity not reported in other organs.
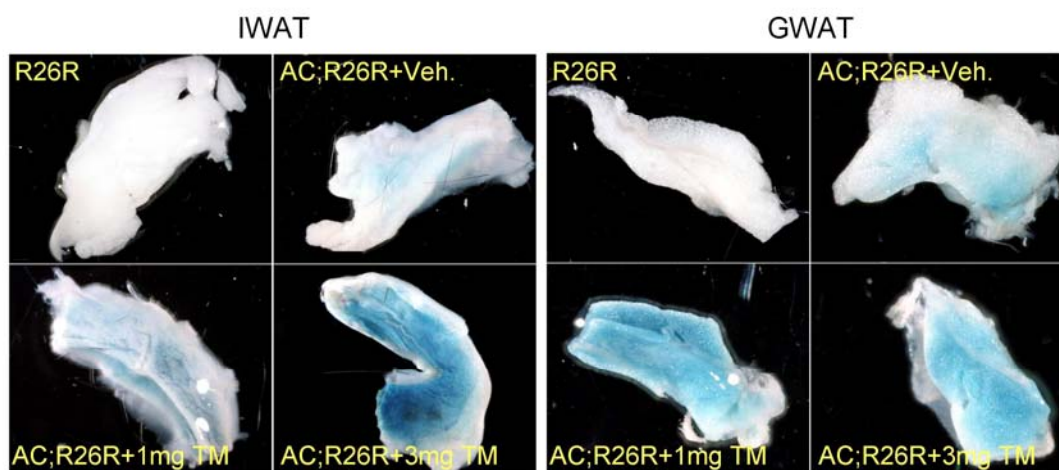
Figure 1.12.   Tamoxifen induced Cre activity in adipose tissues from aP2-CreER^{T2} (AC) knock-in mice.   R26R and aP2-CreER^{T2}; R26R mice were induced by vehicle alone (AC; R26R+Veh.), 1mg tamoxifen or 3mg tamoxifen for 5 consecutive days, and then adipose tissues (IWAT and GWAT) were harvested and stained for β-galactosidase activity (blue).

The leakiness of aP2-CreER^{T2} makes it a less favorable tool, while at the same time, PPARγ-tTA seems to be more advantageous than aP2-CreER^{T2} in many aspects.   Therefore I performed all my following studies using the PPARγ-tTA tool.   However, aP2-CreER^{T2} could be useful as a complementary tool, and it is a nice addition to the field of fat biology.

Discussion

Adipose tissue is an important organ regulating metabolism, lifespan and reproduction. Too much or too little adipose tissue leads to severe adverse health issues. However, little is known about adipose development *in vivo*. Most of our current understanding of adipogenesis comes from *in vitro* culture systems and cannot be directly translated to the *in vivo* organism. The *in vivo* study of adipose development is largely limited by the lack of genetic tools. To fill in this gap, I generated PPARγ-tTA, PPARγ-rtTA and aP2-CreER^{T2} knock-in mice using gene targeting technology. One of the strains, the PPARγ-tTA knock-in mouse, has strong tTA activity in an adipose-restricted manner that is completely suppressed by Dox. Unfortunately, PPARγ-rtTA cannot be successfully induced to turn on reporter expression. aP2-CreER^{T2}, however, can be induced in adipose tissues by tamoxifen, although it does have some background activity in the absence of induction.

PPARγ-tTA, with its high expression, low background and inducibility, together with the good pharmacological kinetics of Dox, is a useful tool for adipose lineage, development, and functional studies. The use of the PPARγ driver, which is upstream of aP2, allows us to examine the behavior of a putative population potentially more primitive than differentiated aP2-expressing adipocytes. By comparing and contrasting the PPARγ and aP2 driver lines, the effects from this putative population and the adipocyte population could be separated, and any adipose-unspecific effect associated with the driver could possibly be dissected out.

In the following chapters, I will discuss some usages of the PPARγ-tTA tool, which brought us novel perspectives toward adipose lineage specification, proliferation and maintenance. I will briefly touch upon one functional study using this tool. Molecular

regulation of adipose tissue is another important research area, which will benefit tremendously from access to a few complementary genetic tools (such as aP2-Cre, aP2-CreER^{T2}, PPARγ-tTA).

Materials and Methods

Plasmids

pTet-Off and pTRE-luciferase were from Clontech. prtTA2S-M2 was a generous gift from Wolfgang Hillen. Nonsense mutations ($G_{768} \rightarrow A_{768}$, $C_{774} \rightarrow A_{774}$, $C_{777} \rightarrow G_{777}$) were introduced to tTA sequence by site-directed mutagenesis (Promega). $\gamma 1$ fragment (95aa) and $\gamma 2$ fragment (125aa) were fused to rtTA and mutated tTA, respectively. The fusion fragments were then cloned into XhoI-BamHI sites in pcDNA3.1(-) for testing the activity of fusion proteins in NIH3T3 cells. *Renilla* luciferase vector was from Promega.

PPARγ targeting construct was a generous gift from Rosen M. Evans (*32*). LacZ-PGKNeo fragment was digested out and replaced by mutated tTA-FRT-PGKNeo-FRT fragment or rtTA-FRT-PGKNeo-FRT fragment. The targeting constructs were linearized by SalI digestion for electroporation into ES cells.

pCreER^{T2} was a generous gift from Pierre Chambon. To construct the aP2-CreER^{T2} targeting construct, 2.2kb 5'arm together with CreER^{T2}-pA were cloned into NheI-KpnI sites and 2.6kb 3'arm were cloned into XhoI-NotI sites of pN-TK2 targeting vector (a generous gift from Eric N. Olson), respectively. The targeting vectors were linearized by AscI for electroporation into ES cells.

Cell Culture

NIH3T3 cells were cultured in DMEM containing 10% calf serum, 10 units/ml penicillin and 10ug/ml streptomycin at 37°C in 5% CO_2. Cells were passed at 80% confluence. Medium was changed every other day. Transfection was carried out with Lipofectamine 2000

(Invitrogen) following manufacturer's protocol. *Renilla* luciferase reporter was co-transfected to control for the transfection efficiency. Cells were analyzed after 48 hours of transfection.

Luciferase Assay

Luciferase activity of the transfected cells was analyzed with Dual-Luciferase Assay System (Promega) following manufacturer's protocol. The analysis was carried out by a POLARstar OPTIMA plate reader (BMG Labtech).

Generation of PPARγ-tTA (rtTA) and aP2-CreER^{T2} Knock-in Mice

PPARγ-tTA-FRT-Neo-FRT targeting construct was electroporated into ES cells. 650 G418-FIAU resistant ES cell clones were isolated and screened for diagnostic Southern blot patterns with a 5' probe external to the recombination cassette. Ten of the G418-FIAU resistant ES colonies exhibited a mutant PPARγ band upon Southern blot analysis; a 3' external probe showed that 4 of these clones were positive for both probes. Two of the recombinant ES cell colonies were injected into C57BL/6 blastocysts, each of which transmitted the PPARγ-tTA-Neo allele into the germline of progeny.

For PPARγ-rtTA, 3 out of 450 clones screened were positive for diagnostic Southern blot with both 5' and 3' external probes. PPARγ-rtTA mice were generated similarly.

aP2-CreER^{T2} knock-in mice were generated similarly. Out of 1600 G418-FIAU resistant ES cell clones screened, 9 clones were identified as positive by Southern blot with both 5' external and 3' external probe.

The following genotyping primers were used to identify the mice with desired knock-in alleles.

Table 1.1.   Genotyping primers used to identify the mice with desired knock-in alleles.

Wild-type allele for PPARγ locus:	
Forward	5' AGGCCACCATGGAAAGCCACAGTTCCTC 3'
Reverse	5' TCCCCACAGACTCGGCACTCAATGGC 3'
PPARγ-tTA specific:	
Reverse	5' CTGTAGGCCGTGTACCTAAATG 3'
PPARγ-rtTA specific:	
Reverse	5' GGGTGCCGAGATGCACTTTAG 3'
Wild-type allele for aP2 locus:	
Forward	5' CCATTGGTCACTCCTACAGTC 3'
Reverse	5' CTGGAGACAAGCTTCCAGGT 3'
aP2-CreER^{T2} specific:	
Reverse	5' CGGCAAACGGACAGAAGCAT 3'

To remove Neo resistance cassette, PPARγ-tTA-Neo mice were crossed with FLPeR (Flipper) mice that express the FLP recombinase in the germ line.   Mice containing both alleles were bred to wild-type mice, and the progeny were selected for the presence of PPARγ-tTA allele but lack of the Flipper allele.   The removal of the neomycin gene was confirmed in these mice, establishing the PPARγ-tTAΔNeo line.

Animals

Mice were housed in a 12:12 light:dark cycle and chow and water were provided *ad libitum*.   Doxycycline (0.5mg/ml in 5% sucrose) was provided in the drinking water, which was changed every 2-3 days.   Tamoxifen was dissolved in corn oil at 10mg/ml, and was injected at 1mg or 3mg/mouse.   tetO-H2B-GFP, Flipper, and R26R were from The Jackson Laboratory. tetO-Cre was a gift of Lisa Monteggia.   All animals were maintained under the auspices of the U.T. Southwestern Medical Center Animal Care and Use Committee according to NIH guidelines.

β-gal Staining

Adipose depot explants were fixed in 2% formaldehyde, 0.2% glutaraldehyde, PBS for 30 minutes and then rinsed with three 15-minute changes of wash buffer (2mM $MgCl_2$, 0.02% NP-40, 0.1M sodium phosphate buffer, pH7.3). The tissues were stained in wash buffer containing 1mg/ml X-gal, 5mM potassium ferrocyanide, 5mM potassium ferricyanide overnight at room temperature on a rocker. Stained tissues were observed with Leica M420 dissection scope and pictures were taken with Nikon Digital Camera SXM1200.

Microscopy

GFP from adipose tissue explants were observed and photographed with a Zeiss Stemi SV11 microscope.

References

Ailhaud, G., Grimaldi, P., and Negrel, R. (1992). Cellular and molecular aspects of adipose tissue development. *Annu Rev Nutr* **12**, 207-233.

Avram, A. S., Avram, M. M., and James, W. D. (2005). Subcutaneous fat in normal and diseased states: 2. Anatomy and physiology of white and brown adipose tissue. *J Am Acad Dermatol* **53**, 671-683.

Barak, Y., Nelson, M. C., Ong, E. S., Jones, Y. Z., Ruiz-Lozano, P., Chien, K. R., Koder, A., and Evans, R. M. (1999). PPAR gamma is required for placental, cardiac, and adipose tissue development. *Mol Cell* **4**, 585-595.

Bjorntorp, P. (1974). Size, number and function of adipose tissue cells in human obesity. *Horm Metab Res* **Suppl 4**, 77-83.

Bulcao, C., Ferreira, S. R., Giuffrida, F. M., and Ribeiro-Filho, F. F. (2006). The new adipose tissue and adipocytokines. *Curr Diabetes Rev* **2**, 19-28.

Daniels, J. (2006). Obesity: America's epidemic. *Am J Nurs* **106**, 40-49, quiz 49-50.

Farley, F. W., Soriano, P., Steffen, L. S., and Dymecki, S. M. (2000). Widespread recombinase expression using FLPeR (flipper) mice. *Genesis* **28**, 106-110.

Farmer, S. R. (2006). Transcriptional control of adipocyte formation. *Cell Metab* **4**, 263-273.

Friedman, J. M., and Halaas, J. L. (1998). Leptin and the regulation of body weight in mammals. *Nature* **395**, 763-770.

Gesta, S., Tseng, Y. H., and Kahn, C. R. (2007). Developmental origin of fat: tracking obesity to its source. *Cell* **131**, 242-256.

Gossen, M., and Bujard, H. (2002) Studying gene function in eukaryotes by conditional gene inactivation. *Annu Rev Genet* **36**, 153-173.

Green, H., and Kehinde, O. (1975). An established preadipose cell line and its differentiation in culture. II. Factors affecting the adipose conversion. *Cell* **5**, 19-27.

Green, H., and Kehinde, O. (1976). Spontaneous heritable changes leading to increased adipose conversion in 3T3 cells. *Cell* **7**, 105-113.

Green, H., and Kehinde, O. (1979). Formation of normally differentiated subcutaneous fat pads by an established preadipose cell line. *J Cell Physiol* **101**, 169-171.

He, W., Barak, Y., Hevener, A., Olson, P., Liao, D., Le, J., Nelson, M., Ong, E., Olefsky, J. M., and Evans, R. M. (2003). Adipose-specific peroxisome proliferator-activated receptor gamma knockout causes insulin resistance in fat and liver but not in muscle. *Proc Natl Acad Sci U S A* **100**, 15712-15717.

Hausman, D. B., DiGirolamo, M., Bartness, T. J., Hausman, G. J., and Martin, R. J. (2001). The biology of white adipocyte proliferation. *Obes Rev* **2**, 239-254.

Hotamisligil, G. S., Johnson, R. S., Distel, R. J., Ellis, R., Papaioannou, V. E., and Spiegelman, B. M. (1996). Uncoupling of obesity from insulin resistance through a targeted mutation in aP2, the adipocyte fatty acid binding protein. *Science* **274**, 1377-1379.

Imai, T., Jiang, M., Chambon, P., and Metzger, D. (2001). Impaired adipogenesis and lipolysis in the mouse upon selective ablation of the retinoid X receptor alpha mediated by a tamoxifen-inducible chimeric Cre recombinase (Cre-ERT2) in adipocytes. *Proc Natl Acad Sci U S A* **98**, 224-228.

Imai, T., Takakuwa, R., Marchand, S., Dentz, E., Bornert, J. M., Messaddeq, N., Wendling, O., Mark, M., Desvergne, B., Wahli, W., Chambon, P., and Metzger, D. (2004). Peroxisome proliferator-activated receptor gamma is required in mature white and brown adipocytes for their survival in the mouse. *Proc Natl Acad Sci U S A* **101**, 4543-4547.

Indra, A. K., Warot, X., Brocard, J., Bornert, J. M., Xiao, J. H., Chambon, P., and Metzger, D. (1999). Temporally-controlled site-specific mutagenesis in the basal layer of the epidermis: comparison of the recombinase activity of the tamoxifen-inducible Cre-ER(T) and Cre-ER(T2) recombinases. *Nucleic Acids Res* **27**, 4324-4327.

Jones, J. R., Barrick, C., Kim, K. A., Lindner, J., Blondeau, B., Fujimoto, Y., Shiota, M., Kesterson, R. A., Kahn, B. B., and Magnuson, M. A. (2005). Deletion of PPARgamma in adipose tissues of mice protects against high fat diet-induced obesity and insulin resistance. *Proc Natl Acad Sci U S A* **102**, 6207-6212.

Kopelman, P. G. (2000). Obesity as a medical problem. *Nature* **404**, 635-643.

Kubota, N., Terauchi, Y., Miki, H., Tamemoto, H., Yamauchi, T., Komeda, K., Satoh, S., Nakano, R., Ishii, C., Sugiyama, T., Eto, K., Tsubamoto, Y., Okuno, A., Murakami, K., Sekihara, H., Hasegawa, G., Naito, M., Toyoshima, Y., Tanaka, S., Shiota, K., Kitamura, T., Fujita, T., Ezaki, O., Aizawa, S., Kadowaki, T., and et al. (1999). PPAR gamma mediates high-fat diet-induced adipocyte hypertrophy and insulin resistance. *Mol Cell* **4**, 597-609.

Lazar, M. A. (2005). PPAR gamma, 10 years later. *Biochimie* **87**, 9-13.

Li, M., Indra, A. K., Warot, X., Brocard, J., Messaddeq, N., Kato, S., Metzger, D., and Chambon, P. (2000). Skin abnormalities generated by temporally controlled RXRalpha mutations in mouse epidermis. *Nature* **407**, 633-636.

MacDougald, O. A., and Mandrup, S. (2002). Adipogenesis: forces that tip the scales. *Trends Endocrinol Metab* **13**, 5-11.

Makowski, L., Boord, J. B., Maeda, K., Babaev, V. R., Uysal, K. T., Morgan, M. A., Parker, R. A., Suttles, J., Fazio, S., Hotamisligil, G. S., and Linton, M. F. (2001). Lack of macrophage fatty-acid-binding protein aP2 protects mice deficient in apolipoprotein E against atherosclerosis. *Nat Med* **7**, 699-705.

Mokdad, A. H., Marks, J. S., Stroup, D. F., and Gerberding, J. L. (2004). Actual causes of death in the United States, 2000. *Jama* **291**, 1238-1245.

Nelson, D. L., and Cox, M. M. *Lehninger Principles of Biochemistry* (ed. 3rd, 2000), pp. 598-619.

Ntambi, J. M., and Young-Cheul, K. (2000). Adipocyte differentiation and gene expression. *J Nutr* **130**, 3122S-3126S.

Ogden, C. L., Yanovski, S. Z., Carroll, M. D., and Flegal, K. M. (2007). The epidemiology of obesity. *Gastroenterology* **132**, 2087-2102.

Pham, C. T., MacIvor, D. M., Hug, B. A., Heusel, J. W., and Ley, T. J. (1996). Long-range disruption of gene expression by a selectable marker cassette. *Proc Natl Acad Sci U S A* **93**, 13090-13095.

Rangwala, S. M., and Lazar, M. A. (2000). Transcriptional control of adipogenesis. *Annu Rev Nutr* **20**, 535-559.

Ross, S. E., Hemati, N., Longo, K. A., Bennett, C. N., Lucas, P. C., Erickson, R. L., and MacDougald, O. A. (2000). Inhibition of adipogenesis by Wnt signaling. *Science* **289**, 950-953.

Soriano, P. (1999). Generalized lacZ expression with the ROSA26 Cre reporter strain. *Nat Genet* **21**, 70-71.

Tanaka, T., Yoshida, N., Kishimoto, T., and Akira, S. (1997). Defective adipocyte differentiation in mice lacking the C/EBPbeta and/or C/EBPdelta gene. *Embo J* **16**, 7432-7443.

Tontonoz, P.,. Hu, E, Graves, R. A., Budavari, A. I., and Spiegelman, B. M. (1994). mPPAR gamma 2: tissue-specific regulator of an adipocyte enhancer. *Genes Dev* **8**, 1224-1234.

Tontonoz, P., Hu, E., and Spiegelman, B. M. (1994). Stimulation of adipogenesis in fibroblasts by PPAR gamma 2, a lipid-activated transcription factor. *Cell* **79**, 1147-1156.

Trayhurn, P., Bing, C., and Wood, I. S. (2006). Adipose tissue and adipokines--energy regulation from the human perspective. *J Nutr* **136**, 1935S-1939S.

Tumbar, T., Guasch, G., Greco, V., Blanpain, C., Lowry, W. E., Rendl, M., and Fuchs, E. (2004). Defining the epithelial stem cell niche in skin. *Science* **303**, 359-363.

Villena, J. A., Kim, K. H., and Sul, H. S. (2002). Pref-1 and ADSF/resistin: two secreted factors inhibiting adipose tissue development. *Horm Metab Res* **34**, 664-670.

Yu, T. S., Dandekar, M., Monteggia, L. M., Parada, L. F., and Kernie, S. G. (2005). Temporally regulated expression of Cre recombinase in neural stem cells. *Genesis* **41**, 147-153.

Zhang, Y., Proenca, R., Maffei, M., Barone, M., Leopold, L., and Friedman, J. M. (1994). Positional cloning of the mouse obese gene and its human homologue. *Nature* **372**, 425-432.

Chapter II

Lineage Tracing on Adipose Tissues Using the PPARγ-tTA Tool

Abstract

Adipose tissues form throughout the body in various places in a stereotypical pattern. Each depot displays distinctive properties at various aspects including anatomical location, morphology, cellular components, and metabolic features. To better understand depot specificity, I applied the PPARγ-tTA tool and performed lineage tracing on adipose tissues to determine the time frames when different adipose depots are specified. I found that adipose depots are specified at very distinctive developmental stages in a sequential manner, suggesting that different adipose depots are derived from distinct origins.

Introduction

Adipose tissue has long been disregarded as part of amorphous connective tissue because of the lack of structures and seemingly simple composition. But with increasing understanding about fat biology and the knowledge on depot-specific features, adipose tissue is starting to be recognized as the largest endocrine organ in the body with great varieties and plasticity.

There are two types of adipocytes with distinct function and morphology: white adipocytes and brown adipocytes (Avram et al., 2005). White adipocytes are usually unilocular, containing one large lipid droplet which pushes the cytoplasm to the periphery to form a rim. The function of white adipose is to store excess lipids in time of abundance while releasing energy to other organs in time of need. On the contrary, brown adipocytes are multilocular and rich in mitochondria, which partially gives rise to the signature color of brown adipose tissue. Brown adipose uniquely expresses UCP-1, which produces heat by uncoupling the proton electrochemical gradient from the generation of ATP. White adipose tissue is the major focus of my research because of its metabolic relevance.

Adipose tissues form throughout the body in various places in a stereotypical pattern (Cinti, 2005). There are several depots with distinctive locations and shapes, such as inguinal, interscapular, gonadal, retroperitoneal, and mesenteric WAT (Figure 2.1). More adipose tissues distribute throughout the body with less defined shape and functions, which hinders further study. Based on the physical location, adipose tissues have two major divisions: subcutaneous WAT and visceral WAT. Fat distribution between these two categories can be simply measured by waist circumference or waist-hip ratio (WHR) in human, which is a better predictor for cardiovascular diseases than BMI (Hamdy et al., 2006). Visceral WAT has a positive association with

metabolic risk factors while subcutaneous WAT has a negative association (Hamdy et al., 2006). Such differential metabolic effects might be due to the physical proximity of visceral fat with the liver through portal circulation or due to the differential gene expression patterns in visceral fat and subcutaneous fat (Gesta et al., 2007).
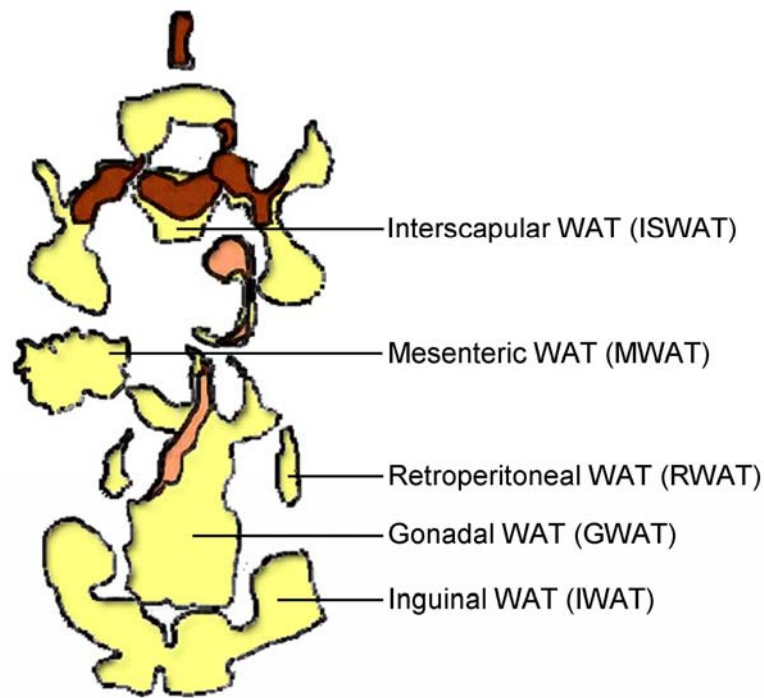
Figure 2.1.   Anatomical locations of mouse adipose tissues.   White adipose tissues are in yellow.   Brown adipose tissues are in dark brown.   Light brown indicates the tissues with both white and brown adipose tissues mixed together.   The depots examined in my study are as labeled. (Modified from Cinti, 2005)

Moreover, any single depot displays distinctive properties when compared to others. For example, inguinal WAT is located at the base of the hind legs of mice, is rich in vasculature, contains white adipocytes with wide range of sizes, and has a significant population of brown adipocytes interspersing among white adipocytes.   On the contrary, gonadal WAT is bound to the reproductive organs (epididymis in male, ovary and uterus in female) by the peritoneal leaflets, is composed almost exclusively of white adipocytes with relatively homogeneous size,

and has much less vasculature when compared with inguinal WAT. The properties of a particular adipose depot might associate closely with its anatomical location and connected organs (Gesta et al., 2007).

The knowledge on the specific features of each depot will help us understand their unique metabolic roles. One interesting aspect is when and how each depot is specified. Adipose tissue formation is part of the developmental program of the whole organism, and each depot is formed at a defined developmental stage. Adipose depots seem to form in an orderly fashion. However, the developmental paradigm for the formation of each depot has not been determined. This includes a few interesting questions. When is each adipose depot specified? Does this specification process occur synchronously or sequentially for different depots? Do adipose depots share the same origin? Lineage tracing in adipose tissue seems to be a good approach to address these questions.

PPARγ is the master regulator for adipogenesis (Rosen and MacDougald, 2006), which makes it a good marker for the lineage specification. Here I use PPARγ-tTA with tetO-Cre; R26R to perform lineage tracing in several adipose depots and show that adipose depots are specified sequentially, and most adipose depots seem to have distinct origins.

Results

In Chapter I, I showed that the PPARγ-tTA knock-in mice are functional in an adipose-restricted manner and tTA activity can be completely suppressed by doxycycline (Dox). The inducibility of tTA and the pharmacological properties of Dox make PPARγ-tTA a good tool for adipose lineage tracing.   I combined PPARγ-tTA with an indelible marker reporter tetO-Cre; R26R, which is an indispensable component for lineage tracing.   My study is limited to the depots with defined shape and anatomy, including inguinal (IWAT), interscapular (ISWAT), gonadal (GWAT), retroperitoneal (RWAT), and mesenteric (MWAT) white adipose tissue.

First, I wanted to determine the time window during which all adipose depots are formed. PPARγ-lacZ is a good reporter for the expression of PPARγ in adipose tissues.   LacZ expression was first reported to appear in the embryonic fat pad as early as embryonic day 14.5 (E14.5) in PPARγ-lacZ mice (Barak et al., 1999).   At postnatal 20 days of age (P20), all the adipose depots studied could be physically identified, and all stained positive for β-galactosidase activity (not shown), indicating that all the depots I studied express PPARγ and are committed to adipose lineage by P20.   To confirm these observations, I initiated the Dox treatment on PPARγ-tTA; tetO-Cre; R26R mice at E14.5 and continued till P30, when the adipose depots were harvested and stained for β-galactosidase activity.   I found that none of the adipose depots had any staining above the background, similar to when I started the suppression at E0 (Chapter I, Figure 1.9).   This indicates that the adipose tissue primordiums have not formed by E14.5 as judged by the expression of PPARγ.   However, when I treated the PPARγ-tTA; tetO-Cre; R26R mice with Dox from P20 to P30, all the adipose depots examined expressed similar level of β-galactosidase as the untreated group, which is consistent with the visual observation that adipose tissues have

fully formed by P20. Therefore, the window of adipose tissue formation was set between E14.5 and P20.

Within the time frame of E14.5 to P20, I'd like to dissect the specific time window for the formation of each depot. To do this, I took the approach depicted in Figure 2.2. I performed a series of Dox treatments starting at various time points between E14.5 and P20, and then continued Dox treatment till P30, staining adipose tissues for β-galactosidase activity. Before the start of Dox treatment, if there is no cell specified by PPARγ expression, continuous Dox treatment should suppress tTA activity, and no cells will be labeled by lacZ. However, if there are some cells in a depot specified and labeled by lacZ before the start of Dox treatment, these cells would retain their labels and pass on to their descendants. Such staining will be detected when the mice are analyzed at P30. Basically, the fate of the cells labeled before the chase period (Dox-treating period) is traced at P30.
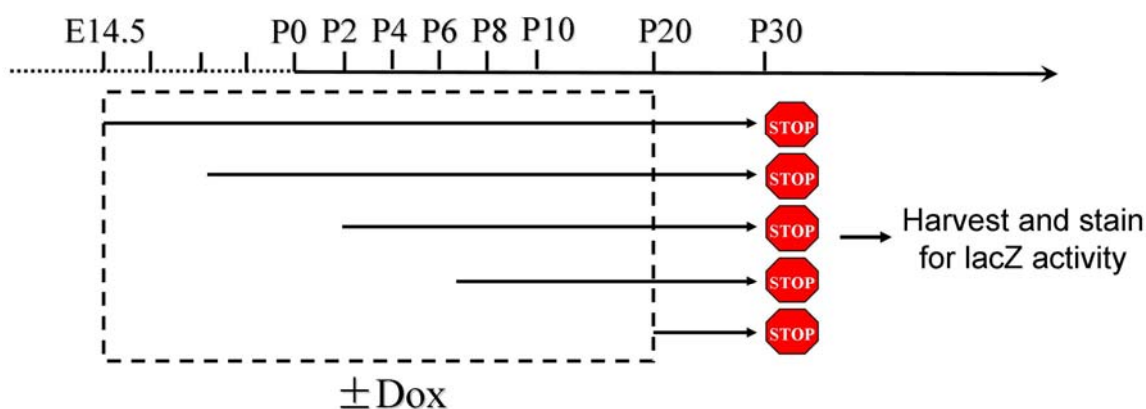
Figure 2.2. The approach for adipose lineage tracing. (See the text for detail.)

Using this method, I found that different adipose depots are formed at different stage during development. For inguinal WAT, I found that the depot starts to form between E14.5 and E18.5. As described above, no lacZ staining was observed for any depot if Dox treatment

started at E14.5.   When started at E16.5, it seemed to be an intermediate state when the lacZ expression was patchy, suggesting that inguinal WAT is in the process of forming the primordium. When started at E18.5, the lacZ staining on IWAT was indistinguishable from the untreated animals, suggesting that IWAT is fully specified by E18.5.

With the same procedure, I identified the time frames when each adipose depot is specified (Figure 2.3).   The results are summarized in Table 2.1.   The beginning of this time frame is set by the latest time point, when Dox treatment was started, that the depot remained non-labeled (white).   The end of this time frame is set by the first time point that the depot becomes fully labeled (blue) and indistinguishable from non-Dox treated depot.   In this way, the time frame described here is broader than the actual process.
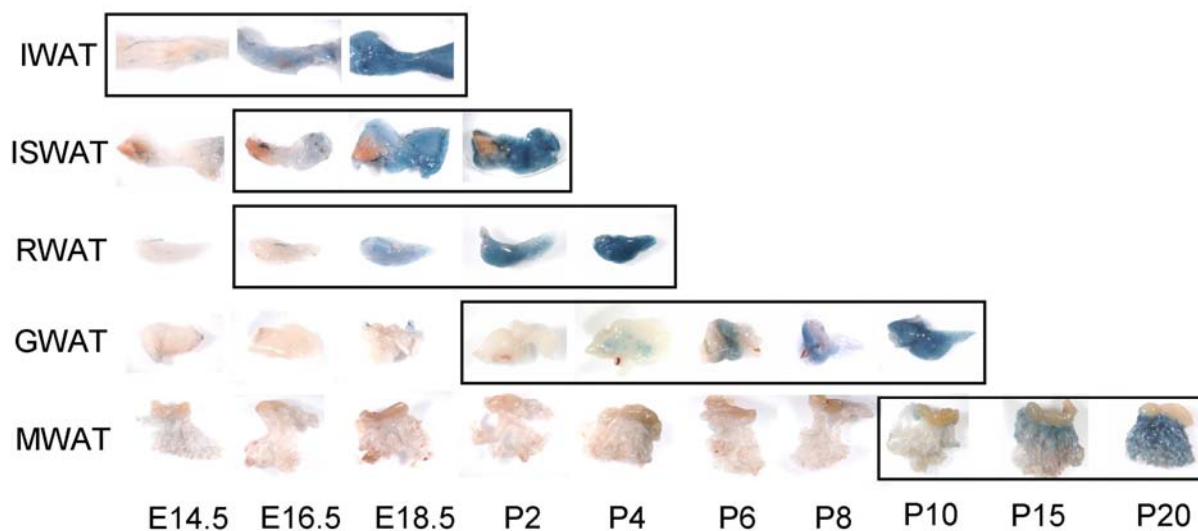
Figure 2.3.   Adipose depots are specified at different developmental stages.   PPARγ-tTA; tetO-Cre; R26R mice were treated with Dox from indicated time points till P30.   Adipose depots as indicated were harvested and stained with X-gal.   The forming time frames are labeled by boxes.

Table 2.1.   The forming time frames for each adipose depot.

WAT	Forming Time Frame
Inguinal (IWAT)	E14.5-E18.5
Interscapular (ISWAT)	E16.5-P2
Gonadal (GWAT)	E16.5-P4
Retroperitoneal (RWAT)	P2-P10
Mesenteric (MWAT)	P10-P20

Discussion

Adipose depots at different locations have distinctive morphology, cellular components and physiological functions, but little is known about when and how each adipose depot is specified. Combining PPARγ-tTA knock-in mice I generated with the permanent reporter tetO-Cre; R26R, I did lineage tracing on adipose tissues and determined the time frames when different adipose depots are specified. I found that different adipose depots are specified at very distinctive embryonic and early postnatal stages. This finding suggests that different adipose depots form at different anatomical locations and are derived from different pools of cells, thus this lineage tracing provides a molecular distinction for different adipose depots.

Another way to characterize the depot specification is to visually observe the formation of each depot in wild-type mice or in PPARγ-lacZ mice by staining for lacZ during development; however, lineage tracing is much more sensitive and technically simpler. Cells that are specified (by expressing PPARγ) and labeled at an early developmental stage will proliferate and pass on the labeling during the chase period, thus exponentially amplifying the signal. For example, when mice were treated with Dox from P4 to P30, GWAT displayed a patchy staining pattern (Figure 2.3). Such staining might be derived from a few cells labeled at P4, which would be impossible to identify by examining pups at P4, but after proliferation during P4-P30, the resulting staining pattern is clearly identifiable. Moreover, the adipose tissues are analyzed at adult (in this case, P30) rather than at embryos or young pups, which provides tremendous technical advantages. The staining pattern observed could be informative in revealing how the tissue formation progresses. For example, the staining pattern for the intermediate state of IWAT (E16.5 Dox treatment) is distinct from the one of GWAT (P4 or P6 Dox treatment),

suggesting that IWAT expands evenly across the tissue while GWAT forms in a wave from inside out.

This method also has its caveats. Here PPARγ is used as a marker for lineage specification based on the findings from in vitro culture models, but more in vivo studies are required to test this notion. The system of PPARγ-tTA; tetO-Cre; R26R artificially impose two thresholds on this lineage tracing process: the threshold for tTA to activate the tetO promoter and the threshold for Cre to delete the stop cassette. Moreover, the tTA and Cre transcripts have to be translated before activation of the PPARγ promoter can lead to permanent deletion of the stop cassette. Therefore, a delay is expected between the actual specification time point and the one identified here.

The study presented here is just the first step to understand the depot specificity of adipose tissues. Based on the finding that different depots are formed at different time windows, it should be possible to alter gene expression at different time points to achieve depot-specific gene manipulation. In this way, gene functional studies could be carried out in a depot-specific manner, which would provide us more knowledge on the differential properties of adipose depots.

Materials and Methods

Mouse maintenance and β-gal staining were as described in Chapter I.

References

Avram, A. S., Avram, M. M., and James, W. D. (2005). Subcutaneous fat in normal and diseased states: 2. Anatomy and physiology of white and brown adipose tissue. *J Am Acad Dermatol* **53**, 671-683.

Barak, Y., Nelson, M. C., Ong, E. S., Jones, Y. Z., Ruiz-Lozano, P., Chien, K. R., Koder, A., and Evans, R. M. (1999). PPAR gamma is required for placental, cardiac, and adipose tissue development. *Mol Cell* **4**, 585-595.

Cinti, S. (2005). The adipose organ. *Prostaglandins Leukot Essent Fatty Acids* **73**, 9-15.

Gesta, S., Tseng, Y. H., and Kahn, C. R. (2007). Developmental origin of fat: tracking obesity to its source. *Cell* **131**, 242-256.

Hamdy, O., Porramatikul, S., and Al-Ozairi, E. (2006). Metabolic obesity: the paradox between visceral and subcutaneous fat. *Curr Diabetes Rev* **2**, 367-373.

Rosen, E. D., and MacDougald, O. A. (2006). Adipocyte differentiation from the inside out. *Nat Rev Mol Cell Biol* **7**, 885-896.

Chapter III

PPARγ-Expressing SV Cells are Adipogenic Progenitors

Abstract

Having an appropriate number and a particular size of adipocytes is critical for the body to maintain energy homeostasis. Understanding the mechanism underlying adipocyte number control is physiologically and pathologically important. Yet the identity of adipose progenitors remains elusive. Exploiting genetic tools I identified a population of PPARγ-expressing cells from adipose SVF that possess characteristics of an adipose progenitor population. These precursors have largely been committed early in the postnatal period, actively proliferate *in vivo* and *in vitro*, and contribute to adipose tissue expansion in response to developmental and pharmacological stimuli. These progenitors are morphologically and molecularly distinct from adipocytes, have high capacity to undergo adipogenesis *in vitro* and, importantly, can form ectopic fat pads after transplantation. The ability to label and prospectively isolate adipose progenitors using the PPARγ-tTA system provide a foundation to explore the mechanisms underlying the poorly understood control of adipose tissue homeostasis *in vivo*.

Introduction

Having an appropriate number and a particular size of adipocytes is critical for the body to maintain energy homeostasis. The importance of forming the appropriate number of adipocytes is highlighted by the significant metabolic disturbances that accompany too few (lipodystrophy) or too many (obesity) adipocytes. Understanding the mechanism underlying adipocyte number control is physiologically and pathologically important.

During the development of adipose tissues, there is a massive increase in the size of WAT depots. This growth is accompanied by the expansion in both cell number (hyperplasia) and cell size (hypertrophy) (Hausman et al., 2001). In adults, weight gain occurs first through cell size increase until adipocytes reach a critical size, and thereafter new cells have to be recruited for further increase of adipose tissues (Avram et al., 2005). In adult rats, it was reported that adipose hyperplasia is responsible for 17%-65% of cumulative adipose growth, depending on the specific depots (DiGirolamo et al., 1998). Adipose hyperplasia is a major contributor in the course of developing obesity, especially severe or morbid obesity (Spiegelman and Flier, 1996; Hausmans, 2006). Therefore, adipose proliferation is actively involved in not only adipose development but weight gain and obesity in adulthood. However, very little is known about how adipose proliferation occurs *in vivo*, although the quest for adipose progenitors started more than two decades ago (Hausman et al., 1980).

The Quest for Adipose Progenitors

Adipose tissue has long been ignored partially because of its seemingly simple composition, but in fact it is rather heterogeneous. Although adipocytes take up more than 80%

of the adipose volume, they represent between one third and half of the total cell number (Ailhaud et al., 1992). The rest of the cells, collectively called the stromal-vascular fraction (SVF), include fibroblasts, endothelial cells, macrophages, blood cells and so called "preadipocytes" (Ailhaud et al., 1992). The procedure to isolate the SVF and adipocytes is depicted in Figure 3.1. Whole adipose tissues are minced into small pieces and digested by type I collagenase. The dissociated cells are further separated by density centrifugation. The lipid-laden adipocytes float to the top and form an adipocyte layer, whereas all the other cell types are collected at the bottom to form the SVF. Studies on the endogenous adipocyte progenitors relied on the analyses of this heterogeneous mixture of cells by *in vitro* culture (Ailhaud et al., 1992; Klaus et al., 1991). So far still very little is known about the identity or biological characteristics of the adipocyte progenitors (Gesta et al., 2007). This area of research is limited by the lack of markers to specifically identify the putative progenitors. A wealth of information suggests that PPARγ is a master regulator of fat formation (Lazar, 2005). Thus marking PPARγ-expressing cells *in vivo* might provide novel insights into adipose lineage specification and the progenitor population.
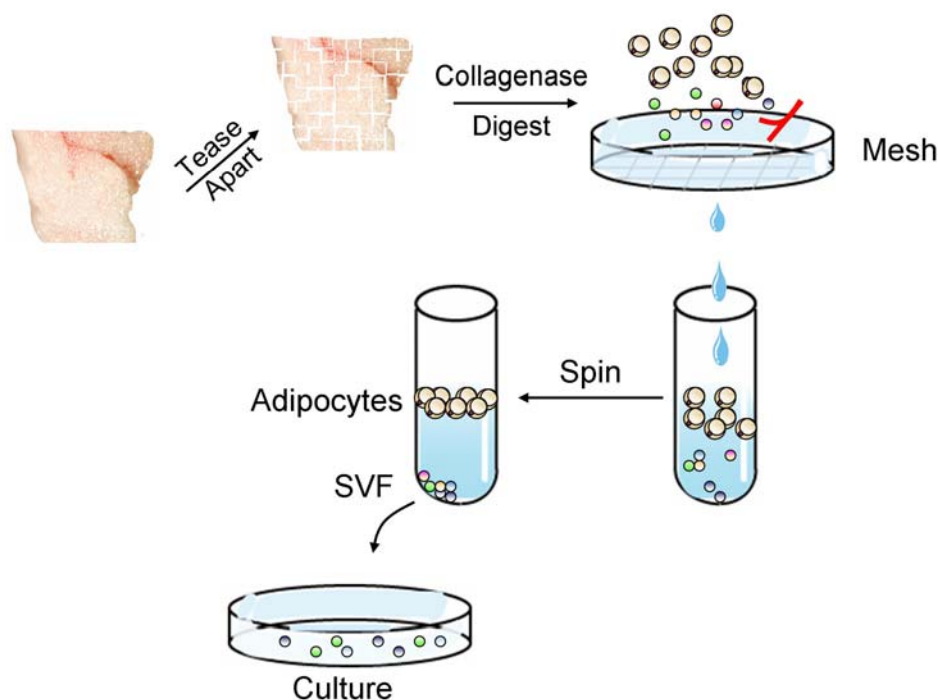
Figure 3.1. Isolation of the stromal vascular fraction (SVF) and the adipocyte fraction from mouse adipose tissues. (See text for detail.)

Introduction to the Reporters

TetO-H2B-GFP and tetO-Cre; R26R are two complementary reporters I adopted for PPARγ-tTA. The properties of these two systems are depicted in Figure 3.2. H2B-GFP is a fusion of GFP to histone H2B, which has been shown to function like histone H2B and stably bind to DNA without much turnover (Kanda et al., 1998). In the setting of PPARγ-tTA; tetO-H2B-GFP, H2B-GFP is stable in post-mitotic cells, both *in vitro* and *in vivo*, but becomes diluted in proliferating cells following inhibition of the Tet system (Kanda et al., 1998; Tumbar et al., 2004). If cells have been labeled with H2B-GFP, but the tetO promoter is shut down, the existing H2B-GFP will be evenly distributed to daughter cells during cell division. Therefore, cell proliferation results in the progressive loss of H2B-GFP labeling, whereas in the absence of cell proliferation, these cells will retain the H2B-GFP label. In contrast, R26R is an indelible

genetic marker. The Cre-mediated deletion of the ROSA26 stop cassette results in an irreversible DNA rearrangement, the recombined allele will be passed on to all progeny derived from these cells, and the descendant cells are readily detected by assaying for β-galactosidase activity.
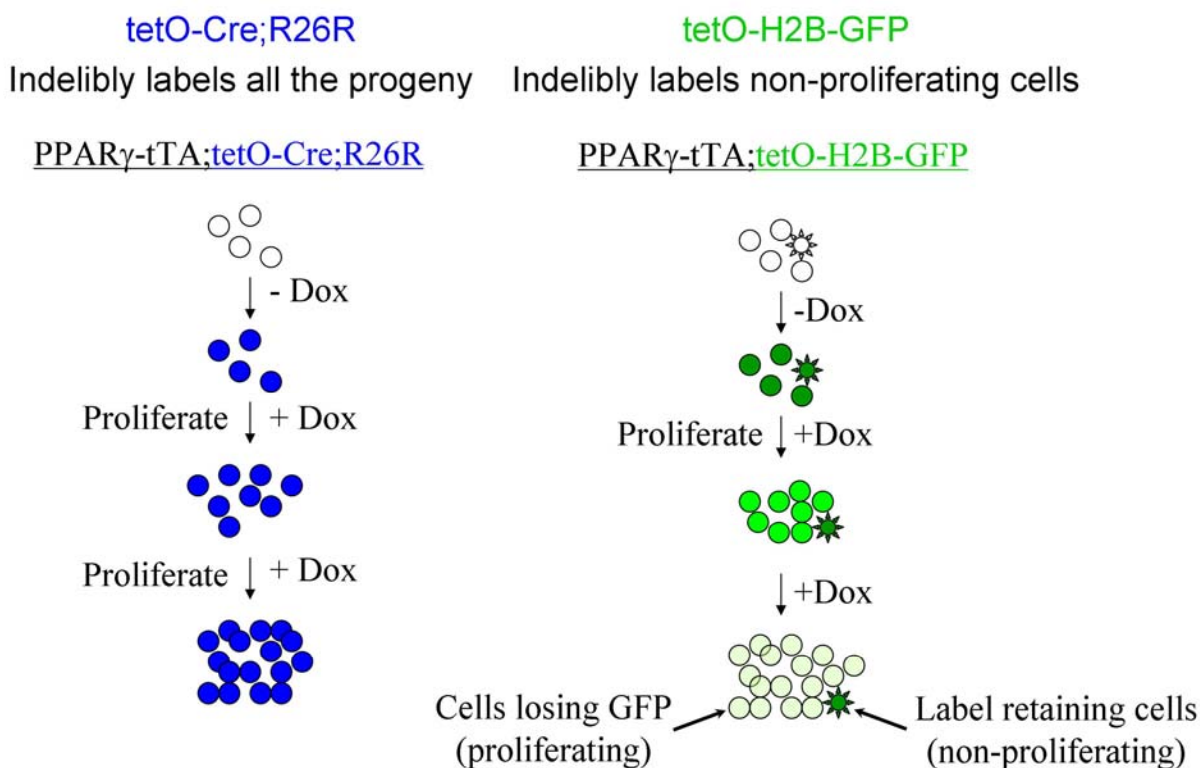
Figure 3.2.   Properties of the two reporter systems when combined with PPARγ-tTA.   In PPARγ-tTA; tetO-H2B-GFP, the non-proliferating cells maintaining the GFP labeling are called "label retaining cells". (See the text for other details.)

PPARγ in Adipogenesis

From cell culture studies, PPARγ has been found to be a central player that initiates the adipocyte differentiation program.   It has been reported that PPARγ is sufficient to induce cell cycle withdrawal (Altiok et al., 1997).   The initiation of its expression was reported to occur

during the clonal expansion period.   After first initiation, a positive feedback mechanism is in place to enforce PPARγ expression till it peaks at day 3-4 after induction (Ntambi and Young-Cheul, 2000).   Therefore, PPARγ is not expected to express in progenitors, but turning on its expression signals the irreversible progression through the differentiation program.

PPARγ Agonist TZD

Thiazolidinediones (TZD), a class of synthetic drugs that enhances insulin action, improves glucose disposal and reduces hepatic glucose output, are widely prescribed for diabetes patients.   TZDs were identified as potent and selective PPARγ agonists (Lehmann et al., 1995), promoting adipocyte differentiation *in vitro* in mesenchymal stem cells and preadipocytes (Kletzien et al., 1992; Hiragun et al., 1988; Sparks et al., 1991).   The degree of potency for different TZDs to activate PPARγ closely matches their anti-diabetic actions, further supporting that TZDs implement their pharmacological actions through PPARγ (Spiegelman and Flier, 1996; Willson et al., 1996).   While improving systemic insulin sensitivity, paradoxically, TZDs increase whole body adiposity.   In fact, TZDs induce significant adipose remodeling, including the redistribution of lipid stores from metabolically adverse visceral fat to subcutaneous fat (Kawai et al., 1999), and the generation of new small adipocyte clusters and shrinkage and/or disappearance of mature adipocytes (Souza et al., 2001).   However, the mechanism underlying the effects of TZD on adipose tissues remodeling is unknown.

Effect of Wnt Signaling

Wnt signaling is an evolutionarily conserved signaling pathway implicated in tissue patterning, cell proliferation, cell differentiation, and cancer etc.   In the canonical Wnt signaling

pathway, β-catenin is the key transcriptional coactivator which helps to elicit downstream target gene expression. In the absence of Wnt, β-catenin is hyperphosphorylated by CKI and GSK3α/β and targeted for degradation. In the presence of Wnt, the destruction complex cannot phosphorylate β-catenin, and the stable β-catenin accumulates in the cytoplasm and translocates into the nucleus, where it binds to and co-activates transcription factor LEF/TCF and activates target gene expression (Clevers, 2006). Activating Wnt signaling has been shown to inhibit preadipocyte differentiation both *in vivo* and *in vitro* (Prestwich and MacDougald, 2007). Wnt signaling might regulate mesenchymal stem cell fate by stimulating osteogenesis while inhibiting adipogenesis. The primary mechanism that Wnt signaling inhibits adipogenesis is through suppressing PPARγ and C/EBPα (Prestwich and MacDougald, 2007).

Here, during the course of exploring the newly generated genetic tool PPARγ-tTA, I identified a population of PPARγ-expressing cells from adipose SVF that possess characteristics of an adipose progenitor population. These cells actively proliferate *in vivo* and *in vitro*, contribute to adipose tissue expansion in response to developmental and pharmacological stimuli, and have high capacity to undergo adipogenesis *in vitro* and, importantly, can form ectopic fat pads after transplantation. The ability to label and prospectively isolate adipose progenitors using the PPARγ-tTA system provide a foundation to explore the mechanisms underlying the poorly understood control of adipose tissue homeostasis *in vivo*.

Results

PPARγ+ Cells Contribute to Adipose Tissue Development *in vivo*

From the lineage tracing results (see Chapter II), it was surprising that the majority of progenitor cells that ultimately contribute to the adult adipose depots are specified within such a narrow and early time window in development. Following this time window, there is a massive growth period where the depots grow by tens of folds in size. However, the results (see Chapter II) suggest that the new adipocytes formed during this growth period seem to mostly descend from the preexisting labeled cells (by tetO-Cre; R26R). For example, inguinal WAT, even though it undergoes massive growth from P2 to P30, retained a similar level of lacZ reporter expression, based upon either inspection or β-gal quantitation (Figure 3.3A, B), when Dox administration started from P2 and continued through P30. This unexpected result indicated that the vast majority of P30 adipocytes are derived from a pre-existing pool of PPARγ-expressing cells, either adipocytes already present in the early postnatal period or proliferating precursors. The possibility that these cells are already formed adipocytes is incompatible with the proliferative increase in adipocytes known to occur over this time frame whereas the notion that PPARγ-expressing cells are progenitors is inconsistent with adipogenic cell line data (Altiok et al., 1997; Rosen and MacDougald, 2006).

To resolve this paradoxical observation that contradicts conventional knowledge of the adipogenic program, and to possibly distinguish between these alternatives, I introduced a complementary reporter system, tetO-H2B-GFP into the same Dox treating experiment, which also allows the control for the proper delivery of Dox into adipose tissues. I examined the response to Dox treatment with PPARγ-tTA; tetO-H2B-GFP ("PPARγ-GFP") and, in contrast to

the PPARγ-R26R data, found markedly reduced adipose depot and adipocyte GFP expression (Fig. 3.3A, C), although scattered GFP+ cells remained (not shown).   It is possible that the diminution in H2B-GFP fluorescence might be due to instability not observed in other cell types (Tumbar et al., 2004), I did similar 1-month Dox treatment on adult mice at 4-month of age, with the notion that adult adipose tissues have less turnover and proliferation than developing tissues, but any intrinsic instability of H2B-GFP would be detectable regardless of age.   The results of this experiment designed to assess the stability of H2B-GFP showed that, the gross GFP intensity reduced roughly to a half or a third during the 1 month Dox treatment (Figure 3.4), but not nearly as much as the P2-P30 Dox treated ones, which was reduced to less than a 1/10 of the -Dox controls (Figure 3.3A).   The apparent reduction of GFP intensity could be due to a hitherto undescribed slow turnover of adipose tissues or the slow degradation of H2B-GFP protein during the one month period of Dox treatment at 4-5 months of age.   In either event, the rather modest reduction due to intrinsic GFP decay points to cell proliferation as the major cause of GFP reduction in P2-P30 Dox treated mouse fat pads.   Furthermore, the presence of some GFP label retaining cells argues against the notion that this dramatic reduction in GFP intensity is the solely due to a general instability of H2B-GFP.   Therefore, it seems likely that PPARγ+ (GFP+) cells divide and thereby dilute H2B-GFP.
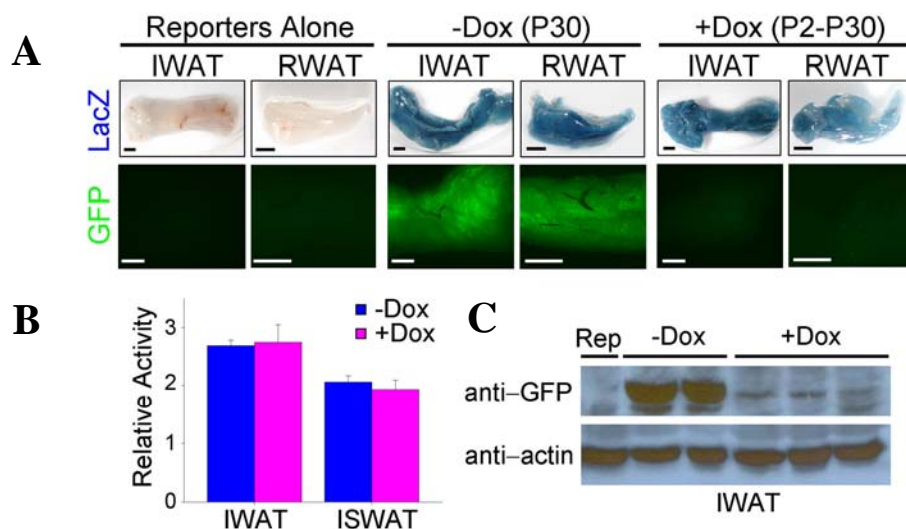
Figure 3.3. PPARγ+ cells contribute to adipose development from P2 to P30. (A) PPARγ-tTA; tetO-Cre; R26R (PPARγ-R26R) (top panels) and PPARγ-tTA; tetO-H2B-GFP (PPARγ-GFP) (bottom panels) mice were treated without or with Dox from P2 to P30 and then IWAT and RWAT were excised and examined for lacZ (blue) or GFP (green) expression.   Left panels are depots of non-Dox treated mice containing either R26R or tetO-H2B-GFP.   (B) In the same experiment, PPARγ-R26R adipose tissues were subjected to a quantitative β-galactosidase assay.   Relative activity is β-galactosidase activity normalized against untreated control tetO-Cre; R26R adipose depots.   IWAT: inguinal white adipose tissue.   ISWAT: interscapular white adipose tissue.   Non-Dox treated group (blue bars).   Dox-treated group (pink bars).   (C) In the same experiment, PPARγ-GFP adipose tissues were harvested, lyzed and examined for GFP expression with Western blotting. β-actin was used as a loading control.   Scale bars: 2mm.
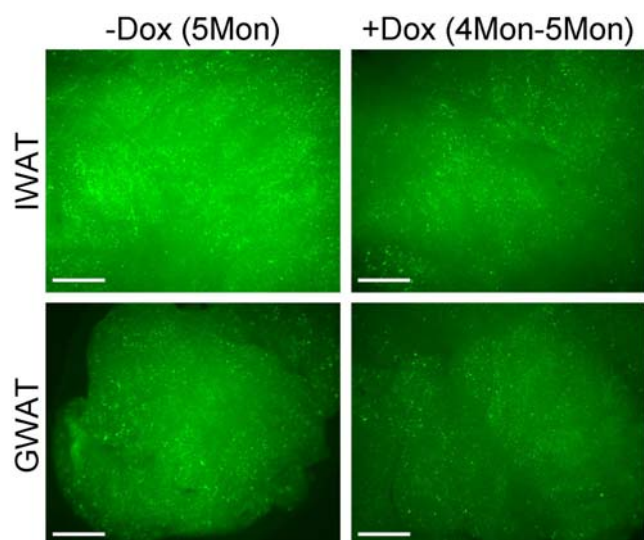

Figure 3.4.   PPARγ-GFP mice partially maintained GFP expression in adipose tissues after one month of Dox-treatment at 4-month of age.   PPARγ-GFP mice at 4-month of age were treated with Dox for one month, and adipose tissues were harvested and inspected for GFP intensity.   Scale bars: 2mm.

The active proliferation in adipose tissue is also supported by BrdU labeling of adipose tissues between P10 and P30 (Figure 3.5). In this experiment, wild-type mice were pulsed daily with BrdU from P10 to P30, and whole mount adipose tissue showed significant incorporation of BrdU into the cells. To further distinguish between adipocyte and SV compartment the contribution to BrdU labeling, I isolated these two fractions and examined BrdU incorporation by immunocytochemistry (ICC). Floating adipocytes are fragile and thus difficult to employ in assays such as ICC. In order to overcome this problem, I extracted nuclei from the floating adipocytes followed by attachment and ICC. Using this modified protocol, I was able to efficiently measure BrdU incorporation in mature adipocytes. The results of this assay indicated that more than 50% of adipocytes, and a similar percentage of SV cells incorporated BrdU during the labeling period (Figure 3.5). Given that the BrdU labeling started at P10 (but not P2) and the injection was a daily pulse instead of continuous infusion, the actual proliferation rate of adipose tissue during the first month after birth is indeed remarkable, again making it difficult to account for the homogeneous lacZ staining observed after Dox treatment unless PPARγ lineage cells proliferate. Together, these data indicate that adipose lineage cells, already instructed to express PPARγ early in the postnatal period, proliferate and are the major source of the spurt of adipocyte development observed in the first month of life.
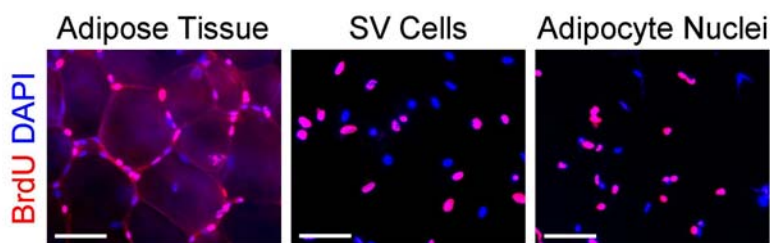

Figure 3.5. Adipose tissues undergo massive proliferation during development (P10-P30). Wild-type mice were BrdU-injected once daily beginning at P10, and at P30 intact adipose depots, SV cells, and nuclei isolated from floated adipocytes were analyzed for BrdU incorporation (red). Nuclei stained with DAPI (blue). Scale bar: 50μm.

PPARγ+ SV cells are the Source for Adipose Tissue Expansion *in vivo*

As the adipose SVF contains adipose progenitors (Ailhaud et al., 1992; Otto and Lane, 2005), it was a possible source from which proliferating PPARγ-expressing cells may originate and ultimately contribute to the burst of adipose tissue expansion described above (Figure 3.3). To test this notion, I examined the SVF from both PPARγ-tTA reporter strains and found that a significant percentage of SV cells expressed lacZ and GFP reporters (Figure 3.6A). To see whether it mirrored the endogenous expression, I stained SV cells from wild-type mice for PPARγ expression by ICC (Figure 3.6B).
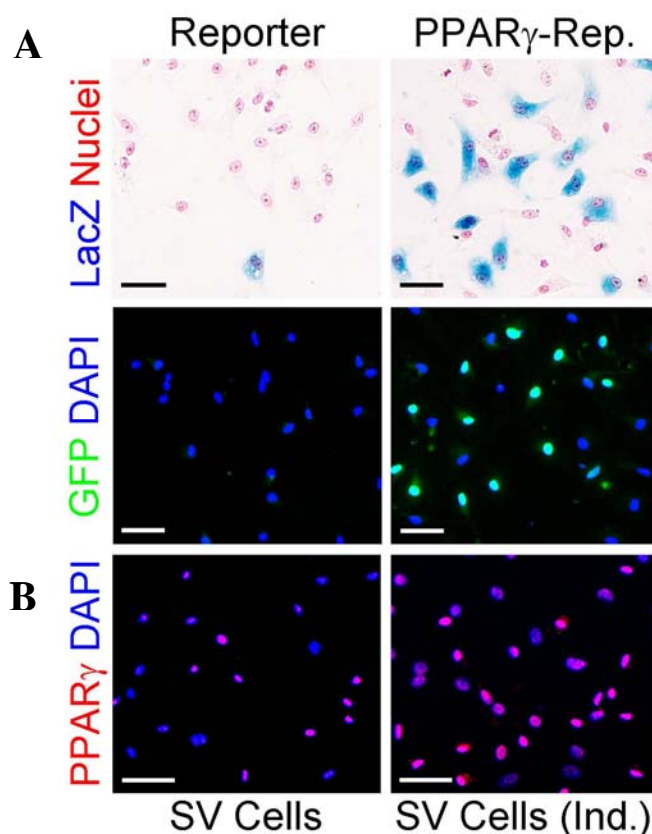
Figure 3.6. PPARγ is expressed in adipose SV cells. P30 SV cells from reporter alone, PPARγ-R26R (A, top panel) and PPARγ-GFP (A, bottom panel), wild-type (B) WAT were examined for reporter expression (A) or for PPARγ expression (red) with ICC (B). (B, right panel) wild-type adipose SV cells were induced for adipogenesis and examined for PPARγ expression with ICC. (A, top panel) lacZ (blue), nuclei counterstained with nuclear fast red (red). (A, bottom panel) Nuclei stained with DAPI (blue), GFP (green). (B) Nuclei stained with DAPI (blue), PPARγ (purple). Scale bar: 50μm.

I detected nuclear expression of PPARγ in a subset of wild-type SV cells and PPARγ level was up-regulated in the differentiated SV cells as expected (Figure 3.6B), supporting the notion that PPARγ indeed expresses in a subset of SV cells.   Moreover, I found that GFP and lacZ reporters largely overlap in terms of the population labeled, since >90% GFP+ cells are lacZ+ while >80% of GFP- cells are lacZ-.   Considering the limited sorting efficiency for GFP reporter and the leakiness of tetO-Cre, these two reporters mostly label the same cell population.
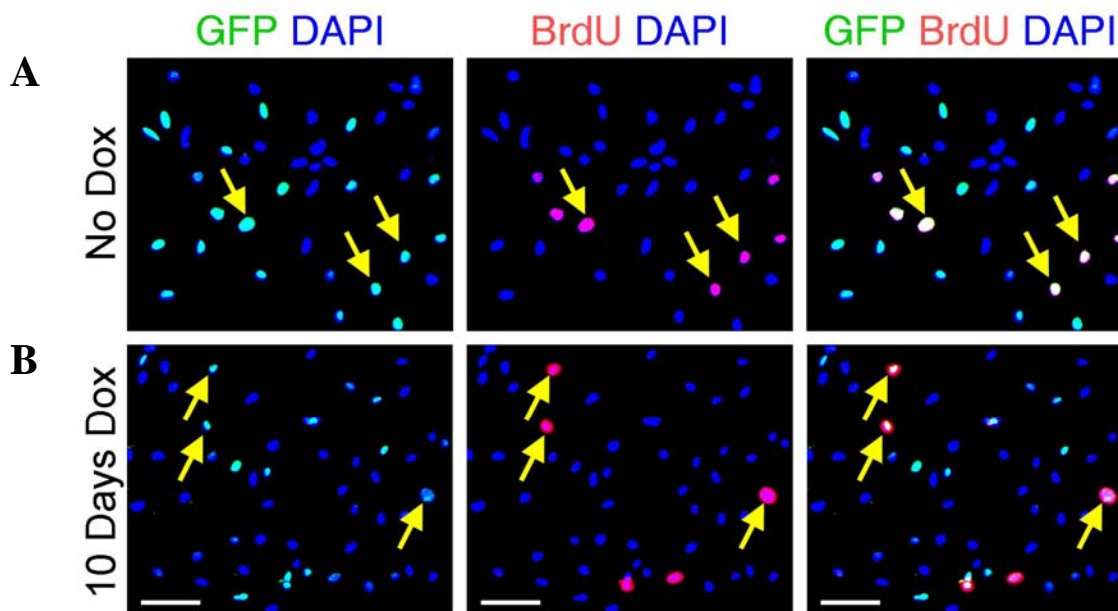
Figure 3.7.   PPARγ+ SV cells actively proliferate during development.   (A) P20 PPARγ-GFP mice were injected with BrdU and 2 hours later, adipose SV cells were isolated, plated and examined for expression of GFP (green) and for incorporation of BrdU (red).   Nuclei stained with DAPI (blue).   (B) GFP+ SV cells incorporate BrdU after 10 days of Dox pre-treatment.   PPARγ-GFP mice were treated with Dox from P15 to P25, then injected with BrdU and 12 hours later, adipose SV cells were isolated and examined for expression of GFP (green) or incorporation of BrdU (red).   Nuclei stained with DAPI (blue).   Note that the intensity of the GFP signal is reduced compared to (A) due to the 10 days of Dox treatment. Yellow arrows indicate cells that are both GFP and BrdU positive (white).   Scale bar: 50μm.

To see whether these PPARγ-expressing cells proliferate, I examined P20 GFP+ SV cells isolated after a BrdU injection and a brief 2-hour chase, designed to trap cells during the cell cycle and before differentiation. I found that many GFP+ SV cells incorporated BrdU (Figure 3.7A). A similar result was observed even when the BrdU pulse-chase was initiated after 10 days of Dox pre-treatment, done to ensure that cells containing both GFP and BrdU expressed GFP prior to initiation of the brief BrdU pulse (Figure 3.7B). Since the SVF contains PPARγ-expressing cells that are actively proliferating during development, they could potentially contribute to adipose tissue development.

To characterize the dynamics of SV resident PPARγ-expressing cells, I analyzed the SVF of P30 PPARγ-tTA reporter mice treated with or without Dox since P2. Flow cytometry profiles showed that Dox-induced a "leftward-shift", significantly decreasing the number and fluorescent intensity of GFP+ SV cells (Figure 3.8A, B), as expected if the cells were dividing and thereby diluting the H2B-GFP label and/or if they were exiting the SV compartment. To assess whether the progenitors remained in the SVF, I analyzed PPARγ-tTA; tetO-Cre; R26R P30 SV cells for expression of the indelible LacZ reporter after treatment without or with Dox for 28 days. I found that Dox did not reduce the number or percentage of SVF LacZ+ cells (Figure 3.8C), indicating that a stable pool of PPARγ-expressing cells is maintained in the SV compartment during the rapid expansion of adipose tissue from P2 to P30. The accumulated data suggest that adipose lineage progenitors, already instructed to express PPARγ very early in life, proliferate, differentiate into adipocytes, and also replenish the progenitor pool.
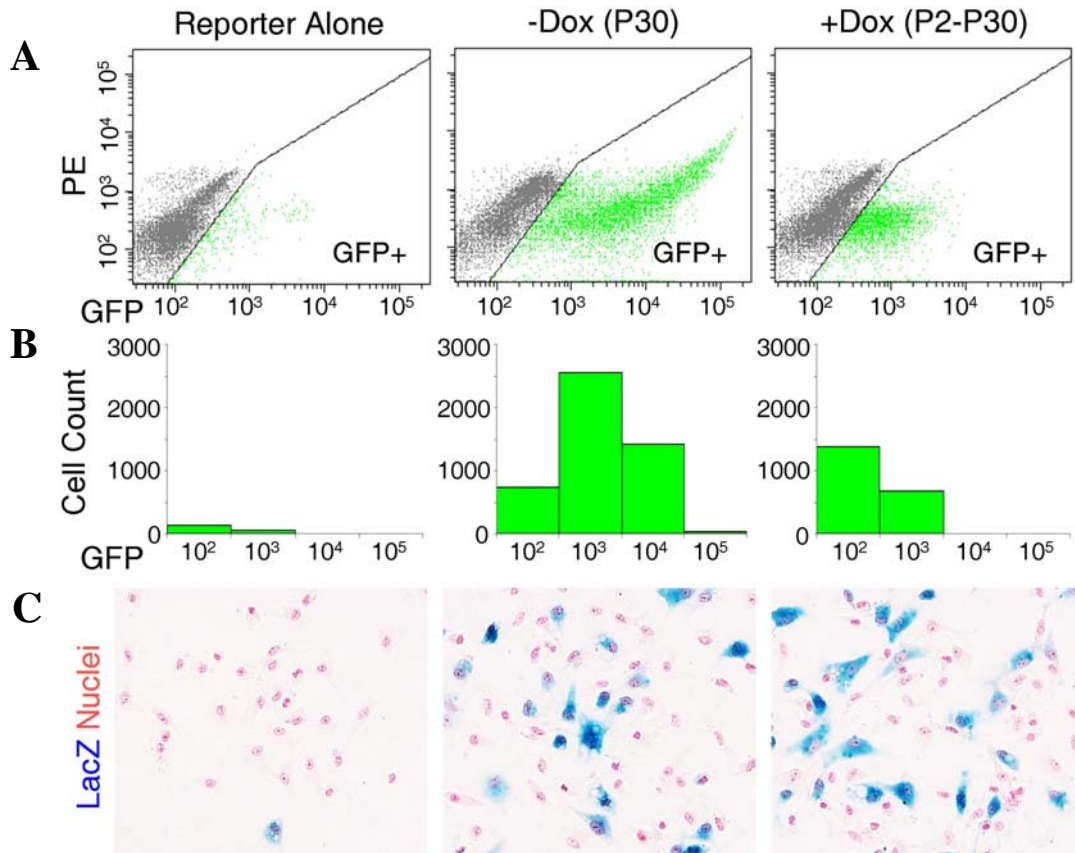
Figure 3.8. **PPARγ+ SV cells proliferate and replenish the progenitor pool during development.** Experimental paradigm is the same as Figure 3.3., except that SV cells were harvested from adipose tissues and examined for GFP and lacZ expression. (A) Flow cytometry profiles of SV cells of untreated tetO-H2B-GFP (left) or PPARγ-GFP treated without (middle) or with Dox (right). X-axis is GFP fluorescence intensity. Y-axis is PE channel to help illustrate the distribution of GFP+ cells. SV cells from tetO-H2B-GFP mice served as a gating control. (B) Quantification of cells gated as GFP+ from the flow cytometry profiles in (A). X-axis is the GFP fluorescence intensity; Y-axis is the cell count of the GFP+ cells per interval of fluorescence intensity with one unit being 1000. (C) SV cells removed from untreated R26R mice or PPARγ-R26R mice treated as indicated were isolated, plated for 4 hours, and stained with X-Gal (blue) and nuclear fast red (red). Dox treatment did not alter the number or percentage of lacZ+ cells based upon statistical analysis of >2,000 cells counted in each group. Scale bars: 50μm.

PPARγ+ SV Cells Respond to TZD

The plasticity of adipose tissues in adulthood is exemplified by the wide range of adiposity seen in human populations. The mechanisms controlling the plasticity of adult adiposity are unknown. Therefore, it would be interesting to test whether the mechanisms governing adipose tissue expansion during early development also operates during adulthood. TZD, PPARγ agonists widely prescribed for diabetes (Spiegelman and Flier, 1996; Lehmann et al., 1995), is a potent stimulus for increased adiposity via an unknown mechanisms, potentially recapitulating events occurring during adipose tissue expansion in the early stages of life.. So I treated adult PPARγ-tTA; double reporter mice at 4-5 months of age with rosiglitazone (one type of TZD) for 2 months in the presence or absence of Dox, and then examined the whole tissue and SV cells for lacZ and GFP expression (Figure 3.9). Similarly, adipose tissues from Dox treated and Dox+TZD treated groups have no less lacZ staining compared to the untreated group, although it is possible that the proliferation from the non-PPARγ source is too subtle to identify. But in fact, Dox+TZD treated adipose tissues have even stronger lacZ staining (Figure 3.9A). GFP intensity is mildly reduced in the Dox treated group, similar to 1-month Dox treatment at 4-month of age (not shown). However, TZD elicited a further reduction in GFP intensity (Figure 3.9B), suggesting a more rapid turnover of adipose tissue. This turnover could be the consequence of proliferation and/or removal of mature adipocytes reported in the literature (de Souza et al., 2001). The corresponding increase in lacZ staining is consistent with the increased proliferation of PPARγ-labeled cells, which brings more lacZ+ cells into the adipose tissues. Inspection of the SV population showed that, similar to the whole depots, the number and fluorescent intensity of GFP+ SV cells were further reduced by TZD in the presence of Dox suppression (Figure 3.9C), indicating that TZD stimulates the proliferation of SV resident

PPARγ+ cells, which might give rise to the small adipocytes that appear following TZD treatment (de Souza et al., 2001).   The effects on these PPARγ+ progenitors could be partially responsible for the therapeutic effects and/or undesirable side-effects of TZD.   The fact that these progenitors respond to TZD suggests physiological and pharmacological relevance of this population.
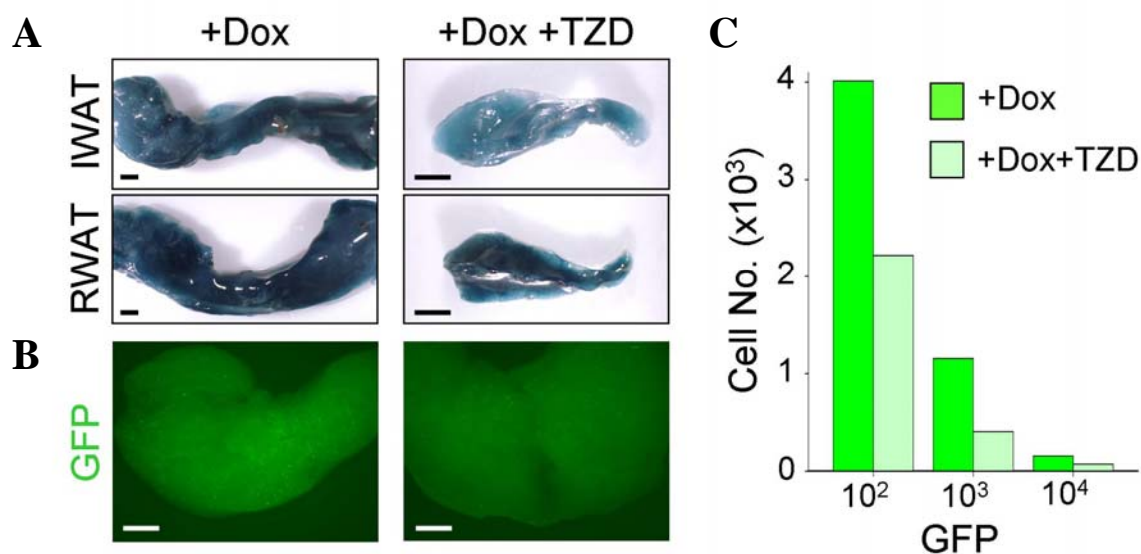
Figure 3.9.   PPARγ+ SV cells respond to TZD treatment in adult mice.   4~5-month old PPARγ-R26R (A) and PPARγ-GFP (B) mice were administered a two-month course of Dox without or with rosiglitazone (TZD).   Intact depots were examined for lacZ (A) and GFP (B) expression; (C) SV cells were examined for GFP expression using flow cytometry as in Figure 3.8 (B).   Scale bar: 2mm.

Together the results indicate that the SV compartment of adipose depots contains PPARγ-expressing cells that proliferate, are mobilized from and also repopulate the SVF, and behave as an amplifying population that contributes to the adipocyte lineage, responding to both developmental and pharmacological cues.

PPARγ+ SV Cells are Distinct from Adipocytes

Due to the nature of the density-based SV fractionation protocol, it remains possible that some GFP+ SV cells isolated could be differentiated adipocytes that had not yet accumulated enough lipids to float.

However, the FACS-isolated GFP+ SV cells (described below) were molecularly distinct from adipocytes, expressing higher levels of the preadipocyte marker Pref-1, the adipogenic inhibitor GATA3, and targets of the anti-adipogenic Wnt (Wisp2) and Hh (Smo, Gli3) pathways and much lower levels of numerous adipocyte markers (e.g. C/EBPs, ACC, FAS, HSL, adipsin, etc.) (Figure 3.10, 3.11).   Rather, expression analyses indicated that the GFP+ SV cells more closely resembled GFP- SV cells (Figure 3.11).   For instance, by RNA expression, PPARγ level in GFP+ SV cells is ~16 times higher than GFP- SV cells whereas PPARγ level in mature adipocytes is ~700 times higher.   These results indicate that the SV fraction may be divided into two distinct populations by the difference in PPARγ expression levels.   This difference has physiological relevance as reflected in the characteristic adipogenic potential of these two populations (see below).
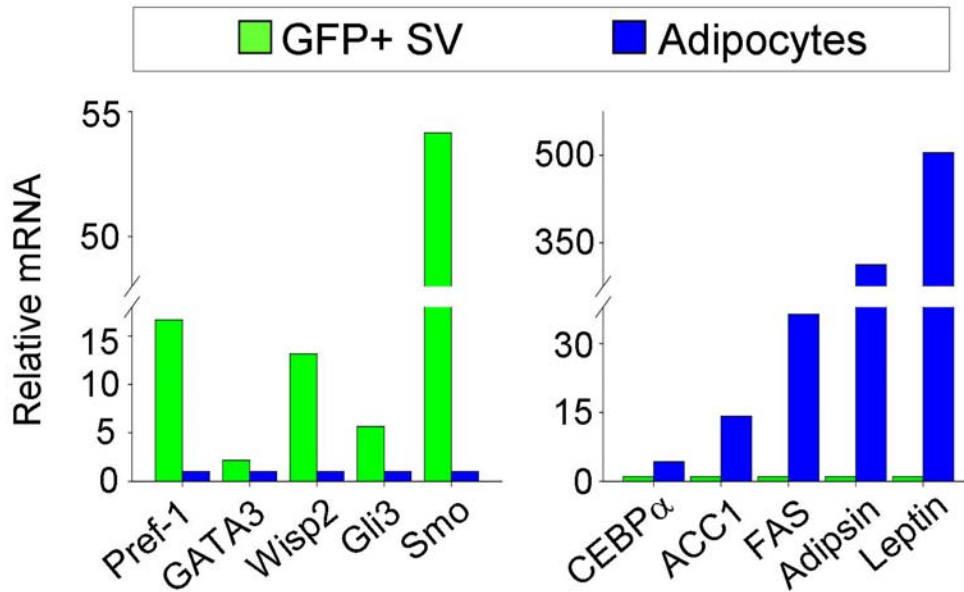
Figure 3.10. GFP+ SV cells are molecularly distinct from adipocytes. FACS-isolated GFP+ SV cells (green bars) and floated adipocytes (blue bars) were analyzed by quantitative PCR (qPCR) for the expression of the indicated markers.

Figure 3.11. GFP+ SV cells molecularly resemble GFP-SV cells more than adipocytes. Quantitative expression analyses of the indicated markers of FACS-isolated GFP- SV cells (purple bars), FACS-isolated GFP+ (green bars), and floated adipocytes (blue bars).
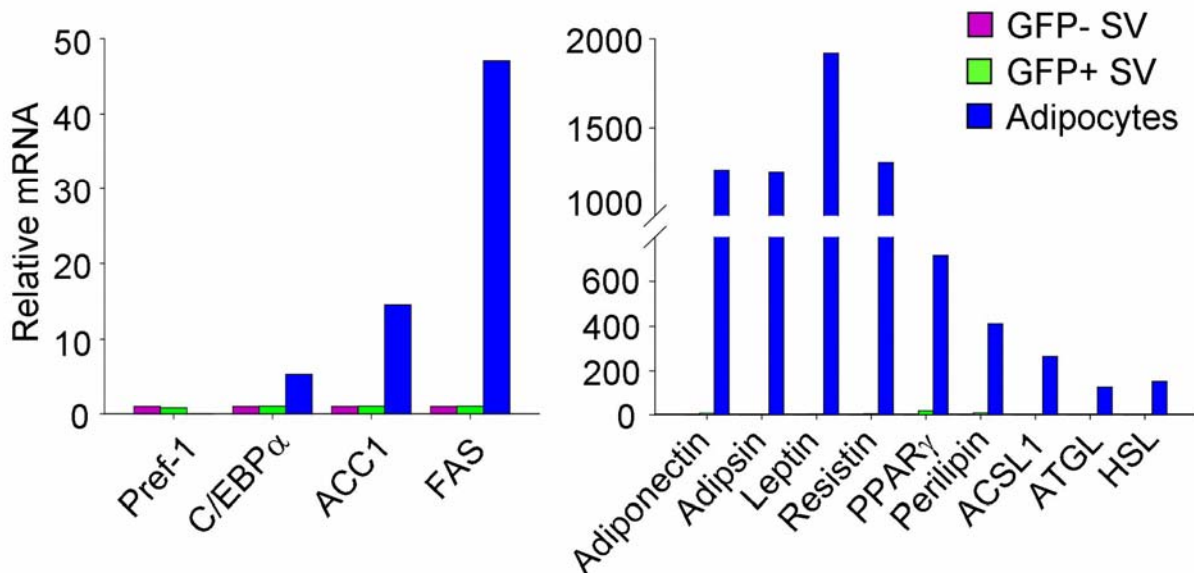
However, molecular, i.e. gene expression, analysis reflects the properties of the whole population instead of individual cells. It is a possibility that the effects of contaminating adipocytes might disproportionately contribute to the gene expression patterns of the whole population. So I examined the individual cells for the expression of differentiation markers such as perilipin and aP2 in adherent GFP+ SV cells (Figure 3.12). Immunocytochemical analyses showed that the GFP+ SV cells did not express perilipin (Figure 3.12A), a classic adipocyte marker which is associated with the periphery of lipid droplets in adipocytes. aP2 is another marker of adipocytes and a PPARγ target gene. To analyze aP2 expression in individual cells, I utilized mice with reporters driven by the 5.4kb promoter/enhancer of aP2 (Graves et al., 1992), which displayed strong expression in adipose depots and adipocytes (Figure 3.12B). Adipose SV cells isolated from aP2-GFP mice have a fraction of GFP+ cells that are comparable to PPARγ-GFP, but ~83% of GFP+ SV cells expressed endothelial marker PECAM and ~73% expressed macrophage marker Mac-1, in contrast to the minor percentages in PPARγ-GFP SV cells (~16% for PECAM, ~6% for Mac-1) (Figure 3.12C). When aP2-GFP SV cells were plated, the adherent cells did not express GFP, unlike PPARγ-GFP reporters (Figure 3.12B). Similar results were produced using aP2-Cre; R26R (Figure 3.12D). The accumulated data suggest that GFP+ SV cells do not express adipocyte markers. Therefore, differentiated adipocytes are either absent, or rare events not detectable by standard methods, within the GFP+ SV cells isolated and studied.
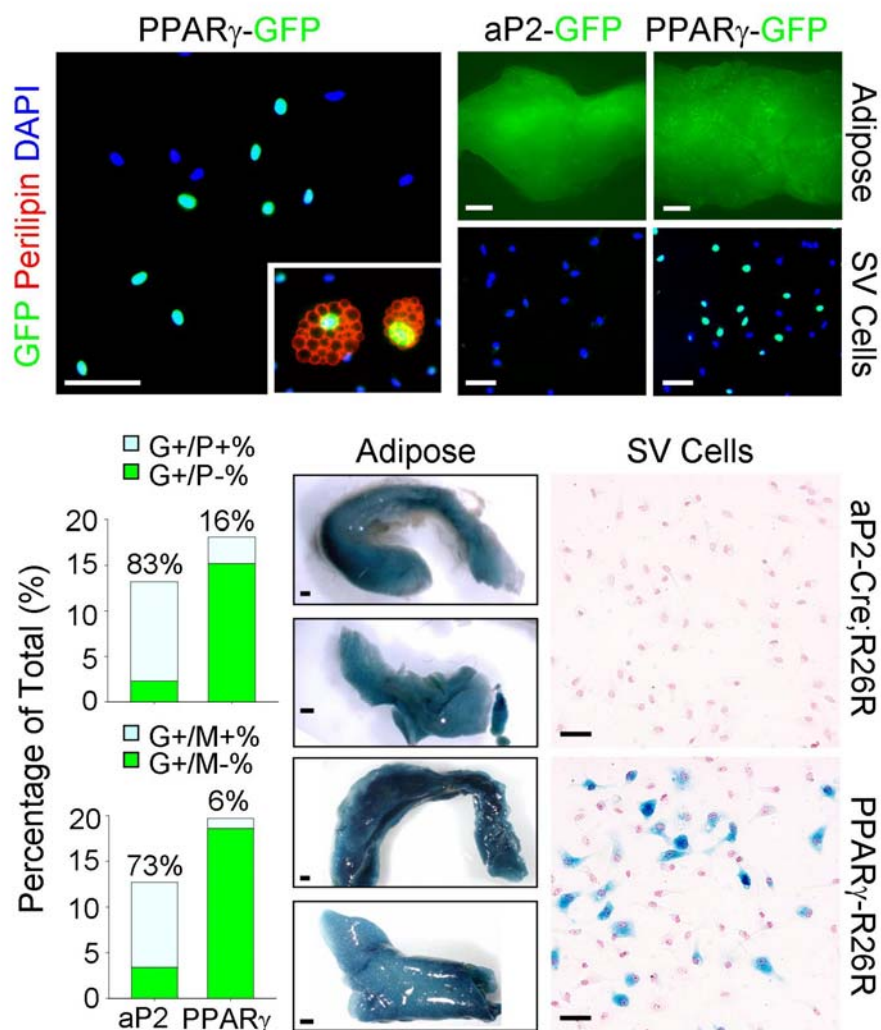
Figure 3.12. PPARγ+ SV cells do not express adipocyte marker perilipin and aP2. (A) adipose SV cells from P30 PPARγ-GFP mice were examined for GFP (green) and immunocytochemically analyzed for expression of perilipin (red), a marker of adipocytes, which serve as a positive control (inset). Nuclei stained with DAPI (blue). (B) Left panels: IWAT (adipose, top) and SV cells (bottom) of aP2-GFP transgenics were analyzed for GFP expression, which was present in the adipose depot but not in the SV cells. PPARγ-GFP serves as a control. (C) aP2-GFP (aP2) and PPARγ-GFP (PPARγ) SV cells were analyzed by flow cytometry with cell surface markers PECAM (P) and Mac-1 (M) and the percentages of GFP+ cells that were positive or negative for PECAM or Mac-1 were shown in bar graphs. The percentages of double possible (GFP and indicated marker) cells in GFP+ cells were shown on top of corresponding bars. (D) aP2-Cre indelible marking labels adipose depots but not stromal vascular cells. β-gal staining of adipose tissues and adipose SV cells from aP2-Cre; R26R and PPARγ-R26R mice, the latter serves as a positive control. For each strain of mice, two representative depots are shown: IWAT (top panel) and GWAT (bottom panel). Nuclei counterstained with nuclear fast red. Scale bar: 50μm (A, B bottom panels, D right panels), 1mm (B top panels, D left panels).

Characterization of PPARγ+ SV Cells

With the aid of the PPARγ-GFP reporter mice and fluorescence-activated cell sorting (FACS), I further analyzed the properties of PPARγ-expressing SV cells directly by flow cytometry and indirectly by sorting followed by *in vitro* culture.   I found that the PPARγ GFP+ (GFP+) SV cells constituted approximately 10% of the total SV pool (Figure 3.13A).   GFP+ SV cells could be detected as early as E16.5, and the dynamics of this progenitor pool at different developmental stages (P10, P30, P120) was monitored by flow cytometry (Figure 3.13B). Starting time point P10 is approximately the earliest time at which quantitation becomes accurate and reproducible.   The size of the total SV pool grows with age, which is not surprising since the vasculature, a major component of the SVF, develops in concordance with adipose depot expansion.   Interestingly, the absolute numbers of GFP+ SV cells per mouse show very little change that is not statistically significant across the various ages examined.   Therefore, as the SV pool increases in number during development, the percentage of GFP+ cells in the total SV pool actually decreases over time.   If this PPARγ+ SV pool is indeed the progenitor pool, my results suggest that this progenitor pool is specified early in development with a defined size, actively proliferating to generate new adipocytes and at the same time replenishing itself to maintain the pool to a fixed size.
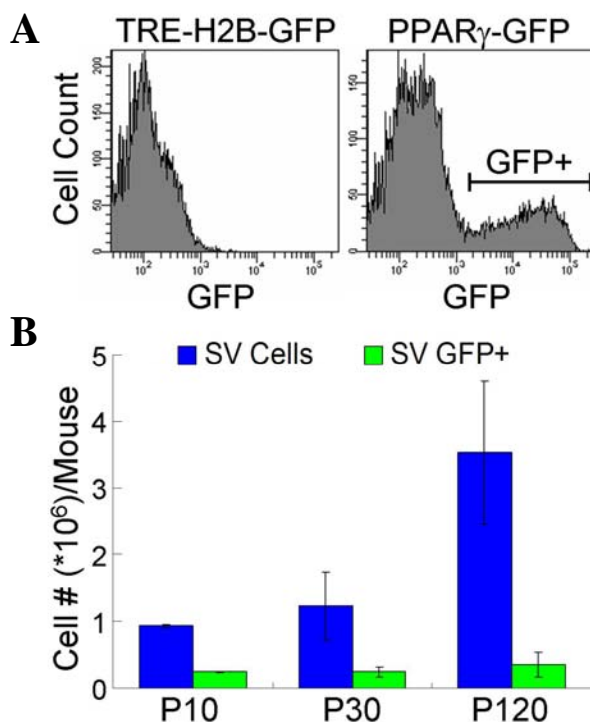
Figure 3.13 GFP+ SV pool maintains a constant size at various ages. (A) GFP+ cells were present in adipose SV fraction of PPARγ-GFP mice. Flow cytometry profiles of SV cells obtained from P30 tetO-H2B-GFP (left) and PPARγ-GFP (right) WAT. The profiles only include cells that had equivalent forward and side scattering as the GFP+ SV pool. (B) The number of adipose depot GFP+ SV cells remains relatively constant in mice during the first six months of life. Flow cytometry quantitation of the number of SV cells and GFP+ SV cells obtained from PPARγ-GFP mice at the indicated ages. Error bars indicate standard error of the mean (SEM). Each experiment was a pool of more than 5 mice of the same age, and each time point includes 3-6 independent experiments.

Cell surface marker analysis showed that the majority of GFP+ SV cells expressed Sca1 (>90%), and only a small percentage (<10%) of GFP+ SV cells expressed CD105, CD45 (hematopoietic lineage), PECAM (endothelial cells) or Mac-1 (macrophages), the latter indicating that the majority of GFP+ SV cells were not macrophages, a cell type in which PPARγ can also be expressed (Tontonoz et al., 1998). Further, adherent sorted GFP+ SV cells had considerable proliferative capacity based upon their growth curve and their ability to incorporate BrdU (Figure 3.14A). However, compared to GFP- cells, the proliferation rate of GFP+ SV

cells is slower (see below).   Moreover, after the GFP+ SV cells were passed in culture for 5-10 times in DMEM+10% FBS, which lasted about one month, they became senescent and stopped proliferating in culture.

Next, I assessed the adipogenic potential of the FACS-isolated GFP+ SV cells *in vitro* and after transplantation.   In culture, the sorted GFP+ SV cells underwent spontaneous and insulin-stimulated adipogenesis that was dramatically enhanced compared to GFP- SV cells (Figure 3.14B, C, D).   GFP+ SV adipogenesis appeared to mirror the gene expression patterns described for preadipocyte cell line adipogenesis (Figure 3.14E) (Ntambi and Young-Cheul, 2000).

To test the adipogenic potential of GFP+ SV cells *in vivo*, I transplanted freshly isolated GFP+ SV cells subcutaneously into nude mice.   After 1 month, I detected formation of a GFP-expressing tumor whose appearance and consistency were characteristic of adipose tissue (Figure 3.15A).   Histological analyses revealed the presence of lipid-laden adipocytes that co-expressed GFP and perilipin (Figure 3.15B, C, D).   In contrast, if GFP- SV cells were similarly transplanted into nude mice, no fat pad was formed.   Only several small cell clusters containing a few lipid-laden adipocytes were scattering inside the matrix (Figure 3.15B).   These cell clusters might be derived from single cells, which could be GFP+ SV cells due to incomplete separation or a "stem" population existing in the GFP- SV fraction.   The accumulated data show that PPARγ-expressing SV cells are phenotypically distinct from adipocytes and have strong adipogenic potential both *in vitro* and *in vivo*, further supporting the notion that they are adipogenic progenitors.
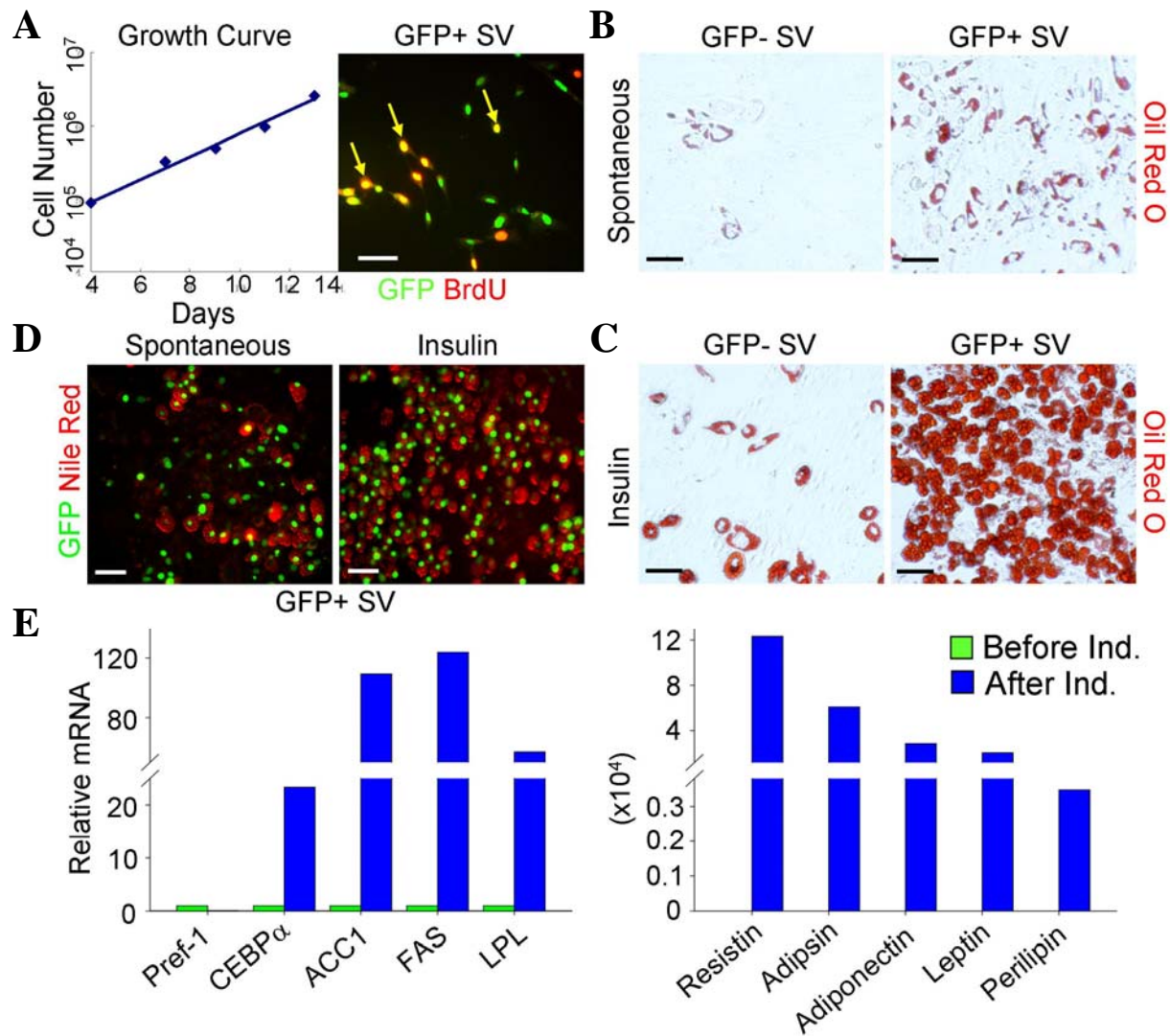
Figure 3.14. GFP+ SV cells proliferate and under adipogenesis *in vitro*. (A) GFP+ SV cells from P30 PPARγ-GFP mice were isolated by FACS and cell proliferation analyzed either with growth curves (left panel) or BrdU (red) incorporation (right panel) GFP (green). Yellow arrows indicate BrdU + GFP cells (yellow-orange). (B, C, D) GFP- and GFP+ SV cells from PPARγ-GFP mice were sorted, plated, cultured to confluence and adipogenesis, occurring either spontaneously (B, D) or in the presence of insulin (C, D), examined with the lipid-specific stains Oil Red O (Red) and Nile Red (Red). In D, sorted GFP+ cells were stained with Nile Red, a fluorescent dye, to allow simultaneous visualization of fat accumulation and GFP expression. (E) Expression levels of the indicated markers were examined in sorted GFP+ cells before and after insulin-stimulated adipogenesis. Scale bars: 50μm (A-D).
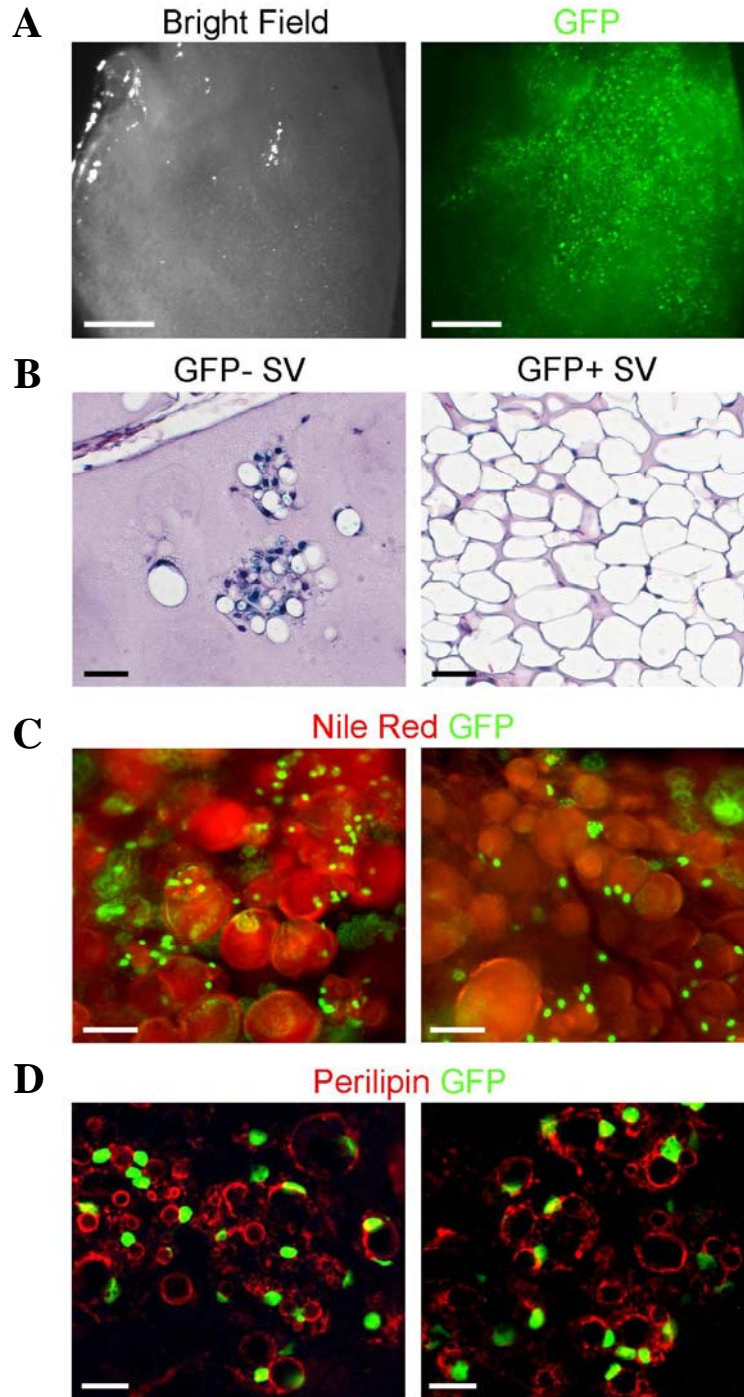
Figure 3.15. GFP+ SV cells formed fat pad after transplantation. FACS-isolated GFP+ SV cells were implanted into nude mice and the tumor that formed after 1 month was photographed with bright field (A, left panel) and fluorescent microscopy (B, right panel) and examined histologically with H&E staining (B, right panel), GFP fluorescence and Nile Red staining (C), and GFP fluorescence and perilipin immunochemistry (D). GFP- SV cells were similarly implanted into nude mice, and the tissues formed after one month was examined histologically with H&E staining (B, left panel). Scale bars: 2mm (A), 50μm (B, C), 20μm in confocal images (D).

Inhibitory Effect of Wnt Signaling on the Adipogenic Progenitors

As Wnt signals inhibit cell culture adipogenesis prior to the expression of PPARγ and potentially before initiation of the terminal differentiation program (Prestwich and MacDougald, 2007), it would be interesting to see how GFP+ SV progenitors respond to Wnt signaling. So I assayed the adipogenic potential of the GFP+ SV cells cultured to confluence and incubated with Wnt3a conditioned medium or LiCl to activate the Wnt signaling pathway (Figure 3.16). In control cells without Wnt3a or LiCl, full induction pushed the majority of cells in the culture to accumulate lipids and become adipocytes. But when the cells were treated with either Wnt3a or LiCl, adipogenesis was almost completely abolished. The responsiveness to the anti-adipogenic actions of Wnt supports the notion that GFP+ SV cells display the characteristics of adipogenic progenitors, similar to preadipocyte cell lines (Ross et al., 2000).

Figure 3.16.   GFP+ SV cell adipogenesis is blocked by activation of Wnt signaling pathway. GFP+ SV cells were cultured in insulin with control- or Wnt3a-conditioned 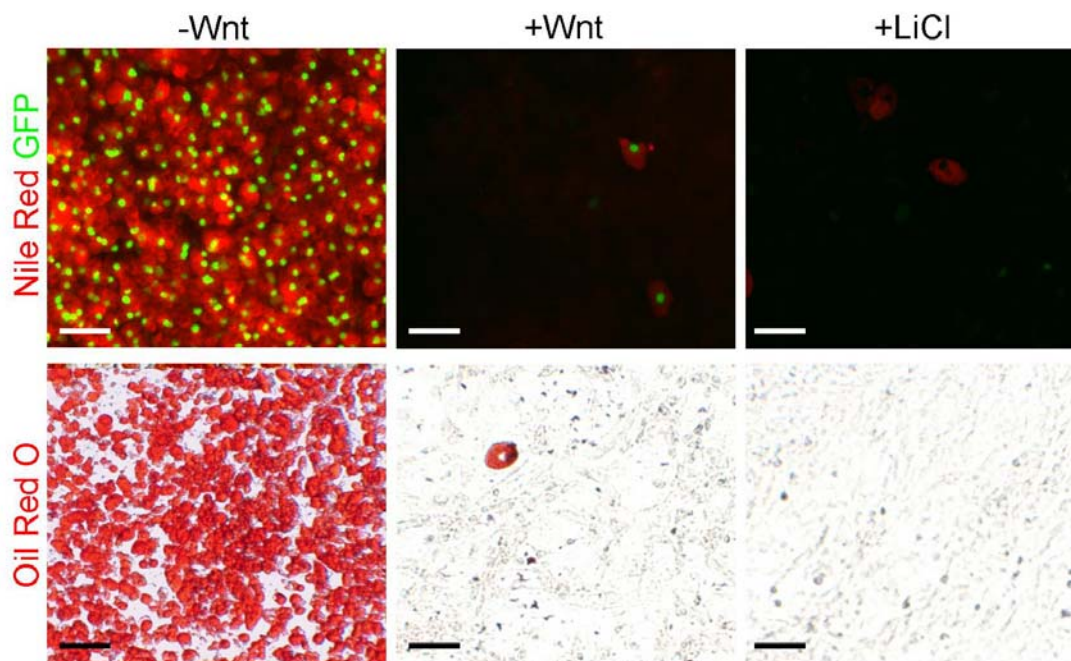media or LiCl and adipogenesis was assed by staining with Nile Red (red, top panel) or Oil Red O (red, bottom panel). Scale bars: 50µm.

To test this effect *in vivo,* I activated the Wnt pathway within PPARγ-expressing cells by breeding PPARγ-tTA; tetO-Cre mice with mice harboring a conditional constitutively active β-catenin allele (Catnb$^{lox(ex3)}$) in which the exon containing the negative regulatory domain of β-catenin is flanked by *loxP* sites (Harada et al., 1999). These mice displayed significantly reduced fat formation (Figure 3.17A). In adipose depots, there was massive reduction in the number of adipocytes (Figure 3.17B), suggesting that the activation of Wnt signaling in the PPARγ+ cells blocks adipogenesis. However, if β-catenin is activated using a late driver such as aP2-Cre, the reduction in adipose formation is marginal (JMS and JMG, in preparation). These observations are consistent with the idea that PPARγ-expressing cells are progenitors, and activating Wnt in these early progenitors will block adipogenesis and hence abolish fat formation. In these adipose tissues, fat formation was blocked and fibrosis took place (Figure 3.17B), which might be an effect brought about by Wnt activation in the progenitors. I also isolated SV cells from PPARγ-tTA; tetO-Cre; Catnb$^{lox(ex3)}$ mice and corresponding control groups (PPARγ-tTA; Catnb$^{lox(ex3)}$ and tetO-Cre; Catnb$^{lox(ex3)}$), and assessed the adipogenic potential. In contrast to the potent differentiation that occurred in control SV cells, Wnt-activated SV cells completely failed to differentiate into adipocytes (Figure 3.17C). I didn't observe any defect in the adipogenic potential of PPARγ heterozygous controls (PPARγ-tTA; Catnb$^{lox(ex3)}$), ruling out PPARγ haploinsufficiency as a potential confounding factor. Even when Dox was added to suppress tTA and shut off any further β-catenin activation after SVF isolation, the blockage of adipogenesis cannot be rescued (Figure 3.17C), supporting the notion that PPARγ+ progenitors are the only source for adipocyte formation *in vivo* and that this population is specified during early development.
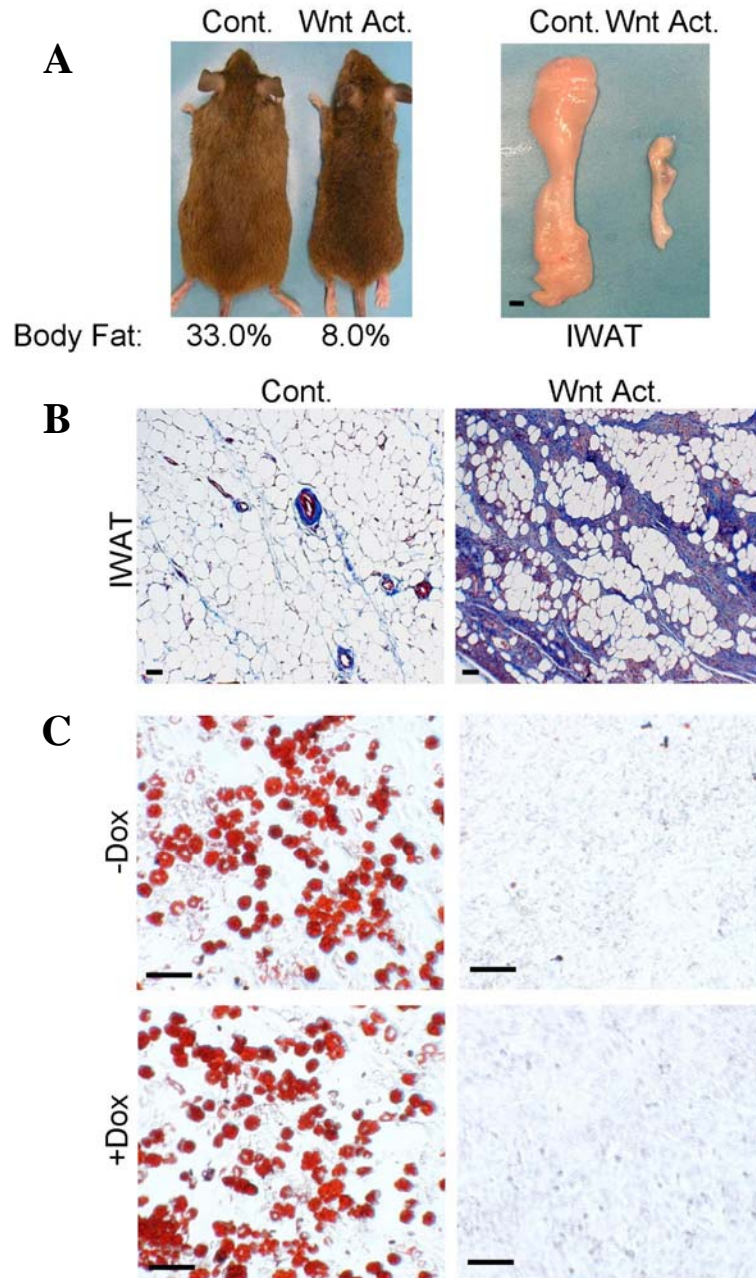
Figure 3.17 **Activation of Wnt in PPARγ-expressing cells blocks adipogenesis *in vivo*.** (A) Left panel: Pictures and body fat content measurements of PPARγ-tTA; tetO-Cre; Catn^blox(ex3) mice (Wnt Act.) and control (Cont.) littermates were taken at 10 months of age. Right panel: Inguinal WAT (IWAT) from control and Wnt-activated mice were dissected and pictures were taken. (B) Trichrome staining was performed on 5um paraffin sections of IWAT from control and Wnt activated mice. Blue: collagen. (C) Adipose SV cells were harvested from control and Wnt-activated mice and cultured to induce adipogenesis in the absence (top panel) and presence (bottom panel) of Dox. Adipogenesis was assessed by Oil Red O staining (red). Scale bar: 1mm (A, right panel), 50μm (B, C).

Age-Dependent Alteration in the Properties of GFP+ SV Cells

Since PPARγ+ progenitors seem to be actively involved in development and TZD-stimulated adiposity, further investigation into the developmental dynamics of this population as a function of age might aid our understanding of obesity.

Because the GFP+ SV pool remains relatively constant in size, it is of interest to examine the relative contributions of proliferation, cell death and differentiation in maintaining this pool. If SV cells differentiate and become adipocytes, they are no longer detected in the isolated SV pool, and this represents another way for GFP+ SV cells to exit the SV pool besides undergoing apoptosis. To maintain a constant size of this pool, the proliferation rate should be similar to the apoptotic rate plus the rate at which these SV cells become adipocytes. Unfortunately, there is no good way to directly measure the rate at which the SV cells become adipocytes. However, the proliferation rate could be measured by detecting BrdU incorporation with flow cytometry 12 hours after a single pulse of BrdU injection. The apoptotic rate could be measured by the presence of apoptotic cell surface markers such as Annexin V (Vermes et al., 1995). Examination of BrdU and Annexin V staining by flow cytometry revealed that P20 GFP+ SV cells have a higher proliferation rate and less apoptotic cells than P120 GFP+ SV cells (Figure 3.18), which in turn indicates that P20 GFP+ SV cells have a higher rate at adipocyte conversion. Some of these findings could be further confirmed by *in vitro* culture studies.

When the proliferation rate was measured by growth curve in culture condition, P20 GFP+ SV cells proliferated much faster than P120 GFP+ SV cells (Figure 3.19A). I compared the adipogenic potentials for P20 and P120 GFP+ SV cells by culturing them and inducing adipogenesis. Strikingly, P20 GFP+ SV cells have much higher adipogenic potential compared to P120 cells in both regular medium and insulin induction (Figure 3.19B). Taken together,

GFP+ SV cells from younger mice proliferate faster and become adipocytes much more efficiently than older mice both *in vivo* and *in vitro*, potentially explaining how the burst of adipose tissue expansion is achieved during postnatal development.
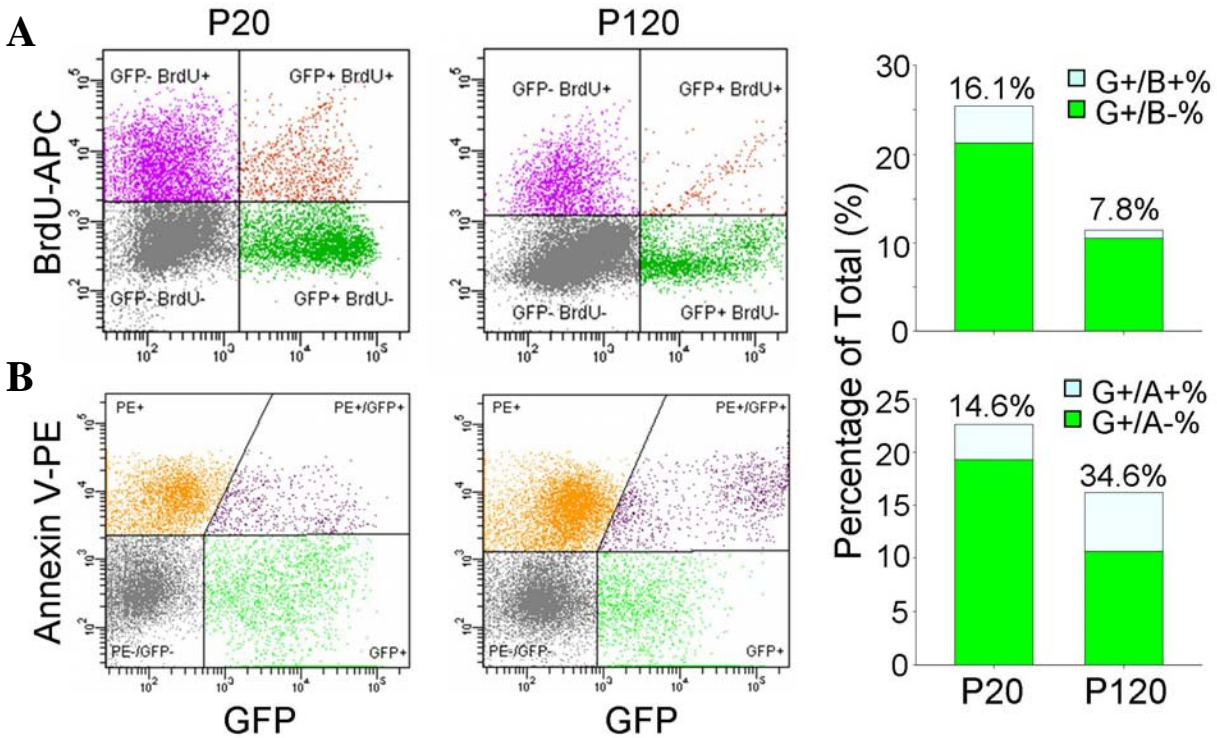
Figure 3.18.   Proliferation rate is higher while apoptotic rate is lower in GFP+ SV cells from younger mice.   (A) Proliferation rates were assessed by BrdU incorporation and detection by flow cytometry in SV cells from P20 (left panel) and P120 (middle panel) PPARγ-GFP mice. The percentages of indicated populations were quantified and plotted into a bar graph (right panel).   The percentages of double positive cells in GFP+ cells were shown on top of the bars. (B) Apoptotic rates were assessed by the detection of Annexin V on the cell surface with flow cytometry and presented as in (A).
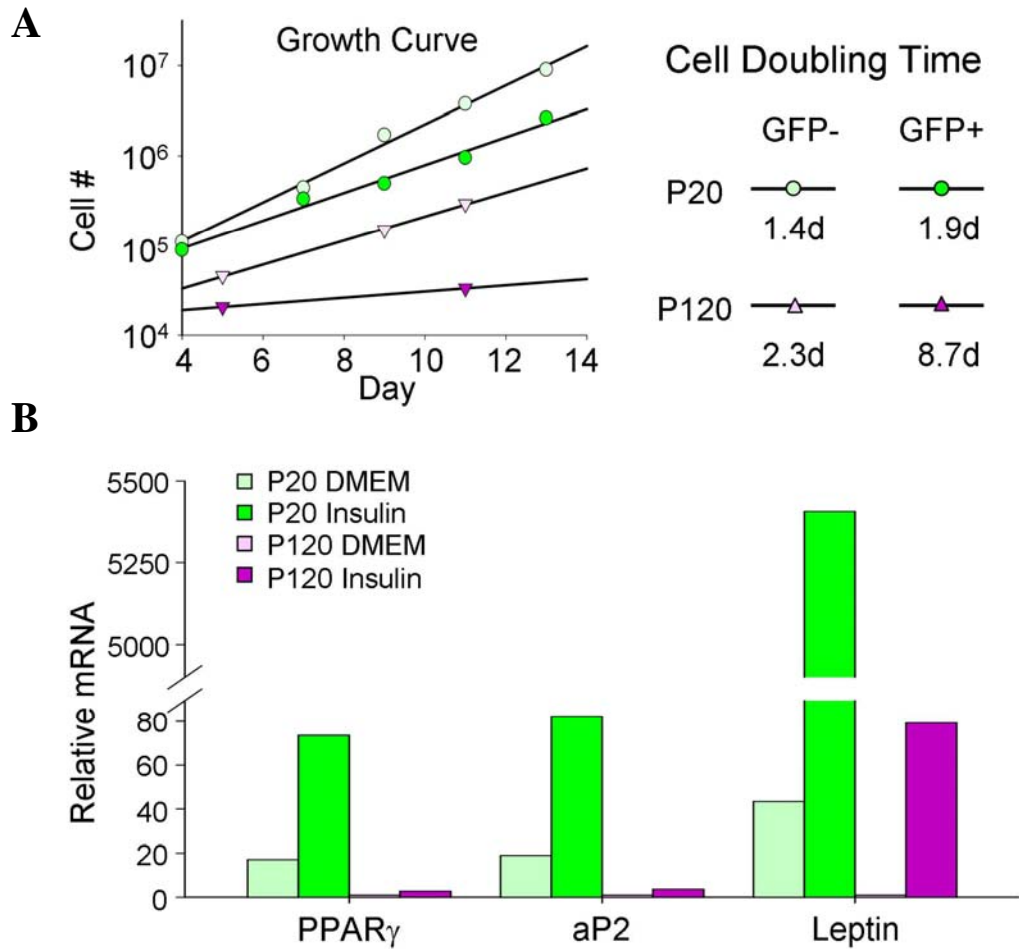
Figure 3.19. P20 GFP+ SV cells proliferate faster and have higher adipogenic potential than P120 GFP+ SV cells. (A) Proliferation rates of P20 and P120 GFP+ and GFP- SV cells in culture were measured by growth curve (left panel). Double time for each population is shown on the right. (B) P20 and P120 GFP+ SV cells were cultured in growth medium (DMEM) or growth medium containing insulin (insulin). Adipogenic potentials were assessed by measuring the expression of PPARγ, aP2 and leptin.

Discussion

The development of the adipocyte lineage is a fundamental and largely uncharacterized biological problem with important ramifications for human health and diseases (Ailhaud et al., 1992; Gesta et al., 2007). Yet the identity of the adipocyte progenitors has remained elusive. Exploiting genetic tools I provide evidence that the pool of murine adipocyte precursors has largely been committed early in the postnatal period. These precursors divide, maintain the progenitor pool, and contribute to adipose lineage in response to developmental and pharmacological cues *in vivo*. These progenitors are morphologically and molecularly distinct from adipocytes, have high potential to undergo adipogenesis both *in vitro* and after transplantation, and respond to the inhibitory effect of the Wnt signaling pathway. The newly established tools allow the prospective isolation of this progenitor population and further characterization of its properties.

With the notion that PPARγ expression could label adipose progenitors, it would be very interesting to revisit the lineage tracing experiment discussed previously (Chapter II) to determine when adipose depots are specified. The time window during which the transition from white-to-blue labeling occurs is when the PPARγ-expressing progenitor pool forms in that particular depot. My findings indicate that the window of time in which progenitor pools form is narrow for most adipose depots, and once the progenitor pool is formed, it functions as a self-renewing population that serves as a source to produce new adipocytes to meet the demand for tissue growth. Anatomically distinct fat depots each display their own distinct and stereotypic timing for the specification of these progenitor pools, thus suggesting that progenitor pools form *de novo* in a depot-specific manner. The notion that various fat depots are derived

from distinct precursor population has long been speculated (Gesta et al., 2007), and the results presented here offer direct support for this idea. Lineage tracing tools marking cells preceding PPARγ expression would be required if depot-specific progenitor pools indeed share a common lineage.

Based on their broad range of GFP intensity, GFP+ SV cells might be a heterogeneous population in terms of PPARγ expression. This heterogeneity becomes more apparent when GFP+ SV cells are FACS-sorted and plated, where a certain fraction of these cells will not adhere to the culture dish or proliferate like the rest. PPARγ expression measured by qPCR is the averaged level of the whole population, and so is PPARγ expression in GFP- SV cells. Within the population, individual cells might display a broader range of PPARγ expression. But as a whole, there is only a modest increase of PPARγ expression in GFP+ SV compared to GFP- SV. Nonetheless, the modest up-regulation of PPARγ expression in GFP+ SV cells could be detected and amplified by the reporter system, providing an *in vivo* label for cells which could not be detected otherwise. On the other hand, the several hundred folds up-regulation of PPARγ in adipocytes is not reflected proportionately by their GFP intensity, indicating that this reporter system is likely saturated in adipocytes that have much higher PPARγ expression. PPARγ+ SV progenitors, although labeled by reporters, can be more accurately described as a "PPARγ^{low}" population, expressing much lower endogenous PPARγ as compared to adipocytes, which likewise can be described as a "PPARγ^{high}" population. If the mechanism discovered in cell culture adipogenesis models also applies here, C/EBPs are responsible for this up-regulation of PPARγ, which in turn requires a "brake" mechanism to restrain the positive feedback loop from excessive reinforcement of PPARγ expression. Alternatively, a novel mechanism might be in place to drive and maintain this PPARγ^{low} progenitor state. Key developmental signaling

pathways might play a role in maintaining the progenitor pool, such as Wnt, Hedgehog, and Notch, some of which have been shown to affect adipogenesis (Rosen and MacDougald, 2006). With the progenitor cells readily labeled, easily isolated and cultured, the involvement of these signaling pathways could be a fruitful avenue for future investigations.

One way to analyze the subpopulations in GFP+ progenitors is to sort the GFP+ cells based on GFP intensity, e.g. GFP^{low}, GFP^{medium}, GFP^{high}, and use microarray or qPCR to look for differential gene expression. It is possible that GFP intensity of these subpopulations mirrors the PPARγ level; given the importance of PPARγ in adipocyte differentiation, the subpopulations might represent the intermediate steps between primitive progenitors and adipocytes. The caveat is that the stability of H2B-GFP limits its ability to dynamically mirror the changes of endogenous PPARγ. Another way to further characterize GFP+ SV population is to separate the subpopulations by cell surface marker analyses. Molecular analysis of the isolated subpopulation combined with adipogenic assays will be instrumental for characterizing the properties of the subpopulations within the GFP+ SV pool.

The nature of GFP- SV cells remains largely uncharacterized in my studies. GFP- SV cells displayed much less adipogenic potential than GFP+ SV cells. Nevertheless, a small fraction of them can still undergo adipogenesis, although much fewer in number and lowered in efficiency as compared to the GFP+ SV cells. What are the properties of these cells? They could actually be contaminating GFP+ SV cells as a result of incomplete separation by FACS. Alternatively, they could have PPARγ up-regulated but not above a threshold to turn on the GFP reporter. The latter is more likely because the GFP reporter and the R26R reporter overlap 80~90%. Although lineage tracing results showed that R26R labeled the progenitors, the GFP reporter was actually used to isolate, characterize, and functionally define the progenitor cells.

Interestingly, roughly 10-20% of GFP- cells are labeled by R26R reporter, which might be responsible for the residual adipogenic potential in GFP- SV fraction.   If progenitor cells are isolated based on the combination of both reporters, and higher purity is achieved by repeated sorting, the GFP- population would be expected to have further reduced adipogenic ability. However, it remains possible that GFP- SV fraction contains the so called "mesenchymal stem cells" that can give rise to adipocytes in culture.   In fact, when I cultured and induced GFP- SV cells from P20 adipose tissues, clusters of adipocytes formed (not shown), which seemed to be derived from single cells.   This effect is less obvious in older mice.   Even though the mesenchymal stem cells might be present in the GFP- SV population, based on the lineage tracing results, they do not account for the rapid expansion of adipose depots during early postnatal development. Rather, they more likely serve as a reservoir for multiple cell lineages and activated under specific situations, e.g., embryogenesis, tissue damage/regeneration, and obesity.

In the past, the presence of adipose progenitors has been widely accepted while their properties are poorly defined.   A multi-step cascade has been proposed for adipocyte differentiation *in vivo* without clear definition.   It is suggested that multipotent mesenchymal stem cells give rise to adipoblasts, and adipoblasts give rise to preadipocytes, which eventually differentiate to adipocytes (Gesta et al., 2007; Otto and Lane, 2005).   The definition for each intermediate population is lacking and no evidence exists to prove the presence of these intermediate steps.   Here using genetic methods, I identified an interesting population of cells that seem to qualify as the adipose progenitors.   The properties of these cells are: 1) the cells proliferate during development; 2) the cells give rise to adipocytes; 3) the cells are not differentiated adipocytes.   Such properties define this unique progenitor population.   Currently

it is hard to fit this progenitor population to any intermediate population described above.   It remains possible that this heterogeneous progenitor population includes some combination of mesenchymal stem cells, adipoblasts, and preadipocytes.   Further characterization of this progenitor population and the rest of the SV pool are necessary to address whether the PPARγ+ SV cells represent the definitive *in vivo* progenitor pool for adipose tissues.

A technical limitation inherent to the PPARγ lineage tool is that PPARγ expresses not only in the progenitor cells presented here, but also in the adipocytes.   For example, the notion that PPARγ+ SV cells directly give rise to adipocytes *in vivo* cannot be directly proved by lineage tracing because PPARγ labels both sets of cells and thus no distinction can be made. However, since this progenitor population can be prospectively isolated and molecularly analyzed by microarray, some genes that have restricted expression in PPARγ+ SV cells but not in adipocytes could be identified.   Using genetic tools made from targeting these hallmark genes, lineage tracing could be performed to rigorously test whether these progenitor cells indeed produce adipocytes *in vivo*.   More importantly, gene functional studies could thus be carried out specifically in progenitor cells.

The results presented here are clinically relevant as the formation of new adipocytes from a heretofore-unidentified progenitor cell is a key event in the development of obesity and diabetes. Current therapies for these prevalent diseases are inadequate and new approaches are urgently required.   With more in-depth knowledge, adipose progenitor cells could be a potential therapeutic target for obesity.   So these studies provide a foundation for new obesity and diabetes therapeutic strategies.

Materials and Methods

Materials

Reagents from Sigma except: type I collagenase (Worthington), BODIPY (Invitrogen), and DAPI (FLUKA), meshes (Small Parts Inc., Miami Lakes, FL), Trizol (Invitrogen), DNase-I (Invitrogen), random hexamers (Invitrogen), M-MLV reverse transcriptase (Invitrogen), rosiglitazone (GlaxoSmithKline), Power SYBR Green PCR Master Mix (ABI), Matrigel Matrix (BD Biosciences), CCLR buffer (Promega), β-galactosidase Assay Kit (Strategene), Micro BCA Protein Assay Kit (Pierce), BrdU Flow Cytometry Assay Kit (BD Biosciences). Antibodies: rabbit anti-GFP (Chemicon), mouse anti-BrdU (BD Biosciences), rabbit anti-perilipin (Sigma), cy2 donkey anti-rabbit, cy3 donkey anti-mouse, cy3 donkey anti-rabbit were from Jackson ImmunoResearch. Flow cytometry antibodies: Sca1-PE (BD Biosciences), Mac1-PE (BD Biosciences), CD45-APC (BD Biosciences), CD105-PE (BD Biosciences), Annexin V-PE (BD Biosicences). Immunohistochemistry images were collected on a Zeiss LSM500 confocal microscope. Immunocytochemical photography was done with an Olympus upright BX40 microscope. Direct GFP fluorescence was observed with a Zeiss Stemi SV11 microscope for tissues, a Zeiss LSM500 confocal microscope for immunohistochemistry, or an Olympus IX70 inverted microscope for cells. Flow cytometry and FACS was carried out on BD FACSCalibur^{TM} flow cytometer. RT-PCR was performed on ABI 7500 Real-Time PCR System. β-galactosidase levels was quantitated with a DU730 Life Science UV/Vis Spectrophotometer (Beckman Coulter) and protein concentration determined and normalized on a POLARstar OPTIMA plate reader (BMG Labtech).

Animals

Mouse maintenance was as described in Chapter I.   BrdU (50mg/kg body mass) was I.P. injected.   For TZD treatment, 5 month-old mice were fed with rosiglitazone at 0.0075% in food for 2 months.   Rosiglitazone intake was estimated to be 15mg/kg body mass/day.   CD-1 nude mice were from Charles River Laboratories.   aP2-GFP mice were generated by Ed Fortuno III. aP2-Cre was a generous gift from Robert Hammer. Body fat content was measured by NMR spectroscopy with the Minispec mq spectrometer (Bruker).

β-gal Staining and Quantification

β-gal staining on the adipose tissue explants was described in Chapter I.   The similar procedure was carried out for cells, with the fixation step and wash steps shortened to 5 minutes. The cells were stained for two days at 37°C, followed by counterstaining with nuclear fast red, and mounted on slides.   To quantify adipose depot β-galactosidase activity, adipose tissues were dissected (50-100mg) and snap-frozen in liquid nitrogen in eppendorf tubes.   The frozen tissues were ground using pellet pestles, 300µl CCLR buffer was added and then the mixture was gently shaken at 4°C for 15 minutes.   The resulting lysates were spun at 12,000xg for 5 minutes and the clarified lysates transferred to a fresh tube and analyzed with a β-galactosidase Assay Kit. The activity of β-galactosidase, assayed in the linear range, was normalized against protein concentration.   The relative activity was then normalized against the same adipose depot from tetO-Cre; R26R Mice.

Western Blotting

Adipose tissues were frozen, ground and lyzed as described above in RIPA buffer (25 mM Tris•HCl pH 7.6, 150 mM NaCl, 1% NP-40, 1% sodium deoxycholate, 0.1% SDS). Western blotting was carried out with standard protocol.

Immunocytochemistry and Immunohistochemistry

Immunocytochemistry was performed on stromal-vascular cells 4 hours after plating, to ensure that the cells could adhere, using standard methods. In brief, the cells were isolated, plated on poly D-ornithine coated coverslips, probed with the antibodies indicated in the figures, and then detected with conjugated secondary antibodies. Specificity controls included no primary or no secondary antibodies, pre-immune sera, and other tissues. For BrdU labeling, the cells or tissues were fixed and washed in H_2O, incubated with 1N HCl at 37°C for 45 minutes, washed in H_2O, incubated in 0.1M $NaBO_4$ for 10 minutes and subjected to immunocytochemistry or immunohistochemistry.

SV Fractionation

The fractionation of SV cells and adipocytes was as described (Klaus et al., 1991) with slight modifications. Briefly, SV cells were isolated from pooled white adipose depots (inguinal, interscapular, gonadal, retroperitoneal) that were explanted and minced into fine pieces (2-5mm^2). The adipose pieces were then digested in adipocyte isolation buffer (100mM HEPES pH7.4, 120mM NaCl, 50mM KCl, 5mM glucose, 1mM $CaCl_2$, 1.5% BSA) containing 1mg/ml collagenase at 37°C with constant slow shaking (~120 rpm) for 2 hours. During the digestion period, the suspension was titurated several times through a pipet to dissociate the

clumps. The suspension was then passed through 80μm mesh to remove undigested clumps and debris. The effluent was centrifuged at 500xg for 10 minutes and the pellet washed once in 5ml PBS. The resultant isolated cells were subjected to FACS or plated in a 24-well tissue culture dish or on poly D-ornithine-coated coverslips placed in a 24-well culture dish. To isolate floated adipocytes, the just described collagenase-treated mixture was passed through a 210μm mesh, centrifuged at 500xg for 10 minutes and floated adipocytes collected from the top.

Isolation of Adipocyte Nuclei

This procedure was performed using standard protocol. Briefly, the adipocytes were isolated as described in SV fractionation and then resuspended in cold nuclei extraction buffer (320mM sucrose, 5mM $MgCl_2$, 10mM HEPES, 1% Triton-X at pH7.4) at 10^6 cells/ml. The cells were vortexed gently for 10 seconds and incubated on ice for 10 minutes. Nuclei were pelleted at 2000xg, and washed twice with nuclei wash buffer (320mM sucrose, 5mM $MgCl_2$, 10mM HEPES at pH7.4). Nuclei in nuclei wash buffer were allowed to attach to silicone-coated slides for 1 hour at 4°C. Then nuclei were fixed in 3.7% formaldehyde in nuclei wash buffer for 10 minutes and subjected to BrdU immunocytochemistry.

Cell Culture

The SV cells were cultured in growth medium (DMEM containing10% FBS, 10units/ml penicillin and 10μg/ml streptomycin). After reaching confluence, the cells were maintained in growth medium for spontaneous adipogenesis or in growth medium with 1μg/ml insulin. Nile Red, BODIPY, and Oil Red O staining were performed as described (McKay et al., 2003; Nishimura et al., 2007). For immunocytochemistry and β-gal staining, the cells were grown on poly

D-ornithine-coated coverslips.   For BrdU labeling, cells were incubated with 10μg/ml BrdU in medium for a 2-hr pulse, followed by immunocytochemistry.   For growth curve analyses, cells were cultured in a 6-well plate in DMEM with 10% FBS.   Upon reaching 80% confluence, the cells were trypsinized, counted using a haemocytometer, split 1:3 and plated for growth.   For Wnt inhibition, conditioned medium from control HEK-293 cells or from HEK-293 cells expressing Wnt3A was diluted 50% with fresh medium and added to the cells after the cells reached confluence and thereafter. LiCl was added at 25mM.

RNA extraction, cDNA synthesis and qPCR

RNA extraction, cDNA synthesis and qPCR were performed as described (Suh et al., 2006). Briefly, total RNA from cells were extracted using Trizol with manufacturer's protocol. RNA was treated with DNase-I and reversed transcribed using random hexamers and M-MLV-reverse transcriptase. qPCR was carried out using Power SYBR Green PCR Master Mix. qPCR values were normalized against β-actin expression.

Transplantation

The transplantation of GFP- and GFP+ SV cells was as described with slight modifications (Hong et al., 2005).   Briefly, adipose SV cells were obtained from 4-week old PPARγ-GFP mice, and GFP- and GFP+ SV cells were isolated with FACS. Then, 5×10^5 FACS-sorted GFP- or GFP+ SV cells were collected, mixed with BD Matrigel Matrix (150μl) supplemented with 1ng/ml bFGF, and injected subcutaneously into the flanks of 2-4 week old CD-1 nude mice.   The transplants were analyzed 4 weeks after injection.   The transplanted tissues were harvested and fixed in 4% paraformaldehyde overnight or snap-frozen in OCT for

cryostat sections and immunohistochemistry.   The fixed tissues were embedded in paraffin.

Histology

Tissues were fixed, dehydrated, embedded in paraffin, and sectioned with a microtome. Hematoxylin and eosin staining (H&E staining) and trichrome staining were as described (Prophet et al., 1992).

References

Ailhaud, G., Grimaldi, P., and Negrel, R. (1992). Cellular and molecular aspects of adipose tissue development. *Annu Rev Nutr* **12**, 207-233.

Altiok, S., Xu, M., and Spiegelman, B. M. (1997). PPARgamma induces cell cycle withdrawal: inhibition of E2F/DP DNA-binding activity via down-regulation of PP2A. *Genes Dev* **11**, 1987-1998.

Avram, M. M., Avram, A. S., and James, W. D. (2005). Subcutaneous fat in normal and diseased states: 1. Introduction. *J Am Acad Dermatol* **53**, 663-670.

Clevers, H. (2006). Wnt/beta-catenin signaling in development and disease. *Cell* **127**, 469-480.

DiGirolamo, M., Fine, J. B., Tagra, K., and Rossmanith, R. (1998). Qualitative regional differences in adipose tissue growth and cellularity in male Wistar rats fed ad libitum. *Am J Physiol* **274**, R1460-1467.

Gesta, S., Tseng, Y. H., and Kahn, C. R. (2007). Developmental origin of fat: tracking obesity to its source. *Cell* **131**, 242-256.

Graves, R. A., Tontonoz, P., Platt, K. A., Ross, S. R., and Spiegelman, B. M. (1992). Identification of a fat cell enhancer: analysis of requirements for adipose tissue-specific gene expression. *J Cell Biochem* **49**:219-224.

Harada, N., Tamai, Y., Ishikawa, T., Sauer, B., Takaku, K., Oshima, M., and Taketo, M. M. (1999). Intestinal polyposis in mice with a dominant stable mutation of the beta-catenin gene. *Embo J* **18**, 5931-5942.

Hausman, G. J., Campion, D. R., and Martin, R. J. (1980). Search for the adipocyte precursor cell and factors that promote its differentiation. *J Lipid Res* **21**, 657-670.

Hausman, D. B., DiGirolamo, M., Bartness, T. J., Hausman, G. J., and Martin, R. J. (2001). The biology of white adipocyte proliferation. *Obes Rev* **2**, 239-254.

Hausman, G. J., and Hausman, D. B. (2006). Search for the preadipocyte progenitor cell. *J Clin Invest* **116**, 3103-3106.

Hiragun, A., Sato, M., and Mitsui, H. (1988). Preadipocyte differentiation in vitro: identification of a highly active adipogenic agent. *J Cell Physiol* **134**, 124-130.

Hong, K. M., Burdick, M. D., Phillips, R. J., Heber, D., and Strieter, R. M. (2005). Characterization of human fibrocytes as circulating adipocyte progenitors and the formation of human adipose tissue in SCID mice. *Faseb J* **19**, 2029-2031.

Kanda, T., Sullivan, K. F., and Wahl, G. M. (1998). Histone-GFP fusion protein enables sensitive analysis of chromosome dynamics in living mammalian cells. *Curr Biol* **8**, 377-385.

Kawai, T., Takei, I., Oguma, Y., Ohashi, N., Tokui, M., Oguchi, S., Katsukawa, F., Hirose, H., Shimada, A., Watanabe, K., and Saruta, T. (1999). Effects of troglitazone on fat distribution in the treatment of male type 2 diabetes. *Metabolism* **48**, 1102-1107.

Klaus, S., Cassard-Doulcier, A. M., and Ricquier, D. (1991). Development of Phodopus sungorus brown preadipocytes in primary cell culture: effect of an atypical beta-adrenergic agonist, insulin, and triiodothyronine on differentiation, mitochondrial development, and expression of the uncoupling protein UCP. *J Cell Biol* **115**, 1783-1790.

Kletzien, R. F., Clarke, S. D., and Ulrich, R. G. (1992). Enhancement of adipocyte differentiation by an insulin-sensitizing agent. *Mol Pharmacol* **41**, 393-398.

Lazar, M. A. (2005). PPAR gamma, 10 years later. *Biochimie* **87**, 9-13.

Lehmann, J. M., Moore, L. B., Smith-Oliver, T. A., Wilkison, W. O., Willson, T. M., and Kliewer, S. A. (1995). An antidiabetic thiazolidinedione is a high affinity ligand for peroxisome proliferator-activated receptor gamma (PPAR gamma). *J Biol Chem* **270**, 12953-12956.

McKay, R. M., McKay, J. P., Avery, L., and Graff, J. M. (2003). C elegans: a model for exploring the genetics of fat storage. *Dev Cell* **4**, 131-142.

Nishimura, S., Manabe, I., Nagasaki, M., Hosoya, Y., Yamashita, H., Fujita, H., Ohsugi, M., Tobe, K., Kadowaki, T., Nagai, R., and Sugiura, S.. (2007) Adipogenesis in obesity requires close interplay between differentiating adipocytes, stromal cells, and blood vessels. *Diabetes* **56**, 1517-1526.

Ntambi, J. M., and Young-Cheul, K. (2000). Adipocyte differentiation and gene expression. *J Nutr* **130**, 3122S-3126S.

Otto, T. C., and Lane, M. D. (2005). Adipose development: from stem cell to adipocyte. *Crit Rev Biochem Mol Biol* **40**, 229-242.

Prestwich, T. C., and MacDougald, O. A. (2007). Wnt/beta-catenin signaling in adipogenesis and metabolism. *Curr Opin Cell Biol* **19**, 612-617.

Prophet, E. B., Mills, B., Arrington, J. B., and Sokin, L. H. AFIP Laboratory Methods in Histotechnology (ed. 1st, 1992), pp. 53-55, 132-133.

Rosen, E. D., and MacDougald, O. A. (2006). Adipocyte differentiation from the inside out. *Nat Rev Mol Cell Biol* **7**, 885-896.

Ross, S. E., Hemati, N., Longo, K. A., Bennett, C. N., Lucas, P. C., Erickson, R. L., and MacDougald, O. A. (2000). Inhibition of adipogenesis by Wnt signaling. *Science* **289**, 950-953.

Soriano, P. (1999). Generalized lacZ expression with the ROSA26 Cre reporter strain. *Nat Genet* **21**, 70-71.

de Souza, C. J., Eckhardt, M., Gagen, K., Dong, M., Chen, W., Laurent, D., and Burkey, B. F. (2001). Effects of pioglitazone on adipose tissue remodeling within the setting of obesity and insulin resistance. *Diabetes* **50**, 1863-1871.

Sparks, R. L., Strauss, E. E., Zygmunt, A. I., and Phelan, T. E. (1991). Antidiabetic AD4743 enhances adipocyte differentiation of 3T3 T mesenchymal stem cells. *J Cell Physiol* **146**, 101-109.

Spiegelman, B. M., and Flier, J. S. (1996). Adipogenesis and obesity: rounding out the big picture. *Cell* **87**, 377-389.

Suh, J. M., Gao, X., McKay, J., McKay, R., Salo, Z., and Graff, J. M. (2006). Hedgehog signaling plays a conserved role in inhibiting fat formation. *Cell Metab* **3**, 25-34.

Tontonoz, P., Nagy, L., Alvarez, J. G., Thomazy, V. A., and Evans, R. M. (1998). PPARgamma promotes monocyte/macrophage differentiation and uptake of oxidized LDL. *Cell* **93**, 241-252.

Tumbar, T., Guasch, G., Greco, V., Blanpain, C., Lowry, W. E., Rendl, M., and Fuchs, E. (2004). Defining the epithelial stem cell niche in skin. *Science* **303**, 359-363.

Vermes, I., Haanen, C., Steffens-Nakken, H., and Reutelingsperger, C. (1995). A novel assay for apoptosis. Flow cytometric detection of phosphatidylserine expression on early apoptotic cells using fluorescein labelled Annexin V. *J Immunol Methods* **184**, 39-51.

Willson, T. M., Cobb, J. E., Cowan, D. J., Wiethe, R. W., Correa, I. D., Prakash, S. R., Beck, K. D., Moore, L. B., Kliewer, S. A., and Lehmann, J. M. (1996). The structure-activity relationship between peroxisome proliferator-activated receptor gamma agonism and the antihyperglycemic activity of thiazolidinediones. *J Med Chem* **39**, 665-668.

Chapter IV

PPARγ-Expressing Adipogenic Progenitors Reside in Adipose Vasculature

Abstract

The microenvironment where progenitor cells reside, or niche, plays an important role in maintaining the identity of progenitors and regulating their behaviours. But such microenvironment for adipose progenitors has not been identified before. Exploring genetic tools, I found that adipose progenitors reside in the mural cell compartment of blood vessels that supply adipose depots and not in vessels of other tissues. Cultured vessels from adipose tissues as well as adipose SV cells sorted based upon expression of the mural cell marker PDGFRβ are highly adipogenic. Lineage studies that trace PDGFRβ-expressing cells support the notion that mural cells contribute to the adipose lineage. Such findings ascribe an adipose precursor function to mural cells in vivo. They suggest that the adipose vasculature supplies cues and a niche for adipocyte development, thereby providing a basis to examine the interplay between adipogenesis and angiogenesis that could be exploited as a new avenue for obesity and diabetes therapies.

Introduction

Stem cells, or progenitor cells, are capable of proliferating and producing differentiated cell types. The microenvironment where progenitor cells reside, or niche, provides factors and signals as well as acts as an anchor to maintain the stem-like capacity of progenitor cells. Some of the most well-documented niches are in the hematopoietic, epithelial, neural and intestinal system (Xie and Li, 2007).

The adipose stromal-vascular (SV) compartment contains adipose progenitors (Ailhaud et al., 1992). The putative progenitor niche, which provides the microenvironment to the progenitors, might play an important role in maintaining the identity of progenitors and regulating their behaviors. But the adipose SV progenitors have traditionally been studied as part of a complex and heterogeneous mixture of cells isolated by enzymatic dissociation and density separation from adipocytes (Hausman et al., 1980). The complete dissociation of adipose tissue results in disruption of any existing microstructure and loss of anatomical context of adipose progenitors. Moreover, the lack of markers for progenitors also hinders the identification of progenitor structures. Therefore, the identity, anatomical location, cellular context, and neighboring cells of adipose precursors are poorly defined. With the help of genetic tools, I was able to mark adipose progenitors by GFP, which allows the direct visualization of progenitor cells. The identification of anatomical location of progenitors and characterization of progenitor niche thus become possible.

Adipose depots are highly vascularized and every adipocyte is intimately juxtaposed with multiple capillaries (Crandall et al., 1997). Adipose development is temporally and spatially correlated with vascular development (Hausman and Richardson, 2004). Targeting adipose

tissue vasculature by using angiogenesis inhibitors or proapoptotic peptide leads to adipose ablation and reversal of obesity (Kolonin et al., 2004; Rupnick et al., 2002). The interrelationship between angiogenesis and adipogenesis has largely been ascribed to autocrine/paracrine between blood vessels and preadipocytes/adipocytes (Hausman and Richardson, 2004). Blood vessel development often precedes adipocyte differentiation and possibly promotes migration of preadipocyte and precipitates adipogenesis (Hausman and Richardson, 2004). Conversely, preadipocytes/adipocytes secret a variety of factors to regulate angiogenesis, such as vascular endothelial growth factor (VEGF), plasminogen activator inhibitor-1 (PAI-1), matrix metalloproteinases (MMP) and leptin (Hausman and Richardson, 2004). However, direct involvement of vascular components in adipogenesis has not been shown before. Nishimura et al. observed so called "adipogenic/angiogenic cell clusters" (Nishimura et al., 2007), in which the sprouting of new blood vessels was coupled with adipocyte differentiation, pointing to the possibility that blood vessels could physically participate in the differentiation process.

Blood vessels are composed of interacting cell types including endothelial cells and mural cells (Armulik et al., 2005). Mural cells, generally referring to vascular smooth muscle cells and pericytes, regulate blood flow, vascular permeability, and blood vessel development. Cultured mural cells display remarkable plasticity and can be induced to undergo adipogenesis (Farrington-Rock et al., 2004), chondrogenesis (Farrington-Rock et al., 2004), myogenesis (Dellavalle et al., 2007) and osteogenesis (Doherty et al., 1998), similar to mesenchymal stem cells (Pittenger et al., 1999). Therefore, mural cells could potentially provide an in vivo progenitor reservoir. Here, exploiting genetic tools, I identified that adipose progenitors are located specifically in the adipose vasculature as mural cells. This finding extends the role of

mural cells as adipocyte progenitors and further supports the notion that mural cells may provide

progenitor repositories for local tissues.

Results

GFP+ SV Cells are Present in the Isolated Blood Vessels

After identification and characterization of adipose progenitors, a lot of interesting questions emerged.   What is the anatomical location of the progenitors?   Do they distribute randomly across the adipose tissues or form some sort of structure?   What is the niche for the adipose progenitors?   To investigate these important aspects of adipose progenitors, I revisited the traditional method to isolate the SVF, which involves mincing adipose tissues into small pieces, enzymatically dissociating the cells and analyzing the isolated cells as a whole.   I reasoned that to better maintain any structure in adipose tissue, a milder digestion should be performed to partially maintain the native SV architecture while removing adipocytes that obscure visualization of the precursor location.   Therefore, the intact tissue should be digested directly instead of being cut into small pieces.   After digestion, usually I collect the cells that pass through the mesh and get rid of the clumps and debris on the top.   But to obtain any possible structure, I collected what remained on the top of the mesh instead.   The modified method is depicted in Figure 4.1.   Interestingly, when I examined the retained structures under fluorescent microscope, I found that GFP+ nuclei were lined up along some structures with various morphologies (Figure 4.2, not shown).   Some were lined up like beads on a thread, some were lined across the wall of a hollow tube, and some simply were part of a clump without any distinguishable shape.   A lot of the structures, named SV particulates (SVP), were reminiscent of blood vessels or capillaries.
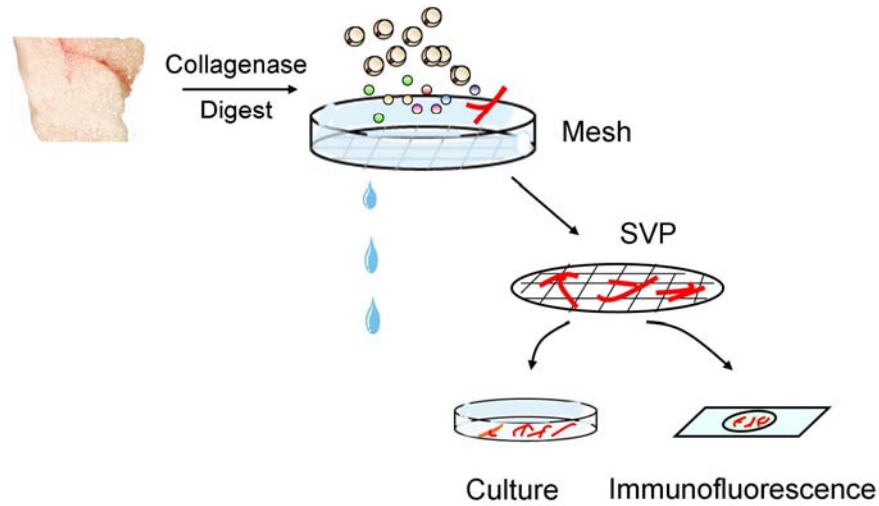
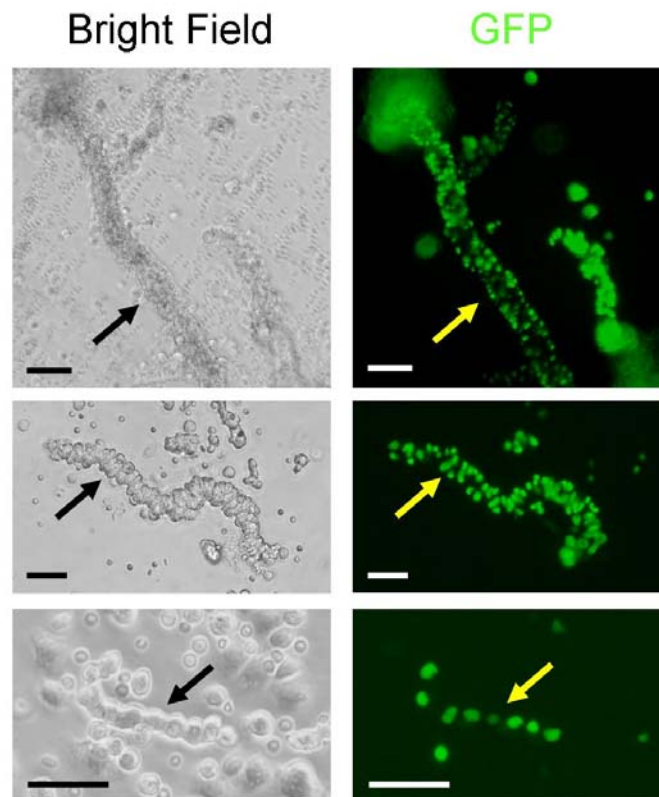**Figure 4.1. Modified method to isolate stromal-vascular particulates (SVP).**

Figure 4.2 GFP+ cells are present in SVP isolated from PPARγ-GFP adipose tissues. SVP structures from P30 PPARγ-GFP mice were photographed with light (left panel) and fluorescent (right panel) microscopy.   Arrows indicate SV tubes containing GFP+ cells.   Scale bars: 50μm.

GFP+ Blood Vessels are Adipogenic

To see whether these structures have any physiological relevance, I cultured and induced them to adipogenesis. I adopted two methods for this adipogenesis assay. One method was to allow the tubes to settle down and attach to the plate, and then induce them. Alternatively, I grew the tubes in suspension and induced them, using non-adherent plates to avoid attachment. The GFP+ cells present in freshly isolated tubes did not contain lipid-droplets based upon inspection and lack of staining with Nile Red or BODIPY (Figure 4.3A, not shown). In contrast, the tubes in culture changed their morphologies and lipid-laden GFP+ adipocytes soon formed along the tubes, indicating that the tube-associated SVP GFP+ cells were adipogenic (Figure 4.3A, B). The induction was particularly potent when the tubes were cultured in suspension. Nearly all the tube-like structures have some lipid accumulation visible within 2-3 days in induction medium. The addition of rosiglitazone dramatically enhanced the adipogenesis, suggesting that these tube-like structures were responsive to TZD (not shown), although this response might be different from the in vivo response. The adipocytes expressed GFP even when the SVPs were isolated and cultured in Dox, indicating that they were derived from a GFP-expressing lineage (Figure 4.3B). Since these tube-like structures contain the PPARγ-expressing progenitors and are adipogenic, they are likely to be the structure of the adipose niche.
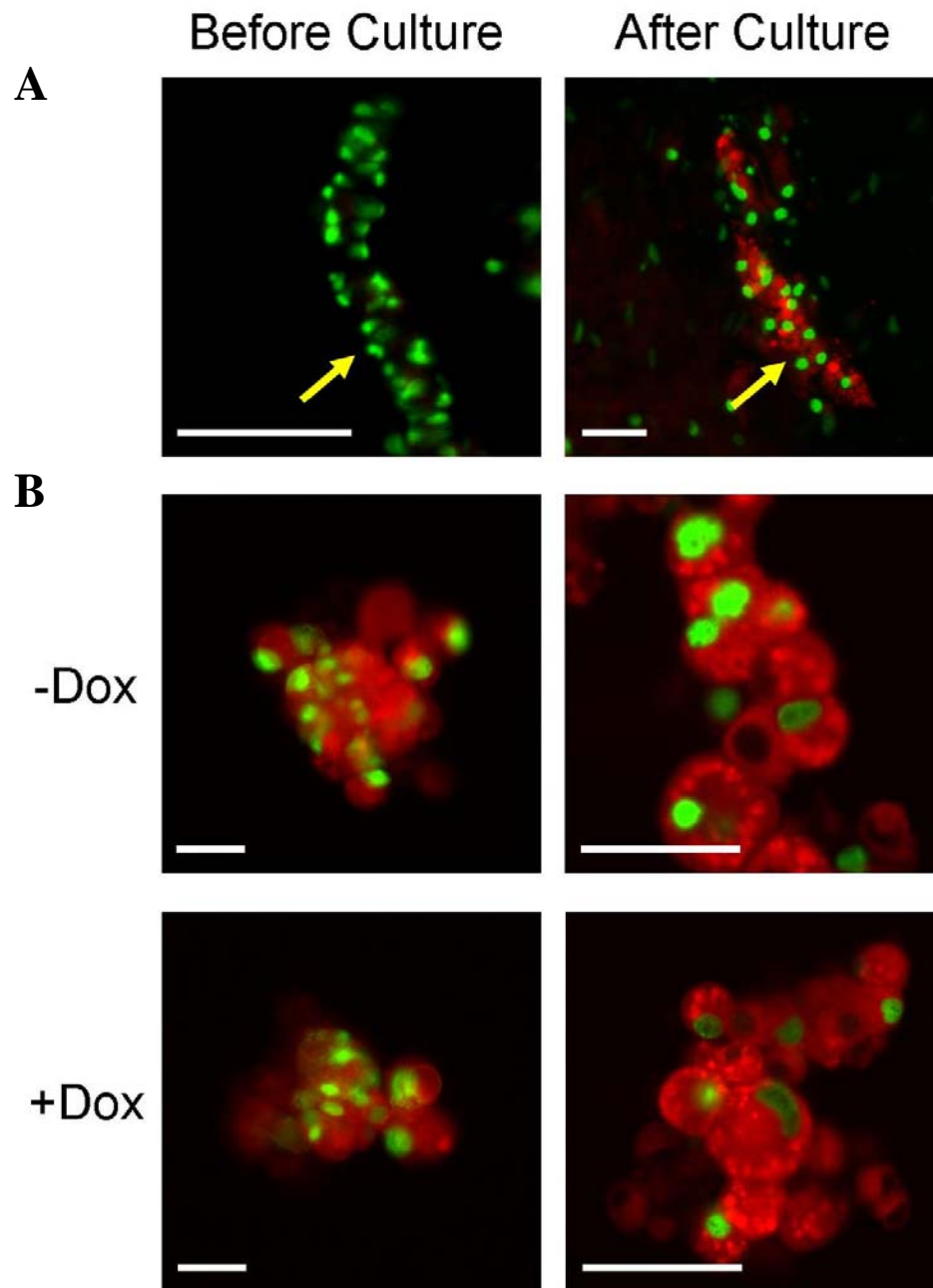
Figure 4.3. **Isolated SVPs are adipogenic *in vitro*.** (A) PPARγ-GFP SVP tubes were isolated and stained with the lipid-specific dye BODIPY either prior to culture (left panel) or after 3 days cultured on petri dishes in insulin (right panel). Arrows indicate SV tube. (B) PPARγ-GFP SVP tubes were cultured in suspension either without (top panels) or with Dox (bottom panels). Formation of adipocytes that derive from the GFP+ tubes was assessed with BODIPY staining (red). GFP (green). Lipid droplets were visualized with confocal microscopy (right panels). Scale bars: 50μm (A, B left panels), 20μm in confocal images (B right panels).

GFP+ SV Cells Reside in Adipose Vasculature *in vivo*

Since the SVP tubes resembled blood vessels, I stained them with antibodies that recognize constituent cells of the vasculature including PECAM (endothelium) and three independent mural cell markers: SMA, PDGFRβ and NG2 (Armulik et al., 2005). The SVP tubes expressed PECAM and were surrounded by cells that expressed SMA, PDGFRβ and NG2, indicating that they were blood vessels (Figure 4.4A). Interestingly, the GFP+ nuclei seemed to co-express mural cells markers, but not endothelial marker (Figure 4.4B). Physically, GFP+ nuclei seemed to be located in the outer layer of blood vessels. This result suggests that the PPARγ-expressing progenitors might be mural cells located along the blood vasculatures.
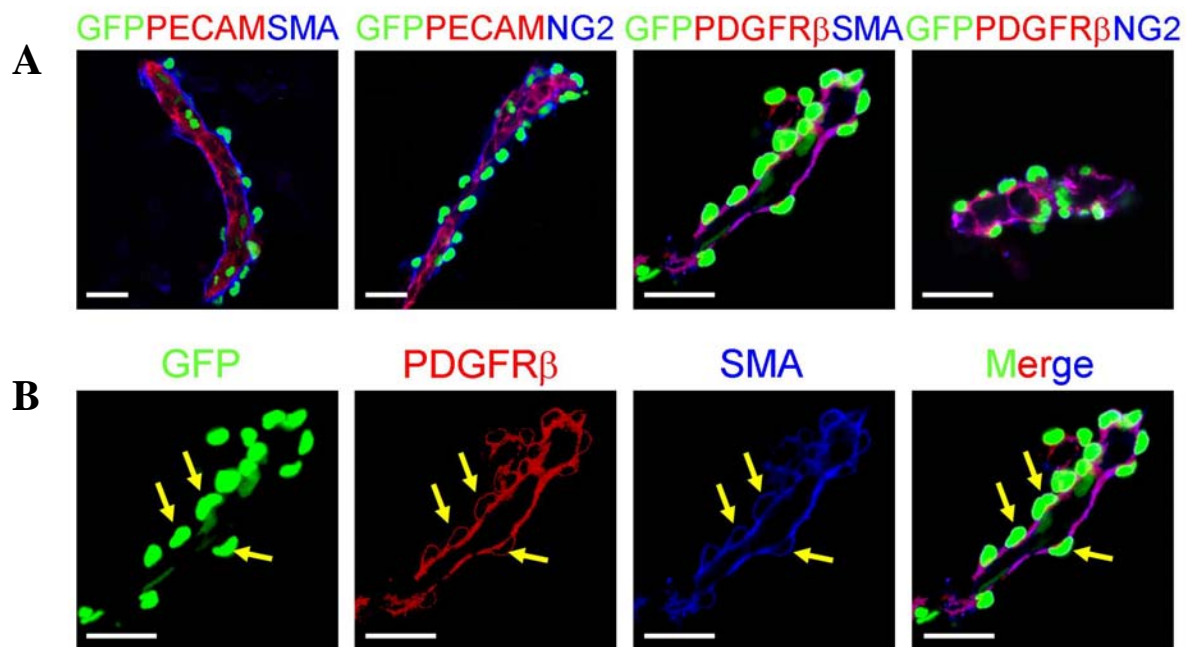

Figure 4.4. Isolated SVP expresses vascular markers and GFP+ cells in SVP express mural cell markers. (A) SVP isolates of P30 PPARγ-GFP mice were examined for expression of GFP (green) and the indicated immunohistochemical markers. Endothelial marker: PECAM (red); mural cell markers: SMA (blue), NG2 (blue), and PDGFRβ (red). Colocalization of GFP+ nuclei and cytoplasmic expression of mural cell markers in the same cells could be visualized in (B). Yellow arrows indicate position of GFP+ nuclei within mural cells. Scale bars: 20μm in confocal images.

To substantiate the notion that PPARγ-expressing cells reside in the adipose mural cell compartment, I examined fresh frozen sections of PPARγ-GFP adipose depots with immunohistochemistry. I observed GFP expression in many vessels that co-localized with mural cell markers (Figure 4.5A, B). This finding is interesting, yet one concern is that expression of the GFP reporter in vasculature might be an artifact introduced by the PPARγ-tTA tool. This expression pattern could be due to leakiness of the Tet system in vasculature or that PPARγ generally expresses in mural cells. To address these concerns, I examined the vasculature in various organs in PPARγ-tTA; tetO-H2B-GFP mice, including retina (which is rich in vasculature and has a high mural cell distribution), kidney, heart, spleen, pancreas and liver. None of these organs has GFP expressed in the vasculature (Figure 4.5C, not shown), suggesting that the presence of PPARγ-expressing cells in vasculature is unique in adipose tissue. This adipose specificity is notable because it indicates that there might be complex interplay between adipose tissue and its vasculature.
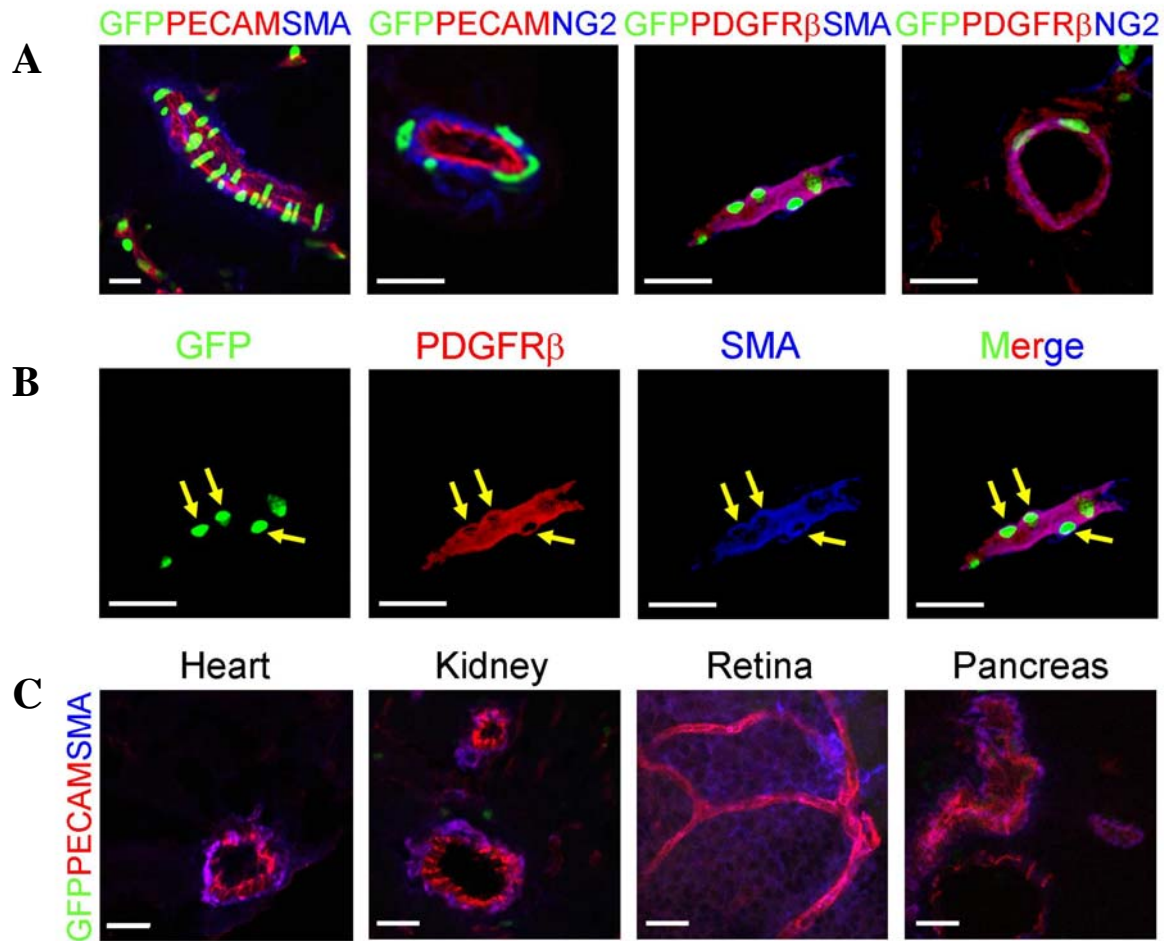
Figure 4.5. **GFP+ SV cells are present in the mural cell compartment of adipose vasculature but not in other organs.** (A) P30 PPARγ-GFP WAT was freshly frozen, cryosectioned, and examined with direct fluorescence for GFP and indirect immunofluorescence for the indicated endothelial (PECAM, red) and mural cell (SMA, blue; NG2, blue; PDGFRβ, red) markers. (B) Cryosection of a PPARγ-GFP adipose depot showing expression of GFP, PDGFRβ, SMA or all three merged. Arrows indicate mural cell nuclei that express GFP. (C) Cryosections of the indicated organs of PPARγ-GFP mice were examined for GFP, PECAM, and SMA as in (A). GFP was not expressed in mural cells of these tissues. Heart, kidney, retina longitudinal view of vessels; pancreas cross-sectional images. Scale bars: 20μm in confocal images (A-C).

I further analyzed progenitor cells with surface markers for mural cells by flow cytometry. Indeed, the majority of GFP+ SV cells express PDGFRβ, although the signal intensity is quite weak (not shown). However, ~35% of GFP+ SV cells express NG2 (not shown), suggesting that GFP+ SV cells are indeed a heterogeneous population. To see whether PDGFRβ-expressing adipose SV cells were competent to undergo adipogenesis, I isolated PDGFRβ positive and negative SV cells from wild-type mice by FACS and induced to adipogenesis. The PDGFRβ positive SV cells had high adipogenic potential and substantially more than PDGFRβ negative cells (Figure 4.6A). To investigate the possibility that PDGFRβ-expressing cells were part of the adipocyte lineage, I performed X-gal staining on adipose depots of P30 mice that contained both a PDGFRβ-Cre (Foo et al., 2006) transgene, which expresses Cre in mural cells and other developing cells, and R26R. As a specificity control, I used SM22-Cre (Boucher et al., 2003), a driver that is expressed in a subset of vascular smooth muscle cells. In these Cre-mediated lineage studies, I found that PDGFRβ-Cre generated strong and relatively homogenous lacZ expression throughout adipose depots in adipocytes and mural cells (Figure 4.6B). In contrast, SM22-Cre did not, although lacZ was expressed in a distinct subset of vessels within adipose depots (Figure 4.6B). These data are consistent with the possibility that adipocyte progenitors reside as mural cells.
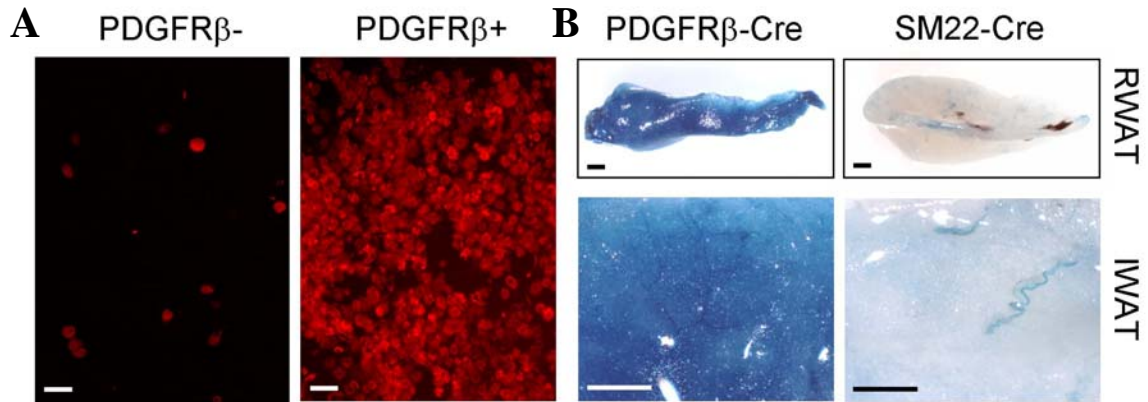
Figure 4.6. Mural cell marker PDGFRβ might mark adipose lineage. (A) SV cells were isolated from P30 wild-type mice and sorted with a PDGFRβ antibody. Confluent PDGFRβ negative and positive cells were cultured in insulin and fat formation assessed with BODIPY (red). (B) RWAT (top panels, 5x) and IWAT (bottom panels, 20x) of P30 PDGFRβ-Cre; R26R and SM22-Cre; R26R mice were stained for β-galactosidase expression (blue). Scale bars: 50μm (A), 1mm (B).

Discussion

The progenitor cell niche provides the microenvironment to maintain the progenitors at the primitive state, signal the progenitors to proliferate, and allow the progenitors to generate differentiated cells and leave the niche. The progenitor cell niche serves to regulate the status and behavior of progenitor cells by feeding signals and cues to progenitor cells. Therefore, in order to understand progenitors and know how to regulate their behaviors, it is critical to know about the niche in which they reside. For adipose progenitors, this area of research has not been studied. Neither the identity of the adipocyte progenitors nor their precise location has been identified. Previously, I have shown that by exploiting genetic tools, one can label and characterize a population of adipose SV cells that have the properties of progenitor cells. These genetic tools offer the advantage to directly visualize the progenitor population, which allows me to identify the anatomical location of adipose progenitor cells. I found that some of these progenitors reside in the adipose vasculature as mural cells, results that are supported by electron micrographs reported over 25 years ago (Iyama et al., 1979; Cinti et al., 1984). This phenomenon is specific for adipose vasculature, which makes it less likely to be an artifact introduced by the labeling system. Thus the adipose vasculature may function as a progenitor niche and provide signals for adipocyte development. The vascular niche is not a novel idea; some tissue stem cells or progenitors, such as pancreatic β-cells, neural stem cells, and hematopoietic stem cells, reside in a vascular niche (Nikolova et al., 2007). However, in adipose tissues, this is first report to identify the progenitors and the presence of a vascular niche. The "adipogenic/angiogenic cell clusters" reported in the literature (Nishimura et al., 2007) might

be a snapshot of how the progenitor in this vascular niche gives rise to differentiated adipocytes. Yet further studies have to be done to see how this process occurs.

Due to the fact that PPARγ labels both progenitors and adipocytes, histologically it is very difficult to distinguish between adipocytes and progenitors residing outside of the vasculature. Therefore it is not clear whether all the progenitors are adipose resident mural cells or if some are scattered outside of the vasculature. A progenitor specific marker is required to address this question.

How adipose progenitors obtain the mural cell identity is an interesting question. One possibility is that mural cells, after receiving the signals from local adipose environment, turn on PPARγ and become a progenitor reservoir. Another possibility is that adipose progenitors are generated during the formation of primitive adipose organ, and get recruited to the vasculature, which stabilize and maintain the progenitor status. Do the progenitor cells acquire the mural cell identity first or the progenitor identity first? The answer to this question helps to delineate the intermediate steps between stem cells and adipocytes. A detail study on the relationship between adipose vasculature and progenitor cells during early adipose development will likely address this issue.

My report here provides a foundation to further characterize the niche and the endogenous cues. Such insights may help define whether and how intervention in adipose lineage formation may be an efficacious therapeutic approach for obesity and diabetes.

Materials and Methods

Materials

Antibodies: rat anti-PECAM (BD Biosciences), mouse anti-α-smooth muscle actin, rat anti-PDGFRβ (eBiosciences), rabbit anti-NG2 (Chemicon), anti-rat PE conjugated antibody (BD Biosciences), cy3 donkey anti-rat (Jackson ImmunoResearch), cy5 donkey anti-mouse (Jackson ImmunoResearch), cy5 donkey anti-rabbit (Jackson ImmunoResearch).

Mouse Studies

PDGFRβ-Cre was a gift of Ralf Adams. SM22-Cre was a gift from Joachim Herz.

Immunocytochemistry and Immunohistochemistry

Immunocytochemistry was performed as described in Chapter III on stromal-vascular particulates after allowing 12 hours for the SVPs to adhere. Immunohistochemistry was performed on either 5-8μm cryostat sections of tissues freshly embedded in OCT using standard methods.

SVP Isolation and Culture

Intact IWAT (cut into 3 pieces), ISWAT, RWAT and GWAT explants were collagenase-treated (1mg/ml, 37°C, 2 hours). The mixture was passed through a 210μm mesh and then a 30μm mesh. The SVP tubes that remained on the 30μm mesh were washed off in DMEM+10%FBS. Alternatively, after passing through 210μm mesh, the SVP tubes were collected with low speed centrifugation (<250rpm, 10 min). SVP tubes were seeded in

gelatinized plates or on poly D-ornithine-coated coverslips, or cultured in suspension on non-coated petri dishes. Adipogenesis was analyzed after cultured in DMEM+10%FBS, which could be stimulated with insulin (1μg/ml).

References

Ailhaud, G., Grimaldi, P., and Negrel, R. (1992). Cellular and molecular aspects of adipose tissue development. *Annu Rev Nutr* **12**, 207-233.

Armulik, A., Abramsson, A., and Betsholtz, C. (2005). Endothelial/pericyte interactions. *Circ Res* **97**, 512-523.

Boucher, P., Gotthardt, M., Li, W. P., Anderson, R. G., and Herz, J. (2003). LRP: role in vascular wall integrity and protection from atherosclerosis. *Science* **300**, 329-332.

Cinti, S., Cigolini, M., Bosello, O., and Bjorntorp, P. (1984). A morphological study of the adipocyte precursor. *J Submicrosc Cytol* **16**, 243-251.

Crandall, D. L., Hausman, G. J., and Kral, J. G. (1997) A review of the microcirculation of adipose tissue: anatomic, metabolic, and angiogenic perspectives. *Microcirculation* **4**, 211-232.

Dellavalle, A., Sampaolesi, M., Tonlorenzi, R., Tagliafico, E., Sacchetti, B., Perani, L., Innocenzi, A., Galvez, B. G., Messina, G., Morosetti, R., Li, S., Belicchi, M., Peretti, G., Chamberlain, J. S., Wright, W. E., Torrente, Y., Ferrari, S., Bianco, P., and Cossu, G. (2007). Pericytes of human skeletal muscle are myogenic precursors distinct from satellite cells. *Nat Cell Biol* **9**, 255-267.

Doherty, M. J., Ashton, B. A., Walsh, S., Beresford, J. N., Grant, M. E., and Canfield, A. E. (1998). Vascular pericytes express osteogenic potential in vitro and in vivo. *J Bone Miner Res* **13**, 828-838.

Farrington-Rock, C., Crofts, N. J., Doherty, M. J., Ashton, B. A., Griffin-Jones, C., and Canfield, A. E. (2004). Chondrogenic and adipogenic potential of microvascular pericytes. *Circulation* **110**, 2226-2232.

Foo, S. S., Turner, C. J., Adams, S., Compagni, A., Aubyn, D., Kogata, N., Lindblom, P., Shani, M., Zicha, D., and Adams, R. H. (2006). Ephrin-B2 controls cell motility and adhesion during blood-vessel-wall assembly. *Cell* **124**, 161-173.

Hausman, G. J., Campion, D. R., and Martin, R. J. (1980). Search for the adipocyte precursor cell and factors that promote its differentiation. *J Lipid Res* **21**, 657-670.

Hausman, G. J., and Richardson, R. L. (2004). Adipose tissue angiogenesis. *J Anim Sci* **82**, 925-934.

Iyama, K., Ohzono, K., and Usuku, G. (1979). Electron microscopical studies on the genesis of white adipocytes: differentiation of immature pericytes into adipocytes in transplanted preadipose tissue. *Virchows Arch B Cell Pathol Incl Mol Pathol* **31**, 143-155.

Kolonin, M. G., Saha, P. K., Chan, L., Pasqualini, R., and Arap, W. (2004). Reversal of obesity

by targeted ablation of adipose tissue. *Nat Med* **10**, 625-632.

Nikolova, G., Strilic, B., and Lammert, E. (2007). The vascular niche and its basement membrane. *Trends Cell Biol* **17**, 19-25.

Nishimura, S., Manabe, I., Nagasaki, M., Hosoya, Y., Yamashita, H., Fujita, H., Ohsugi, M., Tobe, K., Kadowaki, T., Nagai, R., and Sugiura, S. (2007). Adipogenesis in obesity requires close interplay between differentiating adipocytes, stromal cells, and blood vessels. *Diabetes* **56**, 1517-1526.

Pittenger, M. F., Mackay, A. M., Beck, S. C., Jaiswal, R. K., Douglas, R., Mosca, J. D., Moorman, M. A., Simonetti, D. W., Craig, S., and Marshak, D. R. (1999). Multilineage potential of adult human mesenchymal stem cells. (1999) *Science* **284**, 143-147.

Rupnick, M. A., Panigrahy, D., Zhang, C. Y., Dallabrida, S. M., Lowell, B. B., Langer, R., and Folkman, M. J. (2002). Adipose tissue mass can be regulated through the vasculature. *Proc Natl Acad Sci U S A* **99**, 10730-10735.

Xie, T., and Li, L. (2007). Stem cells and their niche: an inseparable relationship. *Development* **134**, 2001-2006.

VITAE

Wei Tang was born in Tiandong, Guangxi Zhuang Autonomous Region of People's Republic of China, on September 17th, 1978, the daughter of Runtian Tan and Xihai Tang. After completing her work at No. 3 High School, Nanning, Guangxi in 1995, she attended the University of Science and Technology of China (USTC) at Hefei, Anhui, China. She received the degree of Bachelor of Science with a major in Biology from USTC in June 2000. In September 2002, she entered the Graduate School in the Department of Biology at Hong Kong University of Science and Technology and completed the master course in the laboratory of Dr. Nicholaus J. Sucher. She received the degree of Master of Philosophy in May 2002. In August 2002, she entered the Graduate School at the University of Texas Southwestern Medical Center at Dallas. She joined the laboratory of Dr. Jonathan M. Graff in May 2003. She married Tao Wang in December 2002.

Permanent Address: Rm 509 Unit 1 Bldg 23. 18 Gechun Rd
                       Nanning, Guangxi
                       China, 530023